بسم الله الرحمن الرحيم

ACOUSTIC AND RESISTIVITY STUDIES OF THE KHOBAR MEMBER, THE DAMMAM FORMATION, EASTERN PROVINCE, SAUDI ARABIA

BY

MOHAMMAD AHMAD MOHAMMAD

A Thesis Presented to the

DEANSHIP OF GRADUATE STUDIES

KING FAHD UNIVERSITY OF PETROLEUM & MINERALS

DHAHRAN, SAUDI ARABIA

In Partial Fulfillment of the
Requirements for the Degree of

MASTER OF SCIENCE

In

GEOLOGY

May, 2000

DHAHRAN 31261, SAUDI ARABIA

DEANSHIP OF GRADUATE STUDIES

This thesis written by MOHAMMAD AHMAD MOHAMMAD under the supervision of his Thesis Committee has been presented and accepted by the Dean of the College of Graduate Studies in partial fulfillment of the requirements for the degree of MASTER OF SCIENCE in Geology.

Thesis Committee

Dr. Abdullatif A. Qahwash
(Chairman)

Dr. Gabor Korvin (Member)

Dr. Mahbub Hussain (Member)

Dr. Mustafa M. Hariri
Department Chairman

Dr. Osama A. Jannadi
Dean, College of Graduate Studies

7/5/2001
Date

Dedicated to

my daughter (shahd)

ACKNOWLEDGMENT

Acknowledgment is due to the Earth Sciences Department at KFUPM for availing me the opportunity to study towards my MS degree.

I wish to express my sincere thanks to Dr. A. Qahwash for his continuous encouragement and advise throughout this work.

My thanks are due to Dr. M. Hussain and Dr. G. Korvin, my committee members, for their invaluable suggestions and comments. Also, I would extend my gratitude to Dr. A.Al-Ka'abi of the Research Institute for allowing me to use the resistivity core test unit. Dr. Al- Majid of Petroleum Engineering Department for preparing the thin sections, and helping in the porosity and permeability study, Dr. K. Al-Hanai of the Research Institute for providing the LANDSAT TM scene 164-42 image of the Eastern Province. Also, I would like to thank Dr. Zulfigar Ahmad, Mr. Lameed Babalola, and Dr. B. Imam of Earth Sciences Department for assisting in thin section descriptions study.

Special thanks to Mr. Ahmad Al-Saif, Mr. Khalid Al- Ramadhan, Mr. Said Hameed, Mr. Aziz Khan, Mr. Fadhel Al-Khalifa, and Mr. Qasim Mushabab. Also, I would like to thank all my friends who helped me in conducting the field work: Mr. Araf Al-Gonfidhi,, my brother Yousef, Mr. Tariq Al-Rashdi, Mr. Foad Al-Dossary, Sami Ramrm, and all who tried to help.

TABLE OF CONTENT

LIST OF FIGURES

LIST OF TABLES

APPENDICES

ABSTRACT

NAME: **Mohammad Ahmad Mohammad**

TITLE: Acoustic and Resistivity Studies of the Khobar Member, The Dammam Formation, Eastern Province, Saudi Arabia

MAJOR FIELD: Geology

DATE OF DEGREE: May 2000

The Khobar Aquifer is considered one of the important aquifers in the Eastern Province of Saudi Arabia. This research is devoted to study the lithology and petrophysical properties of the aquifer. Lithology was studied by analyzing rock samples using X-Ray Diffraction and thin section studies. A laboratory program was also executed to determine the electrical propreties, the acoustic properties, porosity and permeability of the Al-Khobar aquifer rocks. Furthermore, seismic refraction and electrical sounding surveys were conducted in the field. As a result of these studies, general relationships between ultrasonic wave velocity, resistivity, lithology, and porosity have been established.

MASTER OF SCIENCE DEGREE
KING FAHD UNIVERSITY OF PETROLEUM AND MINERALS
Dhahran, Saudi Arabia
May, 2000

الخلاصة

الاسم: محمد أحمد محمد

العنوان: دراسات سرعة الصوت والمقاومة الكهربائية لخزان الخبر، متكون الدمام، المنطقة الشرقية، المملكة العربية السعودية.

التخصص الرئيسي: جيولوجيا

تاريخ نيل الدرجة: مايو ٢٠٠٠

يعتبر خزان الخبر المائي أحد أهم الخزانات المائية في المنطقة الشرقية من المملكة العربية السعودية. كرس هذا البحث لدراسة نوعية الصخور وخصائص الخزان الطبيعية. درست نوعية الصخور من خلال تحليل عينات الصخور باستخدام طرق انكسار أشعة إكس و دراسة الشرائح الدقيقة للعينات. كما تم تحديد خاصية المقاومة النوعية، الخاصية الصوتية، المسامية، والنفاذية لصخور خزان الخبر من خلال برنامج معملي خاص. بالإضافة، تم عمل مسح حقلي باستخدام الطرق الإهتزازية والمقاومة الكهربائية. وكنتيجة لهذه الدراسات، حددت بعض العلاقات العامة بين سرعة الموجة الصوتية، المقاومة الكهربائية، نوعية الصخر، والمسامية.

درجة ماجستيرالعلوم

جامعة الملك فهد للبترول والمعادن

الظهران – المملكة العربية السعودية

مايو – ٢٠٠٠

CHAPTER ONE

INTRODUCTION

1.1. Introductory Statement

Geophysical methods are applied to explore for oil, gas, water, and minerals. Electrical and seismic refraction methods are used in practice to map the boundaries of an aquifer. In the electrical method, a current is applied into the ground to measure the drop in potential and thereafter the resistivity is calculated. In the refraction method, a mechanical vibration is sent into the ground and detected on the surface after having been refracted along the interface between layers of different acoustic impedances.

1.2. Objectives

The Khobar aquifer is a secondary aquifer in the Eastern Province of Saudi Arabia. Core samples were extracted from different parts of the aquifer's outcrops, and

they were saturated with water of different total dissolved salt (TDS) values. Then, their acoustic and resistivity parameters were measured in the laboratory. Seismic refraction and vertical electrical sounding (VES) using Schlumberger array were also conducted in the field. Comparisons between the laboratory and field results were made. Thin sections were made out of the core samples to identify the rock types and to estimate their porosities. Also, X-Ray diffractometry (XRD) and analysis were done on selected samples to identify the lithology of the aquifer.

In summary, the main objectives of this research are:

1- to study the acoustic and electric parameters of the Khobar aquifer, and

2- to interrelate between these parameters and porosity.

1.3. Location of the Study Area

The study area enclosing the Khobar aquifer lies in the Eastern Province of Saudi Arabia along the Arabian Gulf coast (Figure 1.1). It extends from latitude 26° 30' N to latitude 26° 04' N, and from longitude 50° 00' E to longitude 50° 14' E.

1.4. Geological Setting

1.4.1. Structure and Geologic History of the Arabian Peninsula

The Arabian Peninsula is a huge crustal plate composed of ancient sedimentary and volcanic rocks, deformed and metamorphosed and injected by plutonic intrusions. In Precambrian time, long before the formation of the Red Sea (Cretaceous), the peninsula

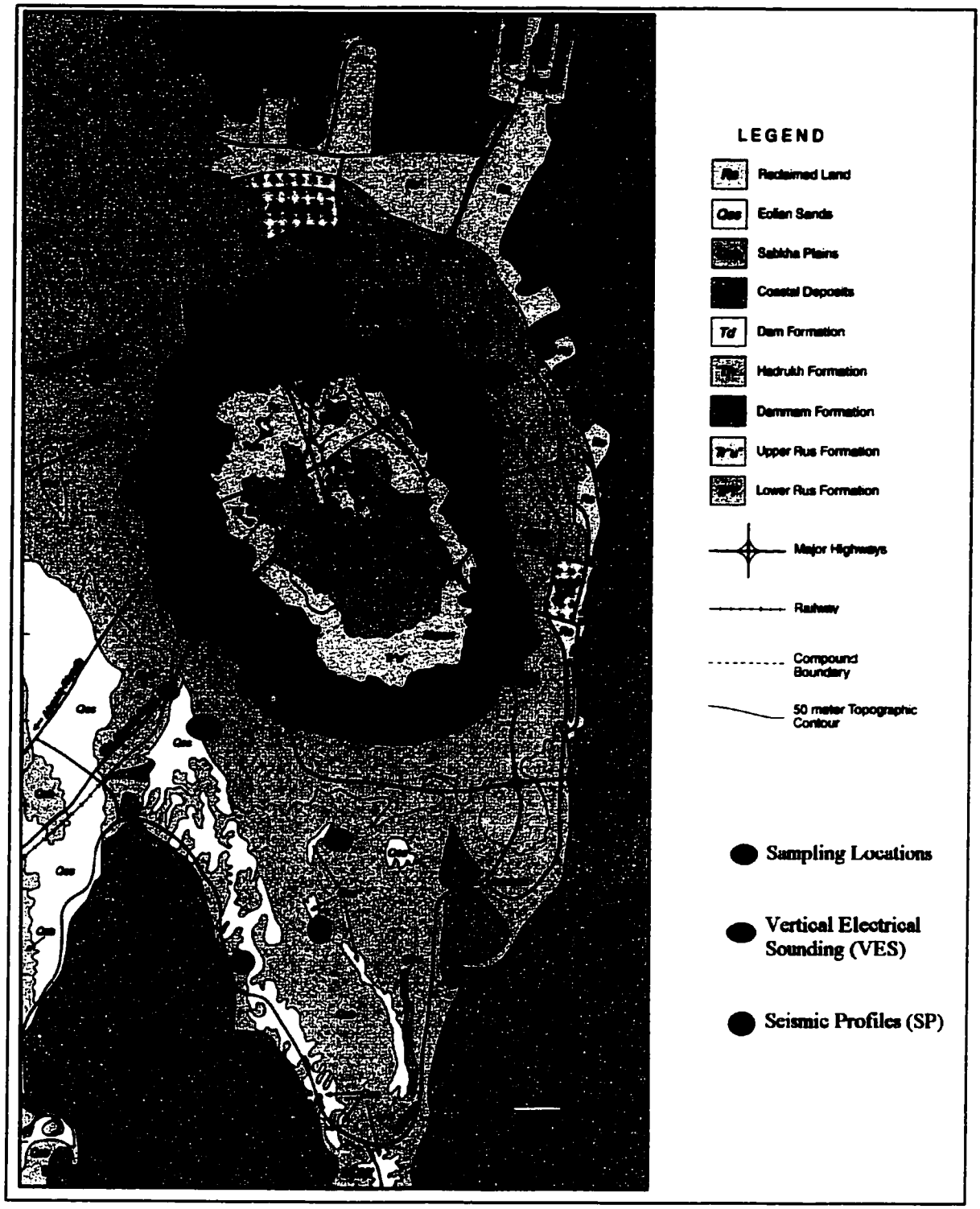

Figure 1.1: Geological Map of Dammam Region (Weijermars, 1999).

was attached to Africa as a part of the African (Nubian) Shield. In late Precambrian, its surface was deeply eroded and peneplaned.

At the beginning of the Cambrian, a great sedimentary basin had developed north and east of Arabia. Throughout Paleozoic, Mesozoic, and early Cenozoic times thousands of meters of continental and shallow-water marine sediments accumulated in a deep, slowly sinking trough of the same Precambrian plate that makes up the shield, resulting in a relatively thin succession of almost flat-lying strata on a number of deep sedimentary basins (Figure 1.2) (Sayari and others. 1978).

Throughout the Paleozoic and Mesozoic and during the Tertiary orogeny. the Arabian plate remained relatively stable, and its cover of shelf sediment was barely disturbed (Figure 1.3).

1.4.2. The Arabian Shelf

Today, the peninsula can be divided into two structural provinces. A western province, known as the Arabian Shield. is a part of the Precambrian crustal plate. generally exposed but locally covered by Tertiary volcanic rocks. An eastern province. called the Arabian Shelf, consists of a thick sedimentary sequence covering about two thirds of the Peninsula.

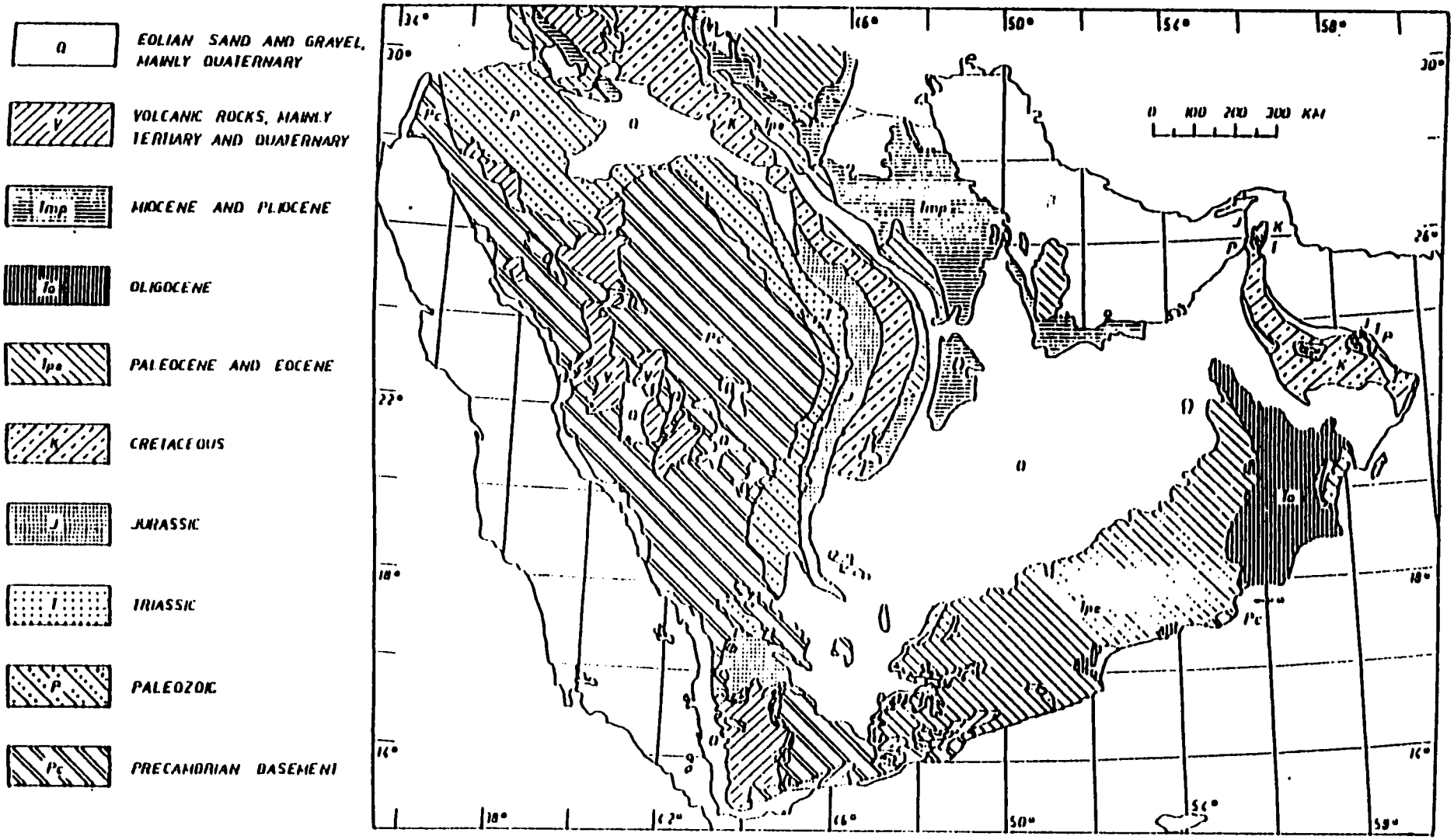

Figure 1.2: Generalized Geologic Map of the Arabian Peninsula (Sayari and Zotl, 1978).

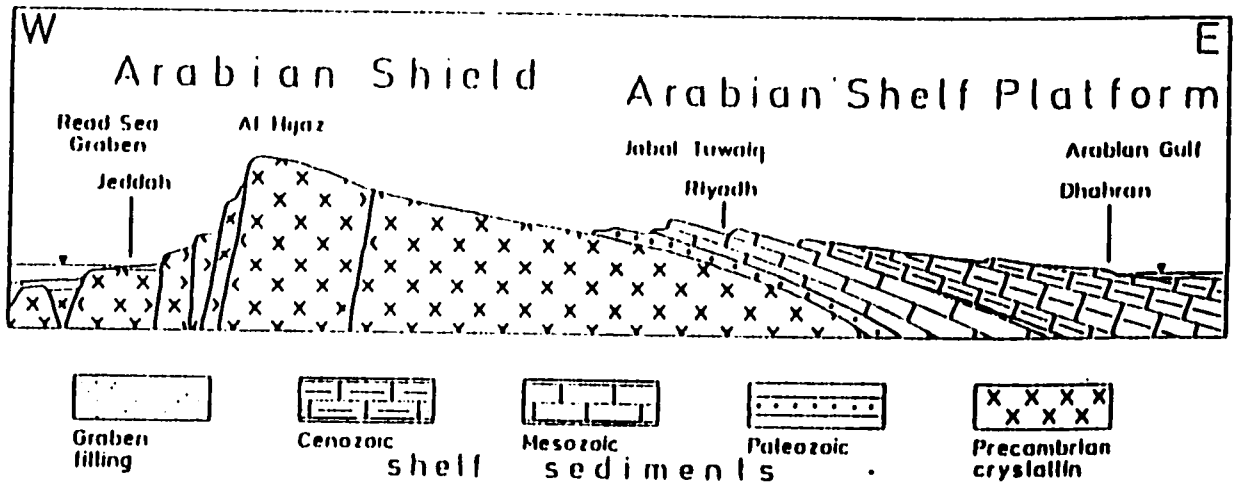

Figure 1.3: Geologic Cross-Section of the Arabian Peninsula from the Red Sea to the Arabian Gulf (Sayari and Zotl, 1978).

The sedimentary section in Saudi Arabia has been divided into eight major divisions: 1. Lower Paleozoic clastic rocks, 2. Permian and Trassic clastic rocks, 3. lower and Middle Jurassic clastic and carbonate rocks, 4. Upper Jurassic and early Lower Cretaceous carbonate rocks, 5. Lower Cretaceous clastic rocks, 6. Middle Cretaceous clastic rocks, 7. Upper Cretaceous to Eocene carbonate rocks, and 8. Miocene and Pliocene clastic rocks; each charactrized by a particular lithology and separated by significant breaks in the geologic records (Sayari and Zotl, 1978)

The Eocene rocks are widely exposed in a belt in the central and northern parts of the Arabian Peninsula, and they are mostly limestone and dolomites with thin layers of marl and shale. The Paleocene and/or Eocene rocks appear again near Abqaiq, Dhahran, Qatar, and in the southeastern Rub' Al Khali. Also, a broad band of Eocene rocks is exposed along the southern edge of the peninsula in the eastern part of the Republic of Southern Yemen and in Dhufar (Tamimi, 1985).

1.4.3. General Geology of Arabian Gulf Coastal Region and Its Hinterland

The Arabian Gulf coastal area is a northwesterly trending belt about 50-100 kilometers wide between As-Summan Plateau and the Arabian Gulf coast (Figure 1.1).
Its surface rocks include consolidated sedimentary formations ranging from Paleocene to Middle Eocene and Miocene to Pliocene. Upper Eocene and Oligocene time is represented by a regional unconformity. Unconsolidated materials include gravel of Tertiary age and various sediments of Quaternary age, comprising beach gravel and sand; gravel and silt in basin deposits, sabkhah sediments, and various eolian sand deposits.

The coastal area is part of the Arabian platform. Formations are thin but extensive, and dips are generally less than 1° northward and eastward toward the Arabian Gulf. A few minor structures break the pattern. The most prominent is the Dammam Dome that is believed to be the result of deep-seated salt intrusion (Sayari and Zotl, 1978). Its major axis trends about N 35° W and with an average dip on the flanks between 1° to 1.5 ° (Tleel, 1973).

This area includes some of Saudi Arabia's major oil and gas deposits. Several formations, notably the Umm Er Radhuma, and the Khobar and Alat Members of the Dammam are important aquifers.

1.4.4 Depositional Environment

During the Paleocene and part of the early Eocene normal marine conditions existed, forming the Umm Er Radhuma limestone. In the early Eocene, evaporitic conditions were controlling the environment, depositing anhydrite of the Rus Formation. In early and middle Eocene, marine conditions prevailed again and shale and limestone were deposited, forming the Dammam Formation. In the middle Eocene, a regional regression of the sea took place, followed by pre-Neogene unconformity where a long period of erosion took place (Mahmoud, 1987).

Towards the end of the Rus time, the sea transgressed and gave way to a more turbid, open marine environment in which shales of Midra and Saila Members were deposited. The sea must have been tropical and clear to permit the deposition of Alveolina limestone. By the end of the Alveolina time, the sea continued to transgress and to be clear, permitting the Nummulites rich Khobar Limestones Member to be deposited (Tleel,

1973). Tables 1.1 and 1.2 show the general lithostratigraphic succession of the study area, and the Dammam Equivalents in the Gulf States.

The Khobar member of the Dammam Formation consists of two units. The upper unit consists predominantly of limestone (Figures 1.4 (a) and (b)). The lower unit consists of light gray to tan dolomitic marl (Figure 1.5). The Khobar limestone Member was deposited in an external shelf on the outer side of an open-sea; very close to a reef in shallow warm water conditions (Layla and others 1992). The structural contour map of the Khobar member is illustrated in Figure 1.6. It is evident that the Khobar Member is at 40 to 60 meters depth in the study area.

1.5. Previous Investigations on the Khobar Aquifer

Many researchers studied the aquifers in the Eastern Province from the point of view of their geology (Sayari and Zotl, 1978; Ghamdi, 1997), numerical modeling (Layla and others, 1986; Rasheeduddin, 1988), development (Layla and others, 1992; Dabbagh and Abderrahman, 1997), hydrochemistry (Hassan, 1998), cavities (Jado and Johnson, 1983). Few studies had dealt with the aquifer geophysically (BRGM, 1977; Hassan, 1995). This research is devoted to study the acoustic and resistivity properties of the Al-Khobar aquifer in the Dammam area.

Table 1.1: Generalized Lithostratigraphic Succession of the Study Area (Hassan, 1998).

Age		Formation	Member	Rock Unit	Generalized Lithologic Description	Thickness (m)	Hydrogeo-logic Unit
Tertiary	Eocene	Dammam	Alat	Limestone	Skeletal detrital limestone	0-110	Aquifer
				Marl	Dolomitic marls with limestone intercalations (orange color)	0-35	Aquitard
			Khobar		Skeletal, detrital, Porous and friable limestones, dolomitic limestone	0-75	Aquifer
			Alveolina		Limestone interbedded with shales and marls	0-20	Aquitard
			Midra and Saila shales		Blue and dark grey, fissile shales with gypsiferous lenses	0-20	Aquitard

Table 1.2: Dammam Equivalents in the Gulf States (Naggar and Nakhal, 1989).

State	Members	Age
Kuwait	1- Bryozoan-peneroplid limestones	Middle Eocene
	2- Nummulitic limestones	
	3- Chalky limestone member	
	4- Chalky & marly limestones	
Southern Iraq	1-Bryozoan- peneroplid and shelf Limestones	Middle Eocene
	2- Nummulitic limestone	
	3- Chalk unit	
	4-Chalky limestones	
Western Iraq	Nummulitic limestone	Early-Late Eocene
Bahrain	1- White Limestone Member	Early-Middle Eocene
	2- Orange Marl Member	
	3- Brown Crystalline limestone Member	
	4- The Shark Tooth Shale Member	
Abu Dhabi	1- Light brown, microcrystalline Dolomite	Middle-Late Eocene
	2- Brown, very finely crystalline Limestone	
Qatar	1- Umm Bab Member	Early-Middle Eocene
	2- Dukhan Member	
	3- The Midra Shale Member	

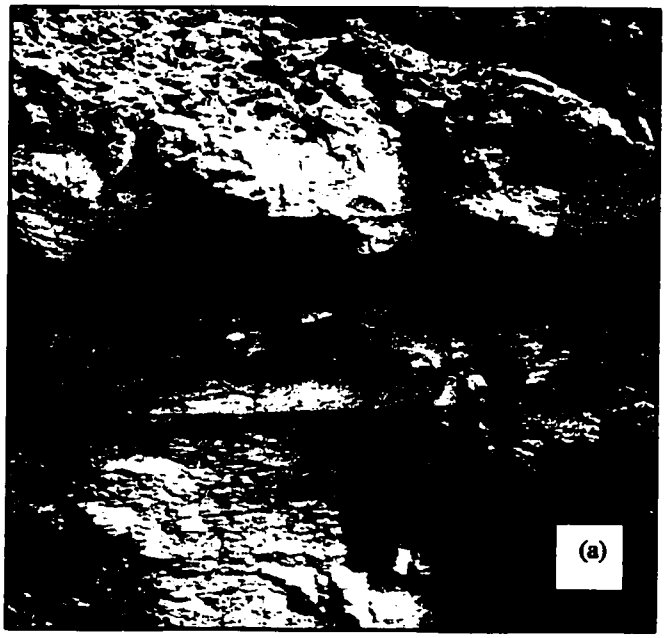

Figure 1.4: (a) The Saila and Alveolina Members. The Lower part shows the shaly members of the Dammam Formation, where the upper part shows the carbonate members of the Formation. (Location 26° 22.12' N, 50 ° 06.11' E – North of Dammam City). (b) Nummulitic Limestone of the Khobar Member. (Location 26 ° 16.57 ' N, 50 ° 10.55 ' E – Thoqba Area close to the Airport City)

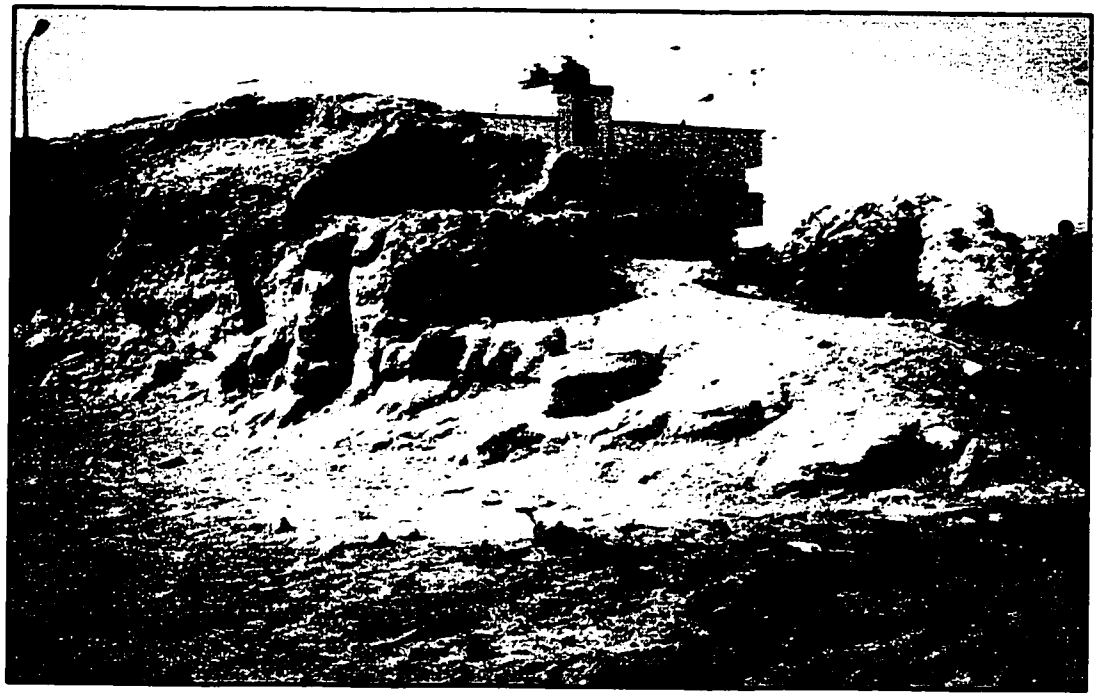

Figure 1.5: The Khobar Limestone Member, showing yellowish gray massive hard nummulitic calcarenitic limestone (upper part), and yellowish brown soft marly limestone (lower part). (Location 26 ° 16.51 ' N, 50 ° 10.57 ' E – Thoqba Area close to the Airport City)

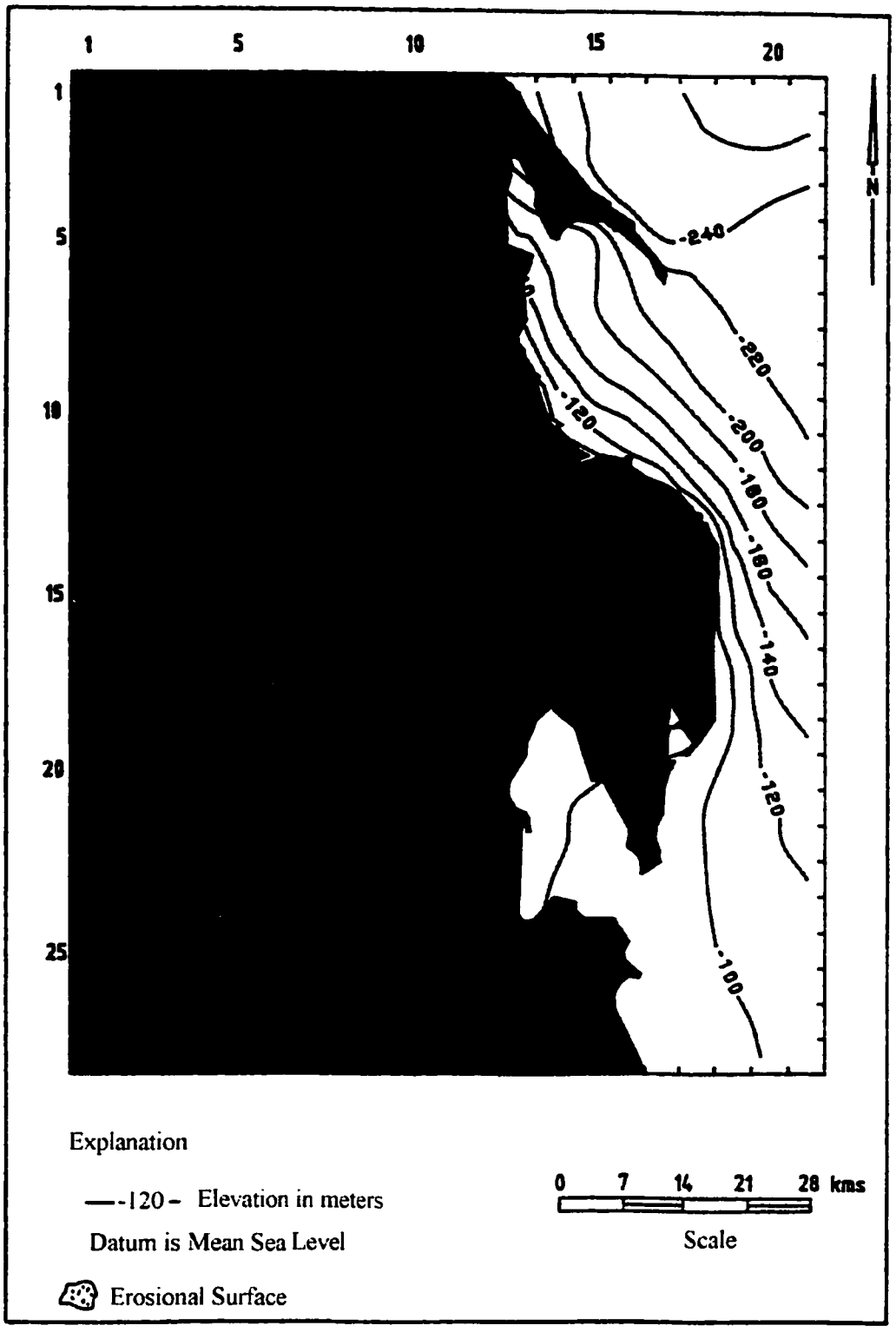

Figure 1.6: Structural Contour Map of the Khobar Aquifer (Rasheeduddin, 1988)

1.5.1. Hydrogeology of the Khobar Aquifer

The Khobar Member is named after the town Al-Khobar and it was introduced by Sander in 1962. The Khobar Member which is composed of fissured and karstified limestone and dolomitic limestones forming the most productive reservoir in the Dammam Formation (Layla and others, 1992; Hassan, 1998; Weijermars, 1999). The Khobar aquifer discharges to springs in both the Qatif and Hasa areas; and to submarine springs off the Arabian Gulf coast.

The Khobar aquifer is characterized by a wide variation of transmissivity and by the presence of a high transmissivity zone in the northeast part of the study area along the Gulf Coast (Layla and others, 1992). Transmissivities increase as a result of the increase in fracturing of the aquifer's rocks. Transmissivity also changes due to changes in lithological and textural properties of the aquifer's rocks.

The Khobar aquifer has a transmissivity of $7.06 \times 10^{-3} - 2.9 \times 10^{-1}$ m^2/s and storativity value of 0.00013×10^{-3} - 7.8×10^{-3}. The low storativity reflects the overall confined nature of the aquifer (Layla and others, 1992; Hassan, 1998). The Khobar aquifer generally has a porosity of more than 3% and a transmissivity range between 10^{-2} and 3×10^{-6} m^2/sec (Rasheeduddin, 1988). The fossil water in the aquifer is more than 30,000 years old (Edgell, 1997).

Total dissolved solid content in the Khobar aquifer increases along the regional groundwater flow in the northeastern direction.

At the Eastern Province, due to the heavy pumping, the water levels of the Khobar aquifer decline continuously, which has resulted in the creation of local, but significant cones of depression and deflections along the flow directions in the aquifer (Mahmoud, 1987).

It can be said that the Khobar aquifer is mainly suitable for rather small withdrawal rates (up to 20 or 30 L/sec) such as for domestic water supplies to small communities. It is not recommended to plan large-scale use of this reservoir. Also, recharge by rainfall of the Khobar aquifer is low, due to the arid conditions. Recharge is mostly from its western intake areas (Edgell, 1997).

In 1992, the water consumption in the Eastern Province's aquifers (Umm Er Radhuma, Dammam, and Neogene) was 1215 million cubic meters (mcm) (Dabbagh and Abderrahman, 1997). The annual recharge of these is almost 900 mcm. So, the rate of consumption is higher than the rate of recharging. In the Khobar aquifer, the estimated groundwater reserve, recharge, and salt content are 45,000 mcm, 200 mcm, and 2600 - 6000 mg/l, respectively (Edgell, 1997).

CHAPTER TWO

Methodology

2.1. Seismic Laboratory Work

The samples were carefully taken from twelve outcrops (Figure 1.1) avoiding obviously weathered ones (Table 2.1). The core samples were saturated with water of different total dissolved solids (TDS) values according to the classification of C.W. Fetter (1988) (Table 2.2). Then, acoustic measurements were made using an ultrasonic tester (Model C368) (Tables 2.3, 2.4, 2.5, 2.6). Also, for some samples, porosity and permeability were measured in the Petroleum Engineering Department (PETE) Laboratory.

Table 2.1: Samples location for laboratory studies.

Location No.	Latitude	Longitude
Loc 1	26° 21.4219' N	50° 07.2098' E
Loc 2	26° 17.5615' N	50° 10.5330' E
Loc 3	26° 17.4286' N	50° 10.5900' E
Loc 4	26° 16.5761' N	50° 10.5518' E
Loc 5	26° 16.5159' N	50° 10.5725' E
Loc 6	26° 23.2052' N	50° 05.1469' E
Loc 7	26° 22.1202' N	50° 06.1139' E
Loc 8	26° 22.5256' N	50° 07.2064' E
Loc 9	26° 22.1202' N	50° 06.1139' E
Loc 10	26° 18.3827' N	50° 10.5518' E
Loc 11	26° 17.1227' N	50° 11.2678' E
Loc 12	26° 20.2495' N	50° 09.3534' E

Table 2.2: Classification of Water based on Total dissolved Solids (TDS) (Fetter, 1988).

	Water Type	TDS (mg/l)
1	Saline Water	10,000 – 100,000
2	Brackish Water	1000 – 10,000
3	Fresh Water	< 1000

Table 2.3: Velocity Measurements for the Saturated Core Samples Using Saline Water.

Sample Location	Sample Number	Velocity (m/sec)	Φ (%)	Rock Type *
2	1	5642.4	3.60	Limestone
2	2	2971.3	17.34	Limestone
2	3	3552.6	16.14	Limestone
3	2	3035.1	6.25	Limestone
4	2	3150.8	4.16	Limestone
5	1	4920.1	11.78	Dolomite
6	1	4510.8	12.95	Limestone
7	2	3711.5	6.06	Dolomite
8	1	4096.1	5.96	Limestone
9	1	4070.1	1.47	Limestone
11	1	5206.8	3.93	Dolomite
12	1	3325.1	17.34	Dolomite

* Based on XRD and Thin Sections

Table 2.4: Velocity Measurements for the Saturated Core Samples Using Brackish Water.

Sample Location	Sample Number	Velocity (m/sec)	Φ (%)	Rock Type *
1	2	2352.1	33.35	Dolomite
2	4	3101.8	3.24	Limestone
2	6	2343.1	10.75	Limestone
2	6	2976.4	10.75	Limestone
3	3	3017.4	8.41	Limestone
4	4	2438.1	2.05	Limestone
4	4	3746.3	2.05	Limestone
5	3	3378.7	10.05	Dolomite
5	3	2809.5	10.05	Dolomite
5	4	3430.1	7.25	Dolomite
6	3	2991.2	16.42	Limestone
6	4	3733.9	3.98	Dolomite
7	3	2572.8	27.18	Dolomite
7	4	2925.7	15.57	Dolomite
7	4	2825.4	15.57	Dolomite
8	2	2205.5	7.11	Limestone
8	2	2090.2	7.11	Limestone
9	2	3250.1	1.11	Limestone
10	2	2870.2	8.52	Limestone
11	2	2304.1	1.75	Dolomite
11	3	2920.1	2.11	Dolomite
12	3	3293.9	14.57	Dolomite
12	3	2272.2	14.57	Dolomite

* Based on XRD and Thin Sections

Table 2.5: Velocity Measurements for the Saturated Core Samples Using Fresh Water.

Sample Location	Sample Number	Velocity (m/sec)	Φ (%)	Rock Type *
1	4	2206.1	16.71	Dolomite
1	5	3016.7	23.64	Dolomite
2	5	4253.5	3.88	Limestone
2	7	3551.1	16.37	Limestone
4	5	4070.1	2.81	Dolomite
5	5	4909.7	11.58	Dolomite
6	5	2650.1	13.98	Limestone
7	5	3210.1	14.49	Dolomite
8	3	4230.1	2.79	Limestone
8	4	3811.9	1.83	Limestone
9	3	3758.7	1.86	Limestone
10	3	4516.4	6.47	Limestone
11	4	2070.1	2.19	Dolomite
11	5	4081.1	27.29	Dolomite
12	4	2088.1	17.08	Dolomite

* Based on XRD and Thin Sections

Table 2.6: Velocity Measurements for the Dry Core Samples

Sample Location	Sample Number	Velocity (m/sec)	Φ (%)	Rock Type *
2	6	1834.1	10.75	Limestone
2	5	2251.6	3.88	Limestone
2	5	2008.7	3.88	Limestone
4	5	2216.1	2.81	Dolomite
5	1	2170.3	11.78	Dolomite
5	3	2065.3	10.05	Dolomite
5	6	1921.5	25.35	Dolomite
6	5	1985.4	13.98	Limestone
6	5	2271.2	13.98	Limestone
6	6	1817.7	12.28	Dolomite
7	4	2330.1	15.57	Dolomite
7	4	2259.5	15.57	Dolomite
8	1	2420.1	5.96	Limestone
8	2	2354.6	7.11	Limestone
8	1	2520.5	5.96	Limestone
8	1	2176.1	5.96	Limestone
9	3	2750.7	1.86	Limestone
9	1	2641.2	1.47	Limestone
10	1	2711.5	3.19	Limestone
10	2	2049.6	8.52	Limestone
10	3	2062.3	6.47	Limestone
11	5	1804.8	27.29	Dolomite
11	4	1904.8	2.19	Dolomite
11	1	2411.5	3.93	Dolomite
11	3	2371.1	2.11	Dolomite
12	3	2466.2	14.57	Dolomite
12	1	2117.1	17.34	Dolomite

* Based on XRD and Thin Sections

2.2. The Seismic Refraction Method

Hydrogeological investigation is one of the most important present-day application of the refraction method. Also, refraction method is applied in civil engineering projects for bedrock investigation in connection with dam sites, hydroelectric power station and large-scale building constructions. Another important application is in the detection of fracture zones in hard rocks in connection with groundwater prospecting and nuclear waste disposal programs.

In refraction method, the purpose is to determine the depths and velocities of the subsurface layers, relying on the fact that earth materials are commonly subhorizontally layered and that seismic velocity normally increases with depth.

Using an energy source to produce seismic waves along a profile, the travel times of waves are measured by a seismograph. Successive impacts are summed to increase the signal-to-noise ratio (Figure 2.1 (a)).

The ES-1225 seismograph from EG & G Geometrics (Figure 2.1 (b)) was used to conduct the seismic fieldwork. It is a multichannel, CRT-display, printing, signal-enhancement, shallow-exploration seismograph. It is microprocessor-based, battery-operated, and has 12 channels. The instrument is a light and portable field unit, yet it displays many sophisticated features typically found on larger systems.

The ES-1225 provides hard copy through a built-in printer/plotter on the front panel; it prints the seismic traces for all twelve channels, plus completes information on acquisition conditions.

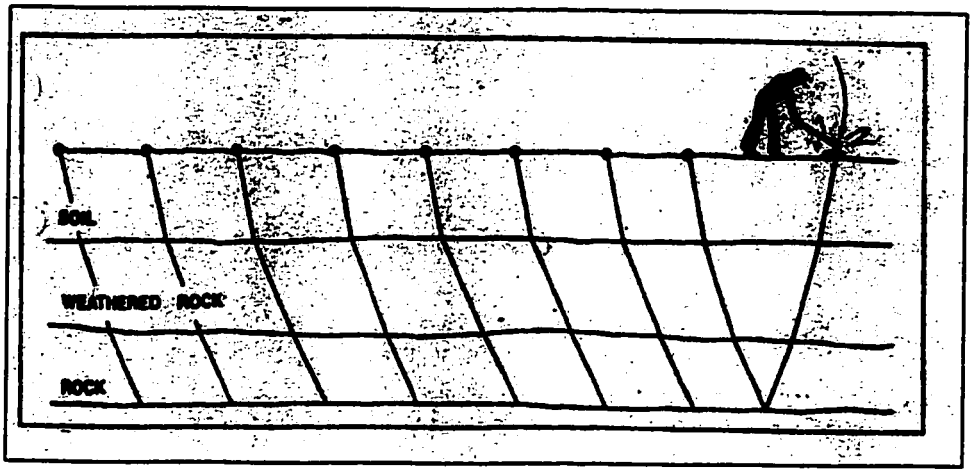

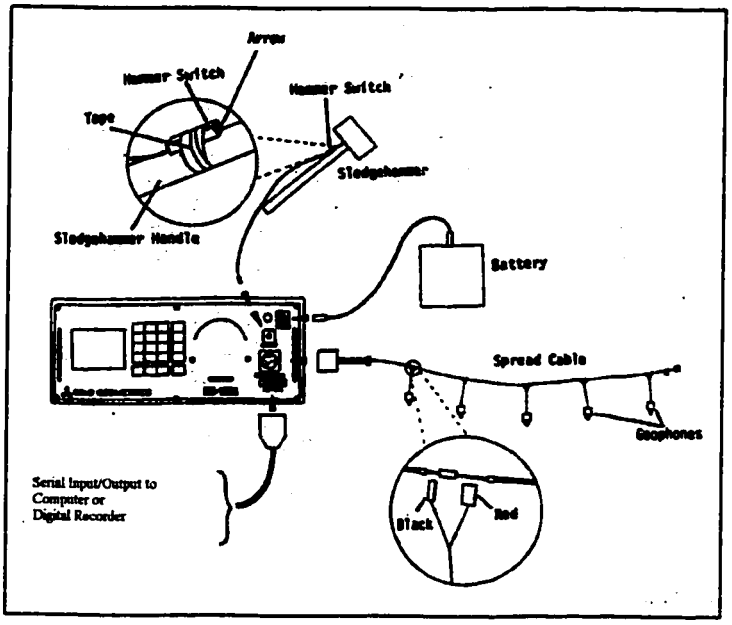

Figure 2.1: (a) Basic Seismograph Refraction Survey Configuration (ES-1225 Manual). (b) Assembly of ES-1225 System (ES-1225 Manual).

Using the ES-1225, refraction profiles were made, at six locations within the Dammam area, to determine the thickness and velocities of the subsurface layers (Table 2.7).

The Seismic Refraction Interpretation Programs (SIP) was used to determine the velocities and thickness of the layers below the surface. It is a computer program developed by the U.S. Bureau of Mines for constructing a two-dimensional, layered earth model as an aid in interpreting seismic refraction field measurements (Scott, 1973).
It consists of:

- SIPIK (for picking first breaks)
- SIPIN (to create input data files for interpretation)
- SIPEDT (to edit input data files for interpretation)
- SIPT2 (for interpreting seismic refraction data)

The following assumptions and conditions apply to the inversion algorithm used by SIPT2.

1. Seismic refracting layers are continuous and extend from one end of the refraction line to the other.
2. Velocity increases with depth.
3. Each refraction layer may be assigned different vertical and horizontal velocities, but these velocities are assumed to remain constant from one end of a spread to the other. In multi-spread data sets, every layer of every spread may be assigned different values of vertical and horizontal velocities. SIPT2 can handle up to 5 spreads in a line for each data set represented by an input data file.

Table 2.7: Seismic Profile Locations (Refraction Method).

Refraction Location No.	Location	Spread Direction
SP 1000	26° 22.86' N 50° 02.66' E	W(S)*----------E
SP 2000	26° 23.34' N 50° 10.76' E	W(S)----------E
SP 3000	26° 24.60' N 50° 05.91' E	E(S)*----------W
SP 4000	26° 14.65' N 50° 03.60' E	S(S)*----------N
SP 5000	26° 22.66' N 50° 10.79' E	W(S)----------E
SP 6000	26° 23.75' N 50° 07.56' E	E(S)----------W

* W(S): Shot point is on the West side of the profile.

* E(S): Shot point is on the East side of the profile.

* S(S): Shot point is on the South side of the profile.

4. The input data file must include the X and Y coordinates, and elevation of each shot-point and geophone in each spread.

5. The input data file must include first-arrival times picked at each geophone for every shot-point, with a layer number assigned to each arrival time. If an arrival time can not be picked with reasonable accuracy, it can be assigned a value of zero to prevent it from being used to formulate the depth model. Layer number 1 is used to specify direct arrivals through the surface layer. Layer numbers 2 through 5 are used to indicate the refracting layers that carry the horizontal component of the refraction ray path. Layer assignments are most easily made or changed on the Time-Distance plot screens of programs SIPIN and SIPEDT.

6. Ranges and limits of input data:

Number of layers in a data set	2-5
Number of spreads in a data set	1-5
Number of shot-points in a spread	1-7
Number of geophones in a spread	6-50

2.3. Resistivity Laboratory Measurements

The electrical resistivity of a substance is its ability to impede the flow of electrical current through that substance. The unit of electrical resistivity is ohm-m. Electrical conductivity is the reciprocal of resistivity, expressed in mhos per meter. Electrical resistivity (ρ_c) of a material is related to its resistance according to the following equation:

$$\rho_c = r_c \bullet (A / L) \qquad \text{(Eq. 2.1)}$$

A = Cross-sectional area of the core through which current flows (in m^2).

L = Length of core in meter.

r_c = Resistance of core in ohm.

ρ_c = Resistivity of core in Ω-m.

It has been established experimentally that the resistivity of a clean formation (i.e. containing no significant amount of clay) is proportional to the resistivity of the brine with which it is fully saturated according to Archie's First Law (Gueguen and Palciauskas, 1994). The constant of proportionality is called formation resistivity factor, F. Thus, the formation resistivity factor (F) is given as:

$$F = \rho_c / \rho_w \qquad \text{(Eq. 2.2)}$$

Where

ρ_c = Resistivity of saturated core

ρ_w = Resistivity of the saturating liquid

Also, F is related to porosity (Φ) by the formula:

$$F = a\,\Phi^{-m} \quad \text{(Archie's law)}, \qquad \text{(Eq. 2.3)}$$

where m is the cementation factor. The constant a is determined empirically. For carbonate rocks, a = 1.

To determine the resistivities of the brine-saturated cores, the resistivity equipment in the laboratory of Research Institute was used (Figure 2.2)

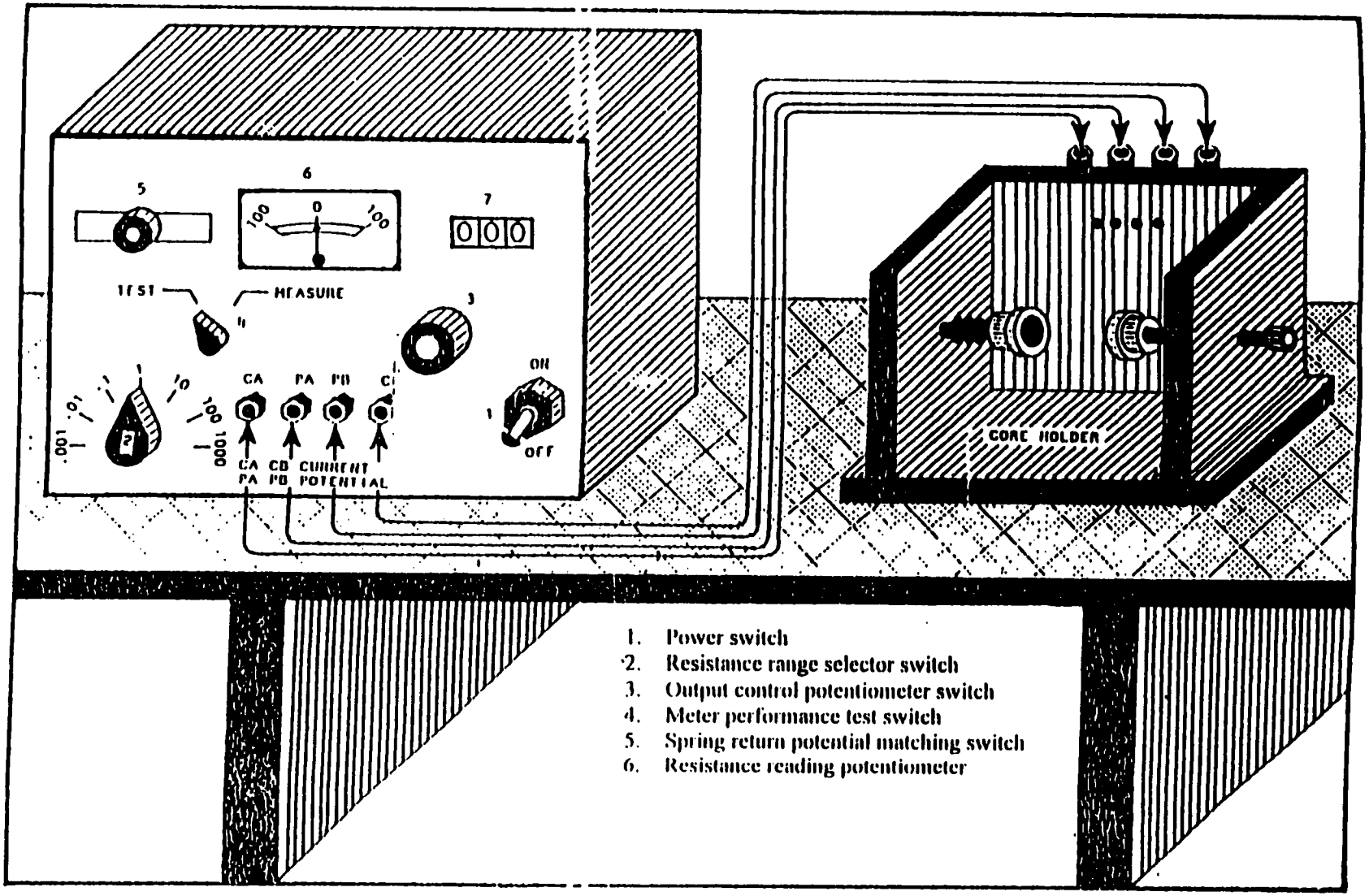

Figure 2.2: Resistivity Test Unit (Lab Experiment Manual, PETE Dept.)- KFUPM

The laboratory steps were conducted in sequence as follows:

1. Two chamois skin discs were soaked in the same brine solution in which the core samples were saturated.
2. The chamois discs were removed thereafter from the brine and then squeezed to spell out the excess water.
3. The squeezed chamois discs were placed over the brass plate electrode of the core holder.
4. The saturated core was removed from the brine solution and wiped off all excess brine solution from the surface.
5. The core was placed between the two electrodes of the core holder
6. The threaded adjustment arm on the core holder was screwed sufficiently to compress the opposite arm spring to firmly hold the core in place.
7. The core holder electrical leads were connected to the resistivity measuring unit

Following these steps, core resistivities (ρ_c), formation resistivity factors (F), and porosity (Φ) were determined using Equations 2.1, 2.2, and 2.3, respectively.
The obtained results are listed in Table 2.8 for saline-saturated core samples, in Table 2.9 for brackish-saturated core samples, and in Table 2.10 for fresh-saturated core samples.

Table 2.8: Resistivity of the Core Samples Using Saline Water.

Sample Location	Sample Number	Measured ρ_e (Ohm-m)	Calculated F	Calculated Φ (%)	Rock Type *
1	1	1.76	8.63	34.03	Dolomite
2	1	156.56	767.48	3.60	Limestone
2	2	6.78	33.25	17.34	Limestone
2	3	7.82	38.37	16.14	Limestone
3	2	52.1	255.8	6.25	Limestone
4	2	117.42	575.61	4.16	Dolomite
4	7	147.62	723.63	3.71	Dolomite
5	1	14.67	71.95	11.78	Dolomite
5	2	2.55	12.52	28.25	Dolomite
6	1	12.14	59.54	12.95	Dolomite
7	2	55.5	272.1	6.06	Dolomite
8	1	57.30	280.90	5.96	Limestone
9	1	939.40	4604.92	1.47	Limestone
10	1	199.62	978.54	3.19	Limestone
11	1	131.51	644.68	3.93	Dolomite
12	1	6.78	33.25	17.34	Dolomite
12	2	7.306	35.81	16.70	Dolomite

* Based on XRD and Thin Sections

Table 2.9: Resistivity of the Core Samples Using Brackish Water.

Sample Location	Sample Number	Measured ρ_c (Ohm-m)	Calculated F	Calculated Φ (%)	Rock Type *
1	2	8.54	8.98	33.35	Dolomite
2	4	903.27	950.81	3.24	Limestone
2	6	82.19	86.52	10.75	Limestone
3	3	134.20	141.26	8.41	Limestone
4	4	2254.56	2373.23	2.05	Limestone
5	3	93.94	98.88	10.05	Dolomite
5	4	180.65	190.16	7.25	Dolomite
6	3	35.22	37.08	16.42	Limestone
6	4	599.61	631.178	3.98	Dolomite
7	3	12.85	13.52	27.18	Dolomite
7	4	39.14	41.20	15.57	Dolomite
8	2	187.88	197.76	7.11	Limestone
9	2	7686.03	8090.56	1.11	Limestone
10	2	130.84	137.73	8.52	Limestone
11	2	3101.80	3265.05	1.75	Dolomite
11	3	2126.95	2238.89	2.11	Dolomite
12	3	44.73	47.08	14.57	Dolomite

* Based on XRD and Thin Sections

Table 2.10: Resistivity of the Core Samples using Fresh Water.

Sample Location	Sample Number	Measured ρ_c (Ohm-m)	Calculated F	Calculated Φ (%)	Rock Type *
1	4	112.72	35.78	16.71	Dolomite
1	5	56.36	17.89	23.64	Dolomite
2	5	2087.56	662.71	3.88	Limestone
2	7	117.42	37.27	16.37	Limestone
4	5	3973.42	1261.40	2.81	Dolomite
5	5	234.85	74.55	11.58	Dolomite
5	6	48.98	15.55	25.35	Dolomite
6	5	161.04	51.12	13.98	Limestone
6	6	208.75	66.27	12.28	Dolomite
7	5	149.90	47.58	14.49	Dolomite
8	3	4039.43	1282.36	2.79	Limestone
8	4	9384.64	2979.25	1.83	Limestone
9	3	9032.72	2867.53	1.86	Limestone
10	3	751.52	238.57	6.47	Limestone
11	4	6535.85	2074.87	2.19	Dolomite
11	5	42.27	13.42	27.29	Dolomite
12	4	107.90	34.25	17.08	Dolomite

* Based on XRD and Thin Sections

2.4. Resistivity Field Work

During the fieldwork, five (5) different sites (Figure 1.1) have been selected in the Dammam area to conduct Schlumberger Vertical Electrical Sounding (VES; Table 2.11).

The objective of the survey was to estimate the quality of the ground water in the Khobar Aquifer.

The flow of direct current through a conductor is described by Ohm's Law, which is expressed as: R=V/I, where R is resistance in ohms, V is potential difference in volts, and I is current in amperes.

In principle, the resistivity of an electrically homogeneous, uniform half space could be measured by passing current through two electrodes at known distance apart and measuring the potential difference between two potential electrodes. The resistivity of the porous medium is largely a function of water content as the mineral grains are generally non-conductive. The conductivity of the water is one of the principal parameters in determining the bulk electrical properties of the medium. The aim of a VES measurement is to obtain the vertical variation in resistivity of the subsurface layers.

In Schlumberger array the current electrodes are spaced much further apart than the potential electrodes along a straight line, as shown in Figure 2.3 (a). The distance between any two electrical electrodes is called AB (2s), and the distance between any two potential electrodes is called MN (a). A current (I) is passed between the outer electrodes A and B and the consequent potential drop (ΔV) is measured between the inner electrodes M and N. Apparent resistivity (ρ_a) is obtained by using the relationship: $\rho_a = \pi/a \cdot (s^2 - a^2/4) \cdot (\Delta V/I)$. The Syscal-R2 (resistivity meter), shown in Figure 2.3 (b), was used in the Vertical Electric Soundings (VES) survey. The Syscal-R2 is an electric resistivity meter

Table 2.11: Vertical Electrical Sounding (VES) Locations.

VES Location No.	Location *	Spread Direction
VES-1	26° 09.31' N 50° 06.90' E	NE-SW
VES-2	26° 11.51' N 50° 07.30' E	NE-SW
VES-3	26° 10.24' N 50° 04.18' E	NE-SW
VES-4	26° 15.29' N 50° 02.57' E	NW-SE
VES-5	26° 30.16' N 50° 01.54' E	NE-SW

* (See Figure 1.1)

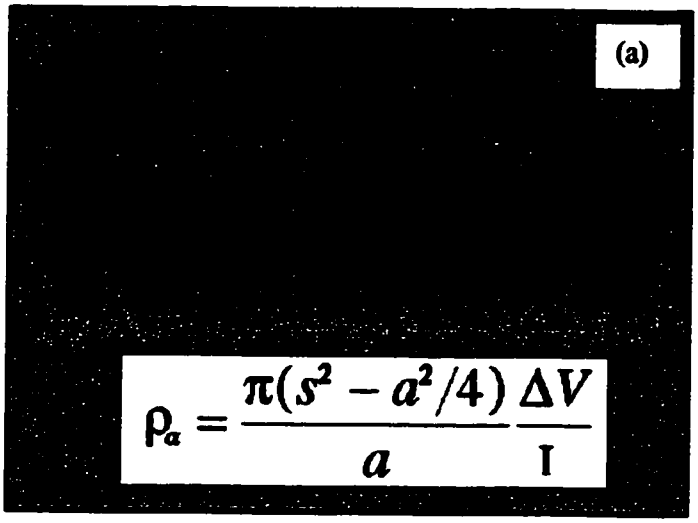

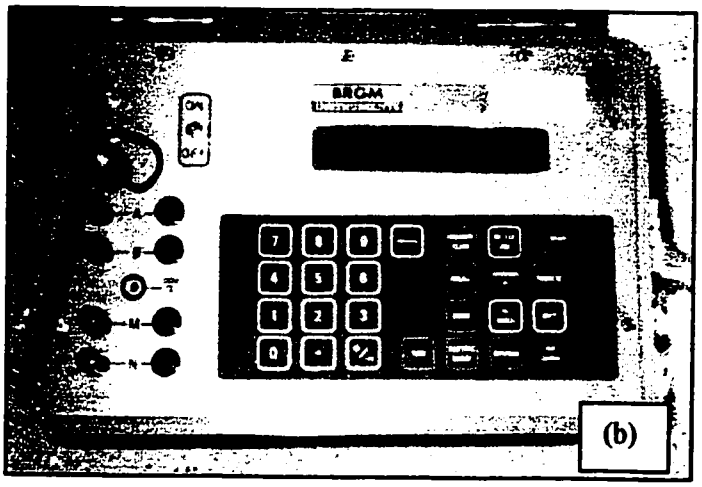

Figure 2.3: (a) The Schlumberger Array (www.mines.edu). (b) The Syscal-R2 System.

with transmission and reception capabilities. It is used as a source of current and a highly sensitive voltmeter. The maximum current supplied to ground is 1.5 ampere DC and the maximum voltage 2.4-volt.

A 2-feet electrode of stainless steel was driven into the soil at each end of the spread. Both electrodes A and B, were connected by two 16-gauge cables to the current sender, which is located at the center. The potential electrodes M and N were connected to the voltage receiver by two coaxial cables whose shielding were grounded at the center.

It is conventional to plot resistivity values on a log-log graph, with horizontal scale being current electrode spacing AB/2 and vertical scale being apparent resistivity to give the sounding curve. The field resistivity data is interpreted using the computer software 'Resix-IP' program. It consists of a forward and an inverse modeling program for interpreting vertical electrical soundings. The forward modeling allows the creation of synthetic resistivity sounding curves for a number of layers on the assumption that each layer is laterally homogenous. Inverse modeling is an interactive iterative process to obtain the best least squares fit to the field data. The results from the inverse modeling are directed to a printer to get a hard copy of the model (Appendix A).

2.5. Rock Identification

A total of eleven (11) thin sections and XRD analysis for nine (9) samples were used to identify and classify rock.

2.5.1. Thin Section Studies

Thin sections were made in RI (The Center for Petroleum and Minerals), KFUPM, using red epoxy to evaluate porosity. Petrographic microscopy was used to describe texture, mineralogy and porosity of tested samples. Petrographic description of eleven thin sections and their photomicrographs are presented in Appendix C.

2.5.2. X-Ray Diffractometry (XRD)

X-ray diffraction works on the principle that, when a sample is irradiated, the X-rays are diffracted in a pattern that is characteristic of the compounds present in the sample under analysis. By measuring the angles at which diffraction peaks occur and their intensities, the mineralogical constituents can be identified.

A total of nine (9) field samples from the Khobar Member were sent for X-Ray analysis. The objective was to identify the chemical/mineralogical constituents of the samples and their relative amounts.

The submitted samples were in a dry powder form and did not require further grinding. The diffraction pattern was generated by a theta-2theta scanning diffractometer. The operating conditions of XRD analysis were Cu board focus tube at 40 kV and 30 mA, divergence slit 1 degree, scatter slit 1 degree, receiving slit 0.2 mm. A nickel filter was used, scanning speed and interval of data collection was 0.001 degree two theta/sec. and angle scanned: 4 to 80 degrees two theta (i.e. 2θ).

2.6. Porosity and Permeability Measurements

2.6.1. Porosity

Porosity is a physical property of the rock describing the ratio of the pores volume within the rock to the total volume of the rock.

$\Phi = V_p / V_b$ (Eq. 2.4)

where

Φ = porosity, fraction

V_p = pore volume

V_b = bulk volume

For regular core sample,

$V_b = \pi \cdot r^2 \cdot L$ (Eq. 2.5)

where,

r = radius of core sample

L = length of core sample

V_p = Weight of Saturating Liquid / Density of Saturating Liquid

The gravimetrical saturation method was used to determine the porosity. The bulk volume of the regular-shaped core sample is calculated by physical calipering of its diameter and length. The pore volume is determined by saturating a cleaned and dried sample with a liquid of known density. The pore volume is calculated from the gain in weight of the saturated sample over that of the dry sample.

The tested rock sample was leached with some solvent, such as carbon tetrachloride or trichloroethane, and then dried in vacuum oven at 100° C overnight. Thereafter, the following steps were followed:

1. The bulk volume was calculated from the geometry of the cylindrical core.
2. The dry, clean core sample's weight was determined.
3. The sample was placed in the saturation apparatus as shown in Figure 2.4 and evacuated for at least half an hour.
4. After evacuation, the liquid valve was opened and the sample was saturated with the saturating liquid for at least half an hour.
5. After saturation, the sample was removed with forcept, weighed as rapidly as possible.
6. The weight of the saturating liquid was calculated by subtracting the dry weight from saturated weight of the core.

Using Equation 2.4, the porosity values were calculated and listed in Table 2.12.

2.6.2. Permeability

The permeability of a porous medium is a measure of its ability to transmit fluids. The liquid permeability of a core sample was determined by measuring the time necessary for a certain amount of liquid at a given temperature to pass through the core under a given pressure gradient.

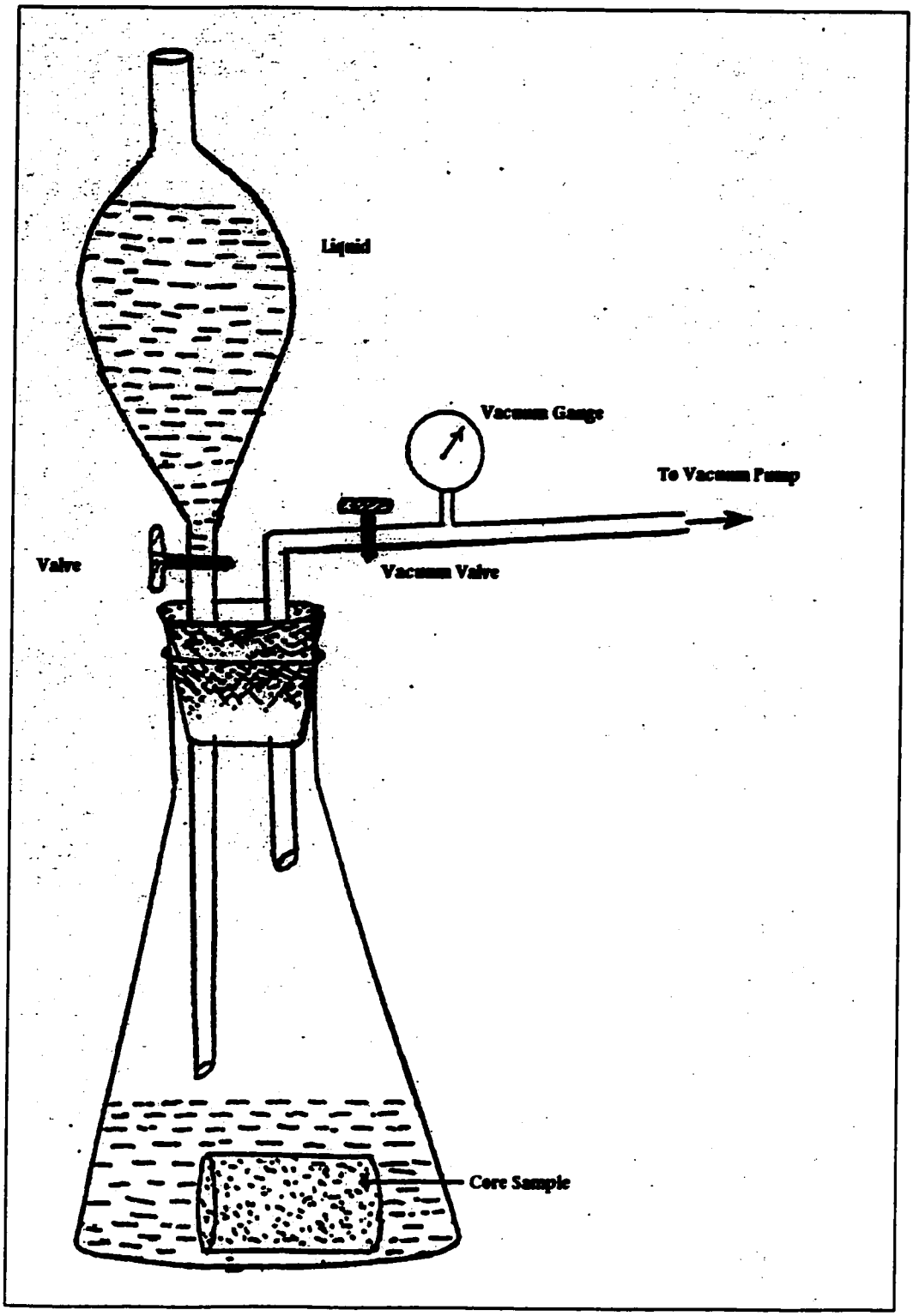

Figure 2.4: Liquid Saturation Apparatus (Schematic Diagram)-(Porosity Experiment Laboratory Manual, PETE Dept., KFUPM)

Table 2.12: Porosity and Permeability Results

Sample Location	Sample Number	Porosity %	Permeability (md)	Lithology
1	6	32.25	387.11	Dolomite
1	7	32.35	398.66	Dolomite
1	8	41.50	148.37	Dolomite
1	8	41.89	148.37	Dolomite
2	8	3.35	1.74	Limestone
2	8	3.25	1.74	Limestone
2	9	17.80	0.73	Limestone
2	10	16.71	5.48	Limestone
2	10	16.72	4.05	Limestone
2	9	18.21	0.73	Limestone
3	6	30.02	11.05	Limestone
3	6	29.50	11.05	Limestone
5	7	12.56	3.37	Dolomite
5	8	11.13	2.13	Dolomite
5	9	9.51	1.32	Dolomite
5	7	12.87	3.37	Dolomite
6	7	15.79	5.03	Limestone
6	7	16.00	5.03	Limestone
6	8	7.78	3.42	Limestone
6	9	11.20	2.81	Limestone
7	6	12.75	66.72	Dolomite
7	7	17.35	269.37	Dolomite
7	8	20.13	33.28	Dolomite
7	8	20.38	33.28	Dolomite
7	9	5.27	2.01	Dolomite
7	10	24.31	1.92	Dolomite
7	11	10.02	1.23	Limestone
7	10	24.92	1.92	Limestone
9	4	1.03	3.65	Limestone
9	4	1.06	3.65	Limestone
12	5	17.19	4.30	Dolomite
12	6	16.67	3.75	Dolomite
12	5	17.01	4.30	Dolomite

* Samples (4) and (11) have not been tested in the PETE lab. However, their properties were evaluated in thin-sections and in laboratory electrical measurements.

A liquid permeameter was used to determine the permeability of consolidated cores. Core samples were cut to size, extracted, dried, evacuated and saturated with test fluid as explained in section 2.6.1.

The core permeability is given by the following formula:

$$K = \mu V L / (A P t) \qquad \text{(Eq. 2.6)}$$

where,

K = Permeability of the sample in darcy

μ = Viscosity in centipoise of the liquid which has been used at the observed temperature

V = Volume in cubic centimeters of liquid flown through the sample during time interval.

t = Time in seconds for the fixed volume (50, 10 or 5 c c.) of liquid to flow through the sample under a given pressure gradient.

P = Pressure gradient in atmosphere, read on the pressure gauge.

L = Length of sample in centimeters.

A = Cross-sectional area of the sample in square centimeters.

Permeability values were calculated using Equation 2.6 and listed in Table 2.13.

Table 2.13: Comparison between Measured and Calculated Porosity Results

Sample Location	Sample Number	Measured Porosity %	Sample Number	Calculated Porosity %
1	6	32.25	1	34.03
1	7	32.35	2	33.35
1	8	41.89	4	16.71
2	8	3.35	1	3.60
2	8	3.25	4	3.24
2	-	-	5	3.88
2	0	17.80	2	17.34
2	10	16.71	3	16.14
2	10	16.72	7	16.37
2	9	18.21	-	-
3	6	29.50	2	6.25
3	-	-	3	8.41
5	7	12.56	1	11.78
5	8	11.13	3	10.05
5	9	9.51	5	11.58
5	7	12.87	-	-
6	7	15.79	1	12.95
6	7	16.00	3	16.42
6	8	7.78	5	13.98
6	9	11.20	-	-
7	7	17.35	3	27.18
7	8	20.13	-	-
7	8	20.38	-	-
7	9	5.27	2	6.06
7	10	24.31	4	15.57
7	11	10.02	5	14.49
7	10	24.92	-	-
9	4	1.03	1	1.47
9	4	1.06	2	1.11
9	-	-	3	1.86
12	5	17.19	1	17.34
12	6	16.67	2	16.7
12	5	17.01	3	14.57
12	-	-	4	17.08

* Samples (4) and (11) have not been tested in the PETE lab. However, their properties were evaluated in thin-sections and in laboratory electrical measurements.

CHAPTER THREE

RESULTS AND INTERPRETATIONS

3.1 X-Ray Diffractometry (XRD) and Thin Sections

With the XRD analysis, the phase identification process involved calculating the 'Most Likely Match Score' for a given phase based on peak intensity and peak position when compared to a data-base of standard phases.

The thin sections and XRD analyses were used together in this study for identification of rock types as well as the relationship between lithology and aquifer characteristics (e.g. porosity, permeability, velocity, and resistivity measurements). The details of the XRD analysis are included in Appendix B. Table 3.1 represents a summary of the XRD results.

The outcomes of the thin sections study are outlined in Table 3.2. Descriptions and photos for the thin sections are also attached in Appendix C.

Table 3.1: Lithology Description from XRD Analysis

Sample Location	Lithology
1	Dolomite
2	Limestone
3	Limestone
4	Dolomite
5	Dolomite
9	Limestone
11	Dolomite
12	Dolomite

Table 3.2: Lithology Description from Thin Sections

Sample Location	Name / Type	Lithology	Porosity %
3	Wackestone	Limestone	< 2
3	Wackestone	Limestone	< 1
4	Crystalline	Dolomite	2-3
4	Grainstone	Limestone	2-3
4	Packstone	Limestone	5
5	Crystalline	Dolomite	20
5	Crystalline	Dolomite	25
5	Crystalline	Dolomite	20
7	Crystalline	Dolomite	25
7	Crystalline	Dolomite	< 10
12	Crystalline	Dolomite	20-25

3.2 Porosity and Permeability

In Figure 3.1, permeability (K) values were plotted versus porosity (Φ) for Al-Khobar Member. It is evident that as porosity increases, permeability increases.

For higher values of K and Φ, the K- Φ data obey a power-law form. From Figure 3.1, it has been found that permeability is related to porosity according to the relation:

$$K = 0.98 \cdot \Phi^{0.7} \qquad \text{(Eq. 3.1)}$$

After plotting the data of Table 2.13, a correlation has been found between the two porosity values, measured in percentages: the one which is derived from resistivity, and the other which represents the measured value (Figure 3.2); i.e.

$$\Phi_R = 0.96\,\Phi_M + 0.5 \qquad \text{(Eq. 3.2)}$$

Figure 3.3 shows how lithology affects porosity values. It is evident that dolomite samples have higher porosity than limestone samples.

3.3 Velocity Measurement for Saturated Core Samples

From Figures 3.4, 3.5, 3.6, and 3.7, it can be concluded that as the porosity of the sample increases, the velocity decreases. This is in conformity with the following Time-Average Equation which was developed by Wyllie et al (1958): $1/V = \Phi/V_f + (1-\Phi)/V_m$, where V_f is the fluid velocity and V_m is the rock matrix velocity.

Moreover, the dry samples have lower velocity values as compared with the saturated ones and there is also an increase in the velocity values with increasing TDS values.

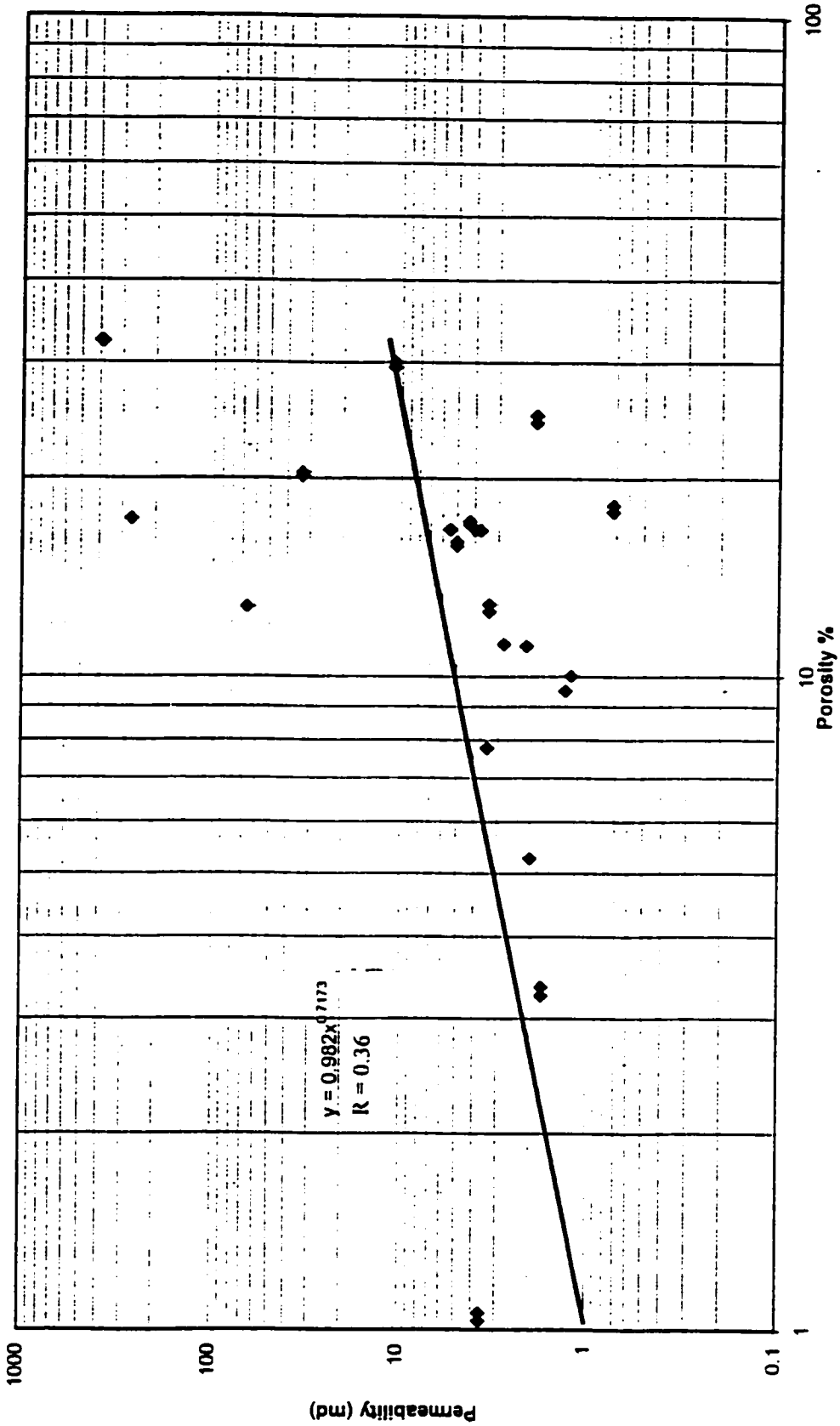

Figure 3.1: Permeability vs. Porosity

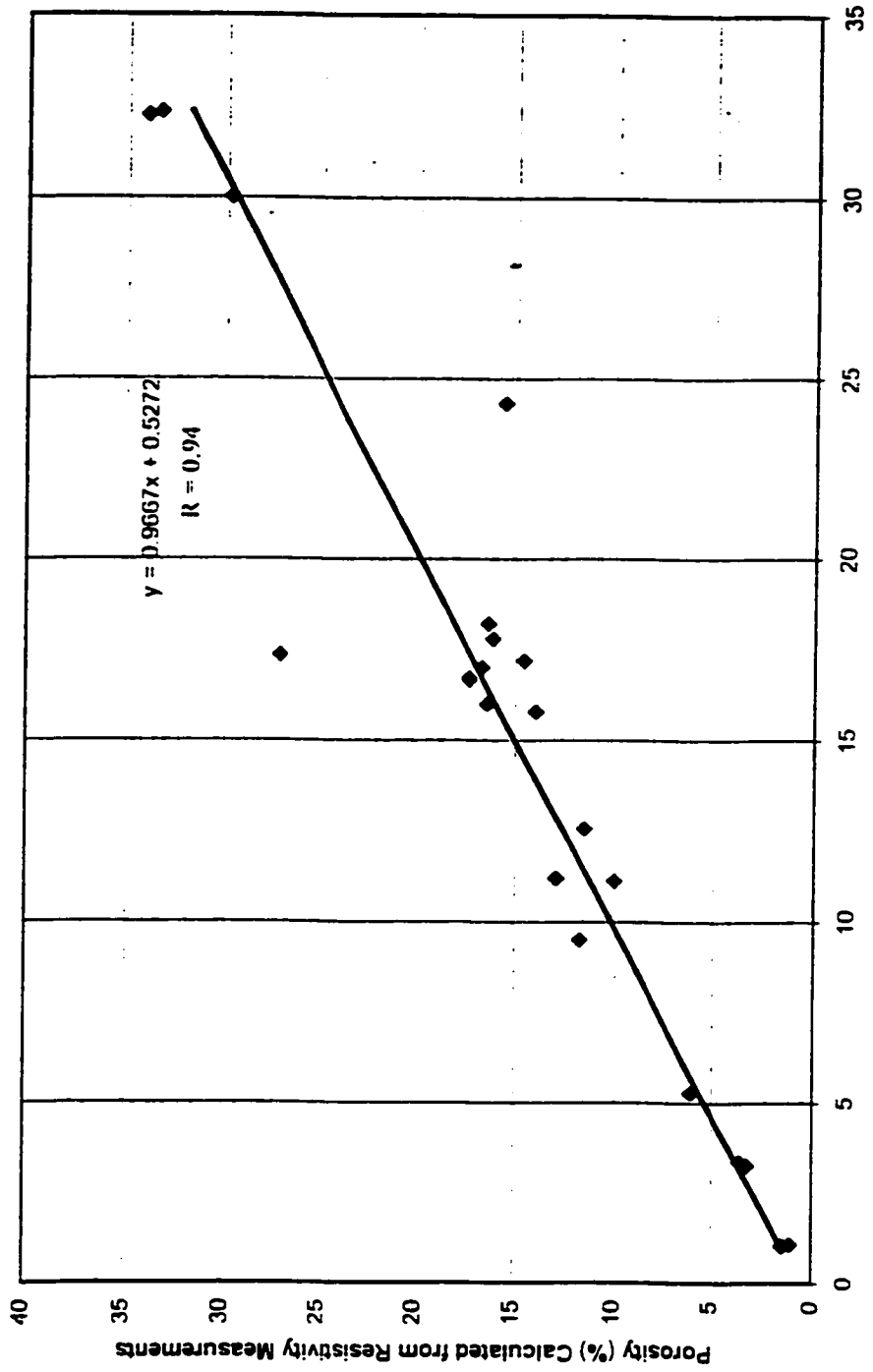

Figure 3.2: Measured Porosity -Porosity Electric Cross-plot

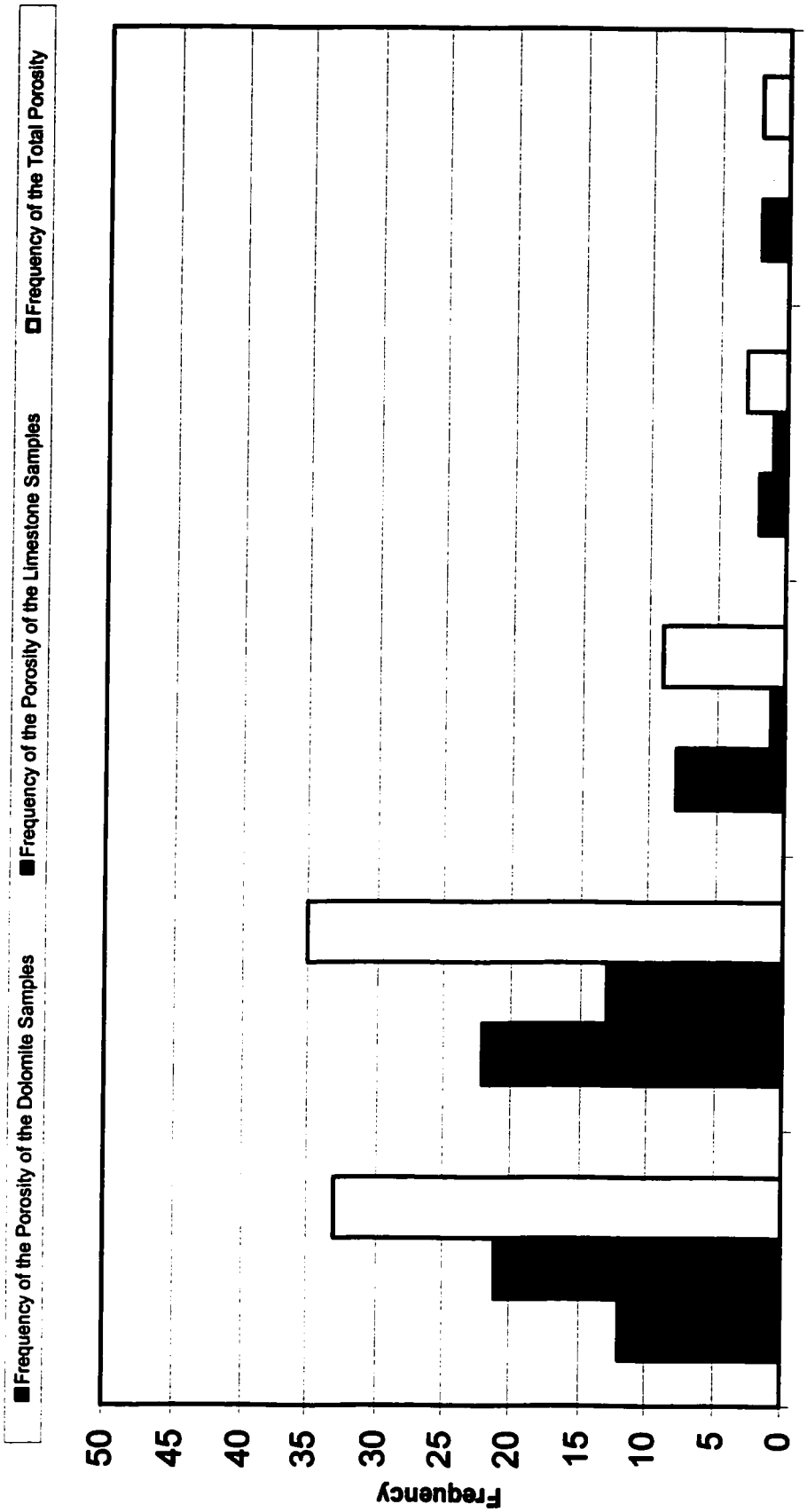

Figure 3.3: Distribution of Porosity

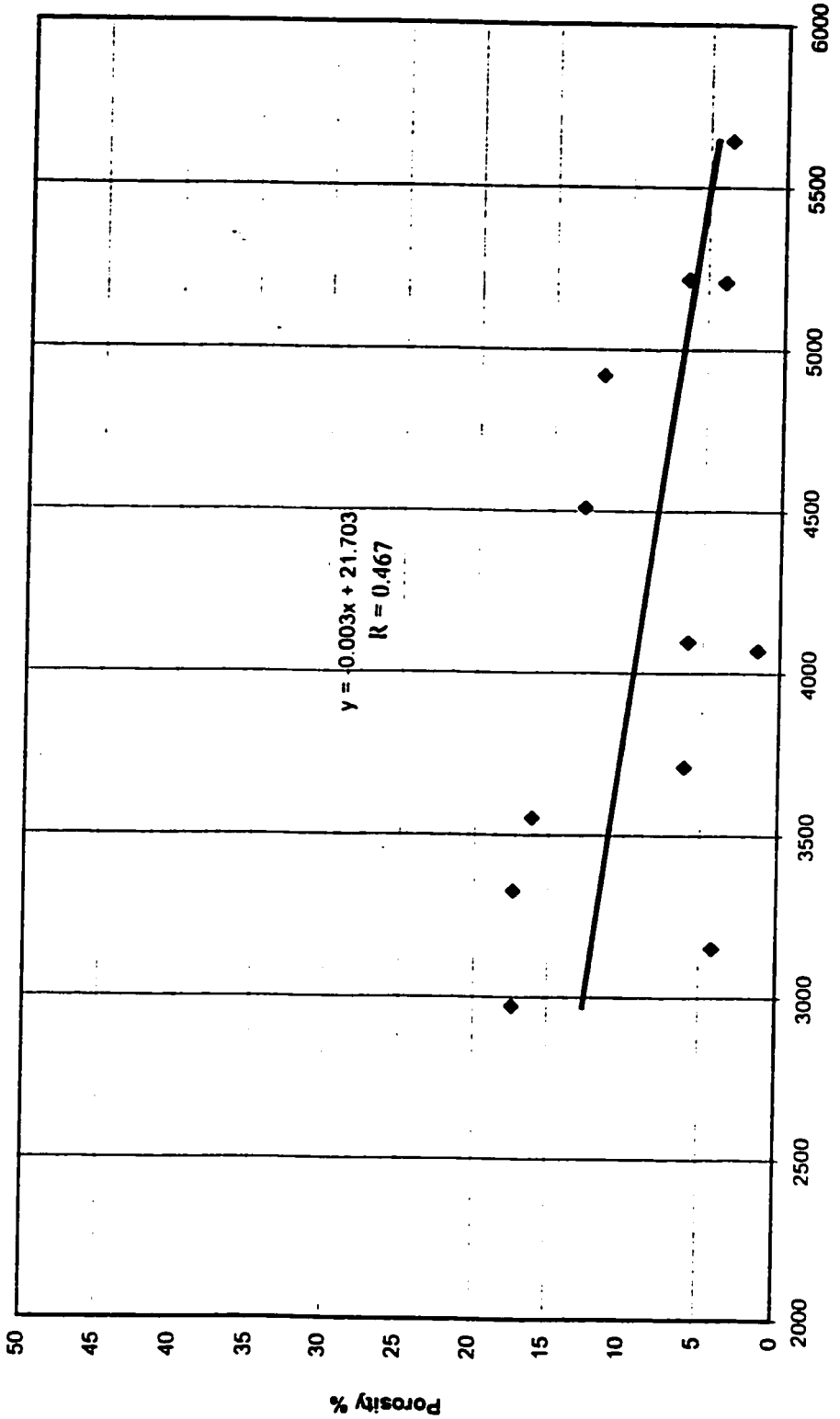

Figure 3.4: Saline Data Velocity

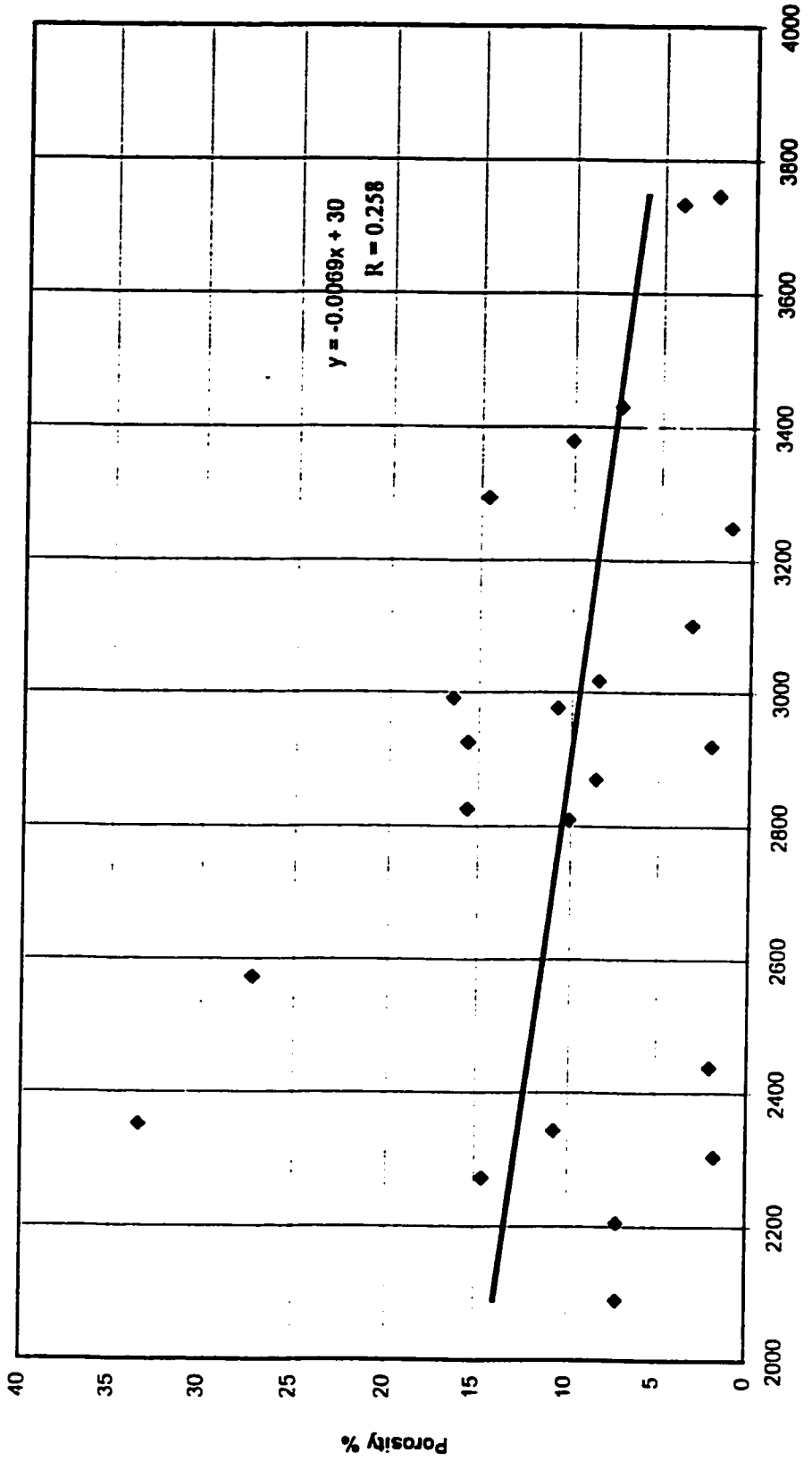

Figure 3.5: Bracklish Data Velocity

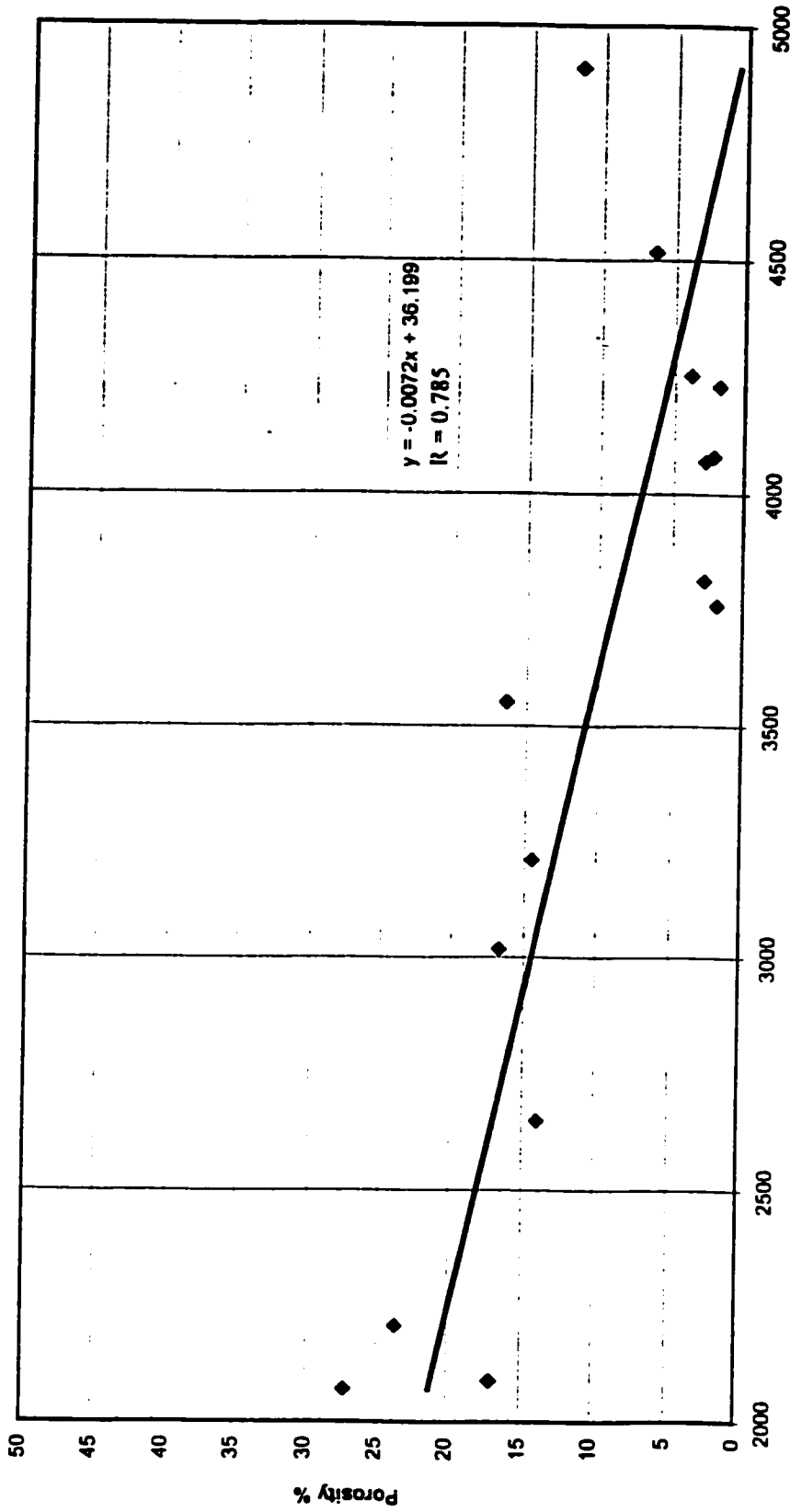

Figure 3.6: Fresh Data Velocity

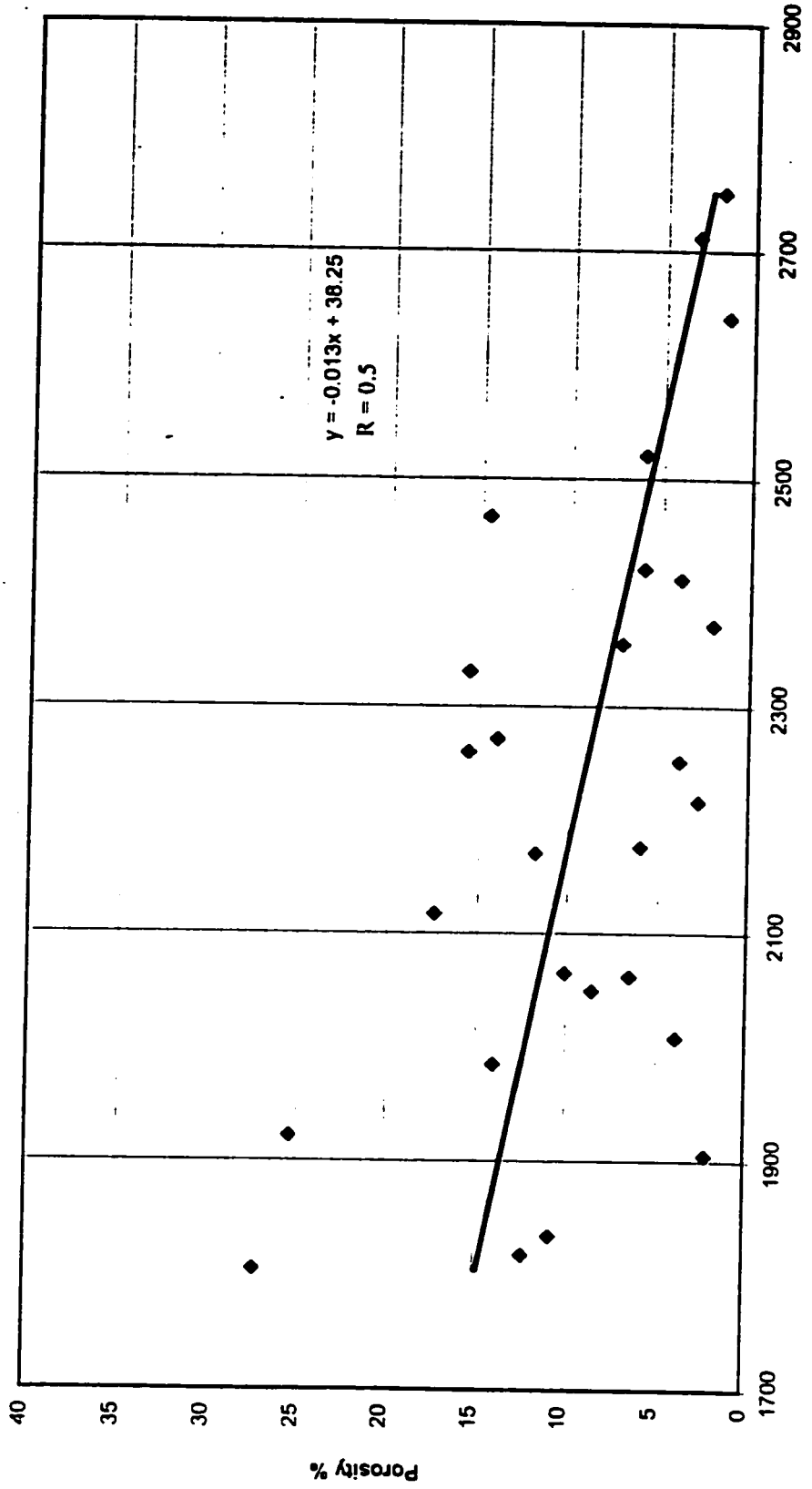

Figure 3.7: Dry Data Velocity

Figure 3.8 shows that the Khobar aquifer velocity lies between 2000 m/s (for a dry dolomite sample with high porosity) to 6000 m/s (for a limestone sample with low porosity).

3.4 Graphical Presentation of Resistivity Data

A histogram of core resistivity for fluid saturated samples as tabulated in Tables 2.8, 2.9, and 2.10 is shown in Figure 3.9 which displays that dolomite samples have lower resistivities than limestone samples. Figure 3.10 shows the formation resistivity factor (F) versus resistivity according to the first Archie's law: $\rho_{rock} = \rho_{fluid} \cdot F$. Figure 3.11 shows the calculated porosity versus Formation factor following the second Archie's law: $F = 1/\Phi^2$. Figure 3.12 represents the relation between resistivity and porosity for different TDS values.

3.5 Refraction Data Interpretation

All the seismic refraction profiles (SP1000, SP 2000, SP 3000, SP 4000, SP 5000, and SP 6000) were close to the outcrop of the Dammam Formation around the Dammam Dome (Figure 1.1).

Seismic interpretation (Appendix D) indicated that the acoustic velocity for the Khobar aquifer ranges between 1800 m/sec (Profile SP 3000) to 3970 m/sec (Profile SP 4000).

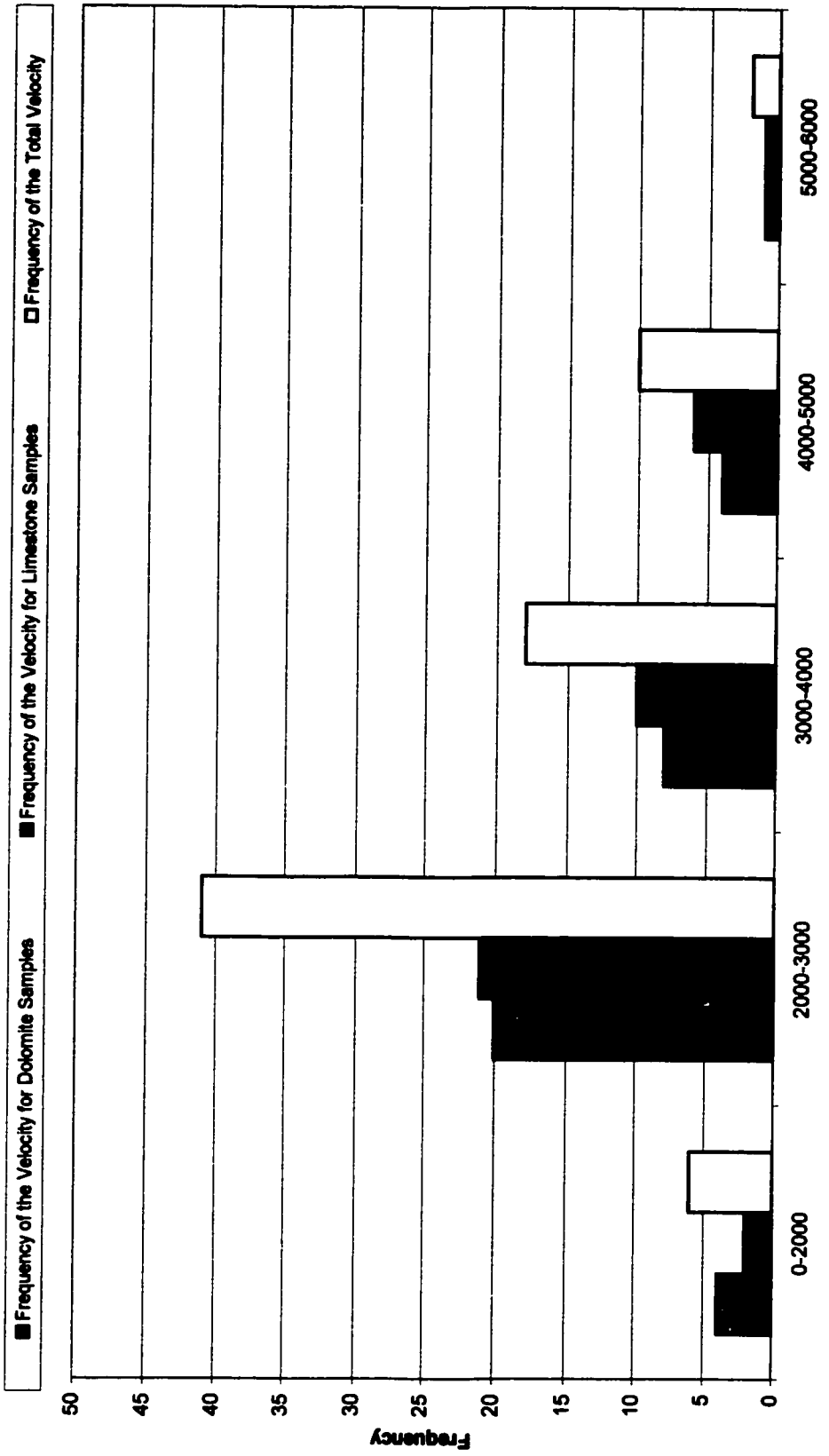

Figure 3.8: The lithology Effect on Velocity.

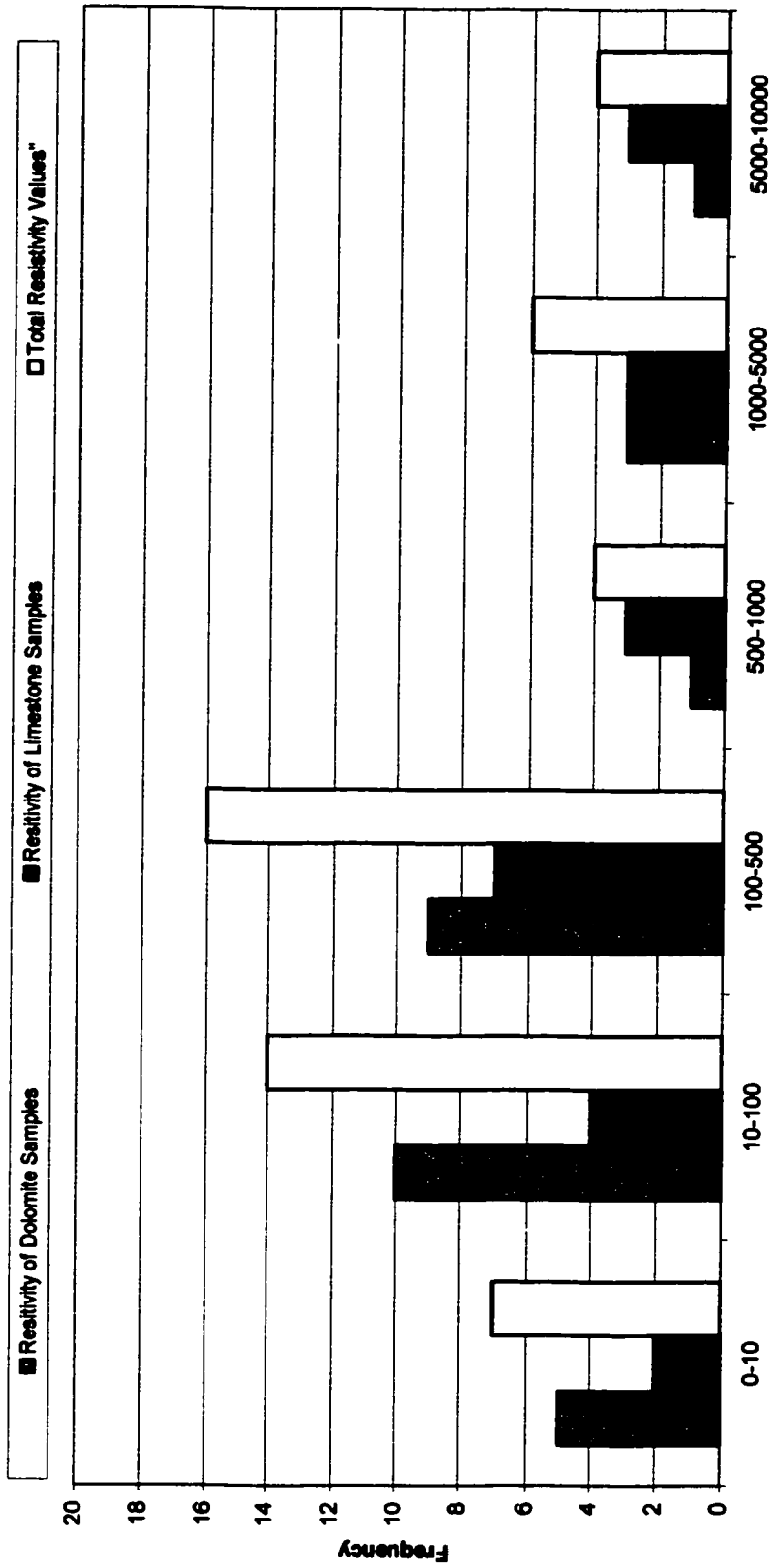

Figure 3.9: Resitivity Distribution for the three different TDS values.

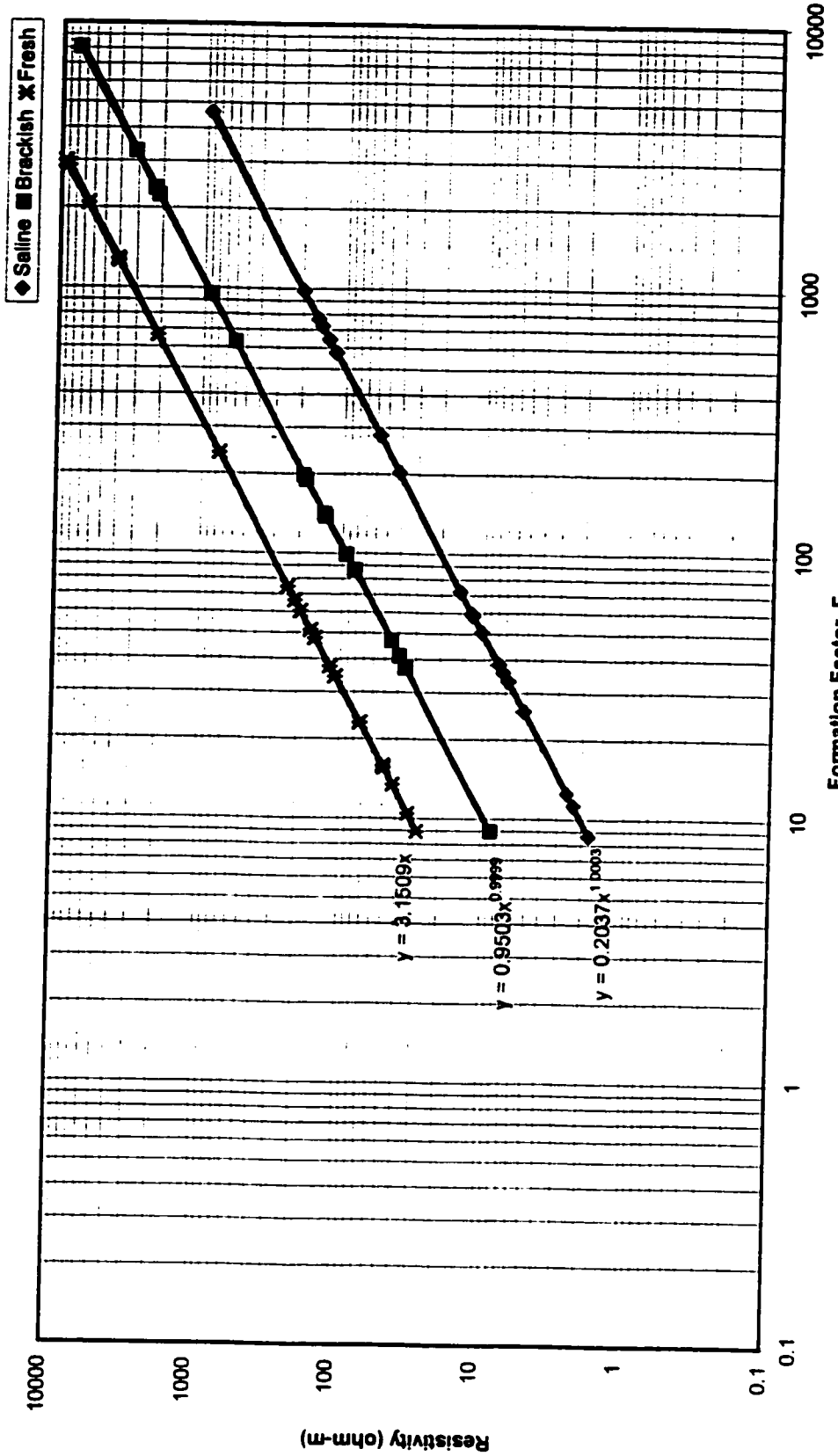

Figure 3.10: Core Resistivity Versus Formation Factor (for different TDS values)

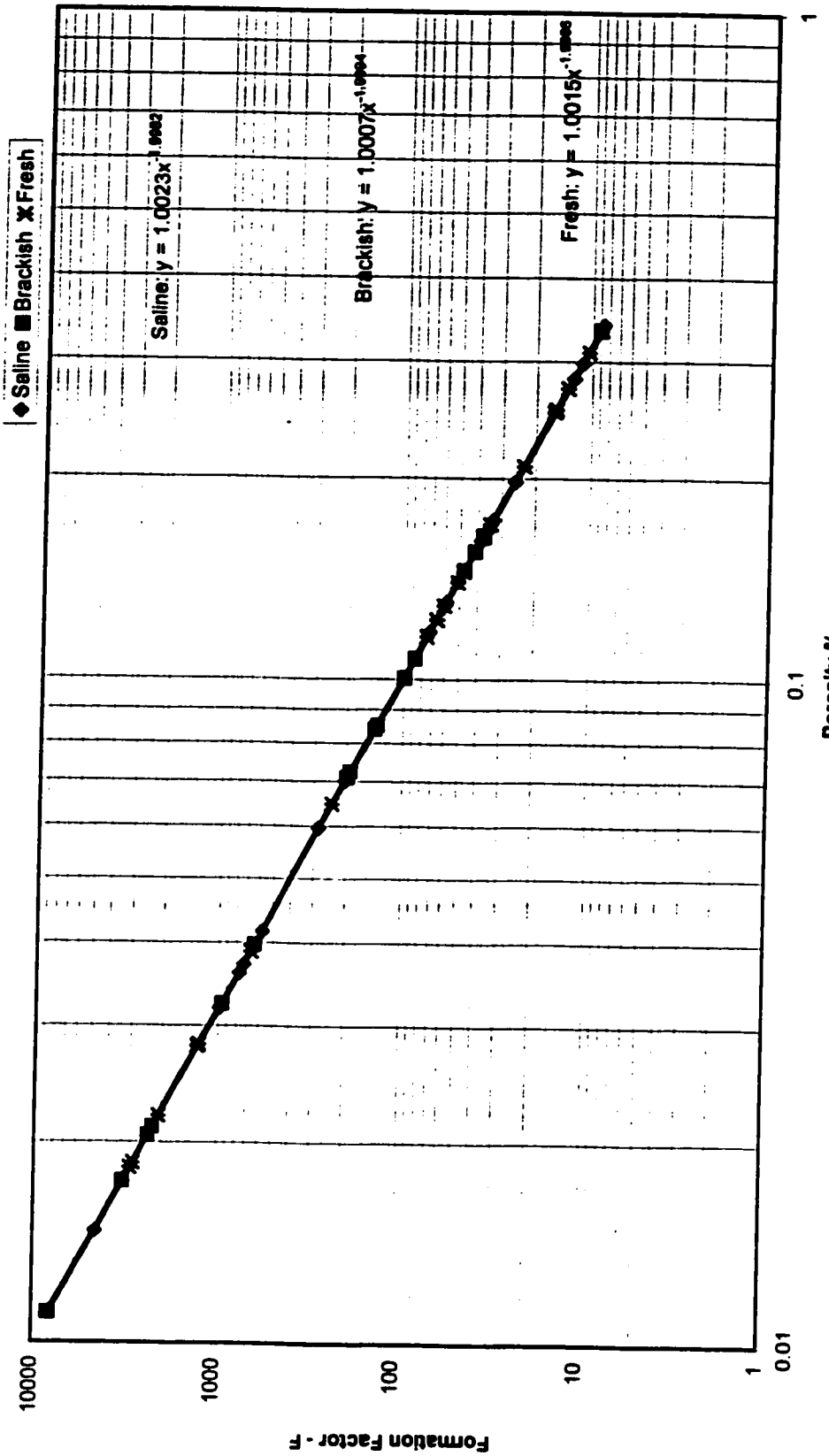

Figure 3.11: Formation Factor Versus Porosity (For different TDS values)

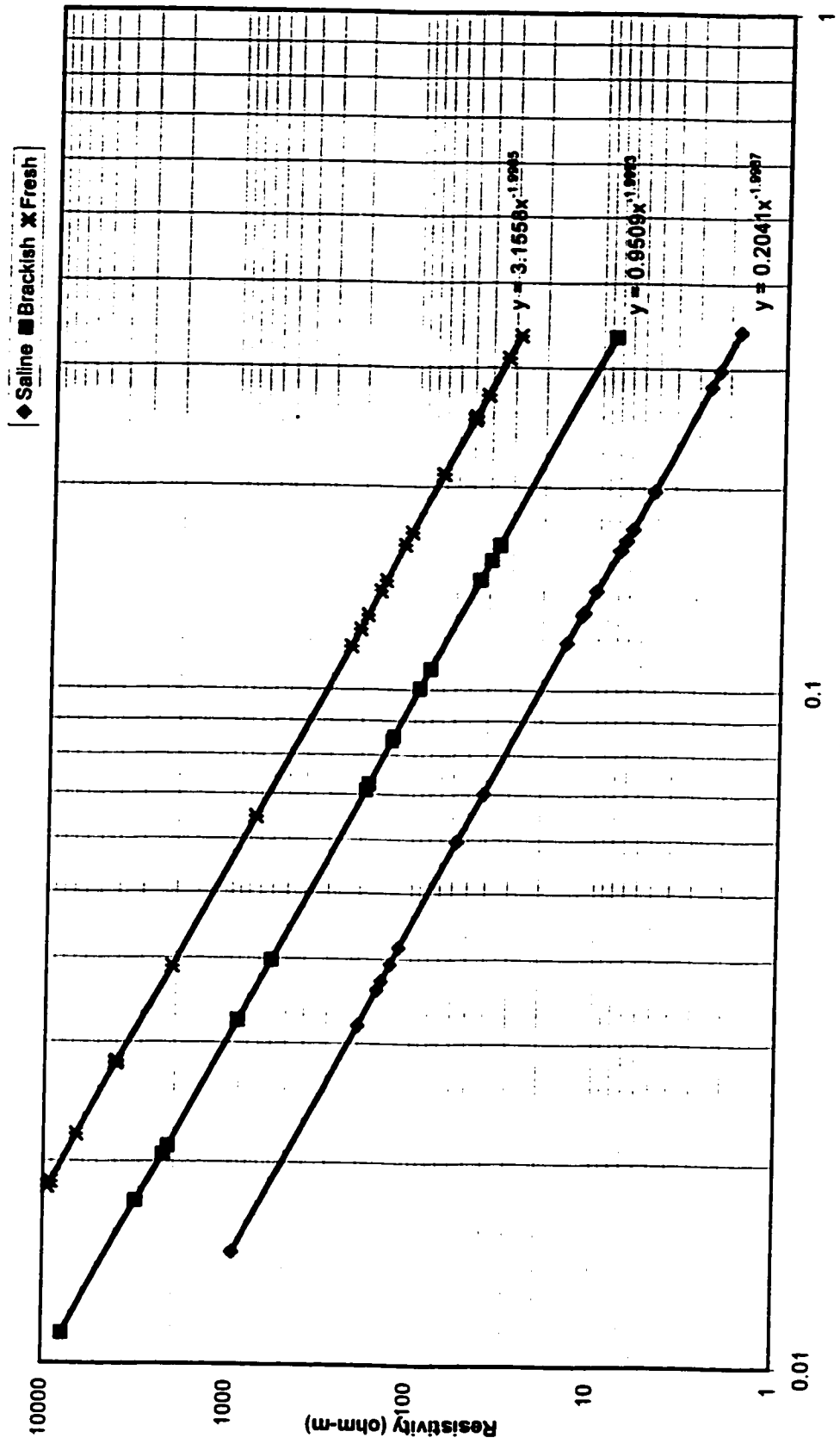

Figure 3.12: Core Resistivity Versus Porosity (for different TDS values)

For the seismic refraction profiles (SP 1000, SP 2000, SP 5000, and SP 6000), the velocity values for the Khobar aquifer are 2500 m/sec, 2336 m/sec, 2547 m/sec, and 2551 m/sec, respectively.

3.6 Resistivity Field Data Interpretation

The field resistivity data is interpreted using the computer software " Resix plus " program produced by the U.S.A's Interprex Ltd. This is a forward and inverse modeling program for interpreting electrical soundings. The forward modeling allows the creation of synthetic resistivity sounding curves for a number of plane layers on the assumption that each layer is laterally homogeneous. Inverse modeling is an interactive iterative process to obtain the best least squares fit to the field data. The results from the forward and inverse modeling are directed to a printer for a hard copy of the model (Appendix A). The Khobar aquifer's depth is in conformity with that in the structural contour map of Figure 1.6.

The detailed results from various sites are presented and discussed below:

Site No. 1 (VES-1)

Layer	Resistivity (ohm.m)	Thickness (m)
1	0.377	30.07
2	2.06	39.07
3	24.1	

The Khobar member in this site has low resistivity value (20.04 ohm.m) at 69.14 meters in depth.

Site No. 2 (VES-2)

Layer	Resistivity (ohm.m)	Thickness (m)
1	0.212	20.09
2	2.82	59.68
3	20.04	

The Khobar member has low resistivity value (20.04 ohm.m) at 79.77 meters in depth.

Site No. 3 (VES-3)

Layer	Resistivity (ohm.m)	Thickness (m)
1	0.282	39.11
2	3.36	40.29
3	33.99	

At this site, the Khobar member has a resistivity of 33.99 ohm.m at 79.4 meters in depth.

Site No. 4 (VES-4)

Layer	Resistivity (ohm.m)	Thickness (m)
1	2.9	23.4
2	1.04	38.73
3	127.2	

At this site, the behavior of the modeled curve and layers indicate that the site has a resistivity of 127.2 ohm.m which is higher than that at the previous sites at 62.13 meters depth. This may indicate a lower degree of salinity of the aquifer at this site.

Site No. 5 (VES-5)

Layer	Resistivity (ohm.m)	Thickness (m)
1	0.247	27.79
2	21.81	77.77
3	106.6	

This site is similar to the site VES-4 where the Khobar member has also a lower degree of salinity.

The electric profiles 3,4, and 5, are plotted in Figure 3.13 (a) together with the corresponding depth-resistivity cross-section in Figure 3.13 (b).

Figure 3.13 (b), which introduces an integrated information about the geoelectric configuration, is based essentially upon the data of the multi-layer models of the three soundings VES-3, VES-4, and VES-5.

The interpretation of the section emphasizes the sequence of three (3) geoelectric layers. On the surface, there is a layer of about 23 to 39 meters thickness of a resistivity value 0.25 to 3 ohm.m. This layer may be equivalent to soil and the Neogene deposits.

This layer overlies another layer of the Alat Member of the Dammam Formation characterized by moderate resistivity (1 – 22 ohm.m) and a thickness of 39 to 78 meters. The third layer is considered to be equivalent to the Khobar Aquifer with lower resistivity values to the south of the study area which might be due to an increase of groundwater salinity. Sayari and Zotl (1978) showed that the flow direction of underground water. in the study area, is NW-SE direction. Therefore, the salinity increases along the flow path. The resistivity range for the Khobar Aquifer is between 34 ohm.m in the south of the area, and 107 ohm.m in the north. The top of the Aquifer is 61 to 104 meters deep below the existing ground surface.

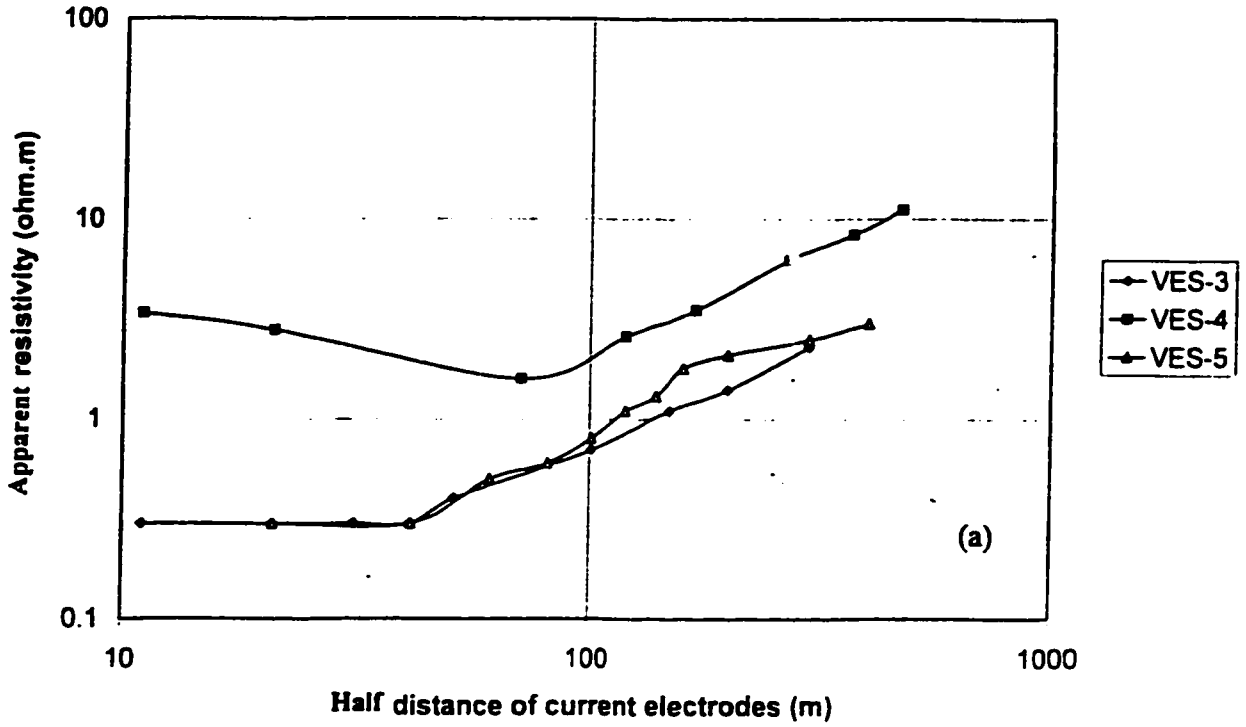

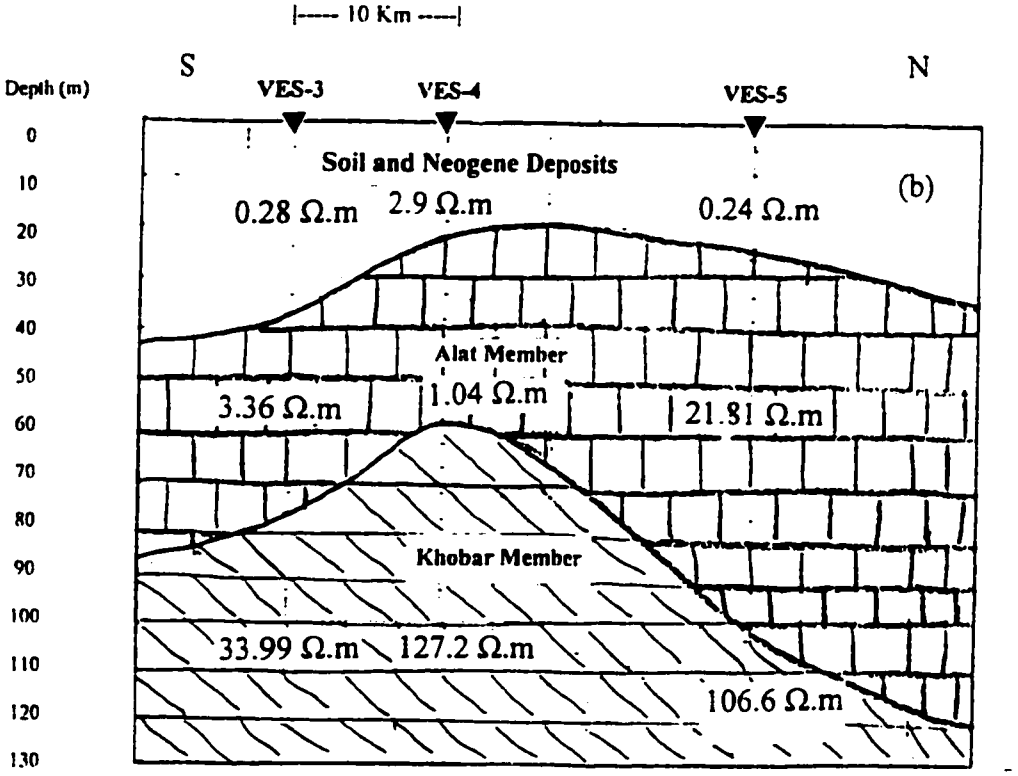

Figure 3.13: (a) The electric profiles 3,4, and 5. (b) Cross-section of VES 3,4, and 5 profiles.

Figures 3.14 and 3.15 show the isoresistivity and depth of the Khobar Aquifer, respectively, as interpreted from the Resix-IP software. Contouring of the isoresistivity map has conducted by dividing the map into two parts: northern part with high resistivity values, and southern part with low resistivity values. In the Dammam area, the isoresistivity map has been compared with salinity maps prepared for the Khobar Aquifer by Layla and others (1992) and Rasheeduddin (1998), Figures 3.16 and 3.17, respectively.

Comparison between these TDS maps and the isoresistivity map is shown in Table 3.3, where the low resistivity values in the southern part correspond to high TDS values and vica versa. This gradual increase in TDS values from North to South may be attributed to sea water intrusion and/or leakage of groundwater with high salinity from the Umm Er Radhuma Aquifer to the Khobar Aquifer (Sayari and Zotl, 1978).

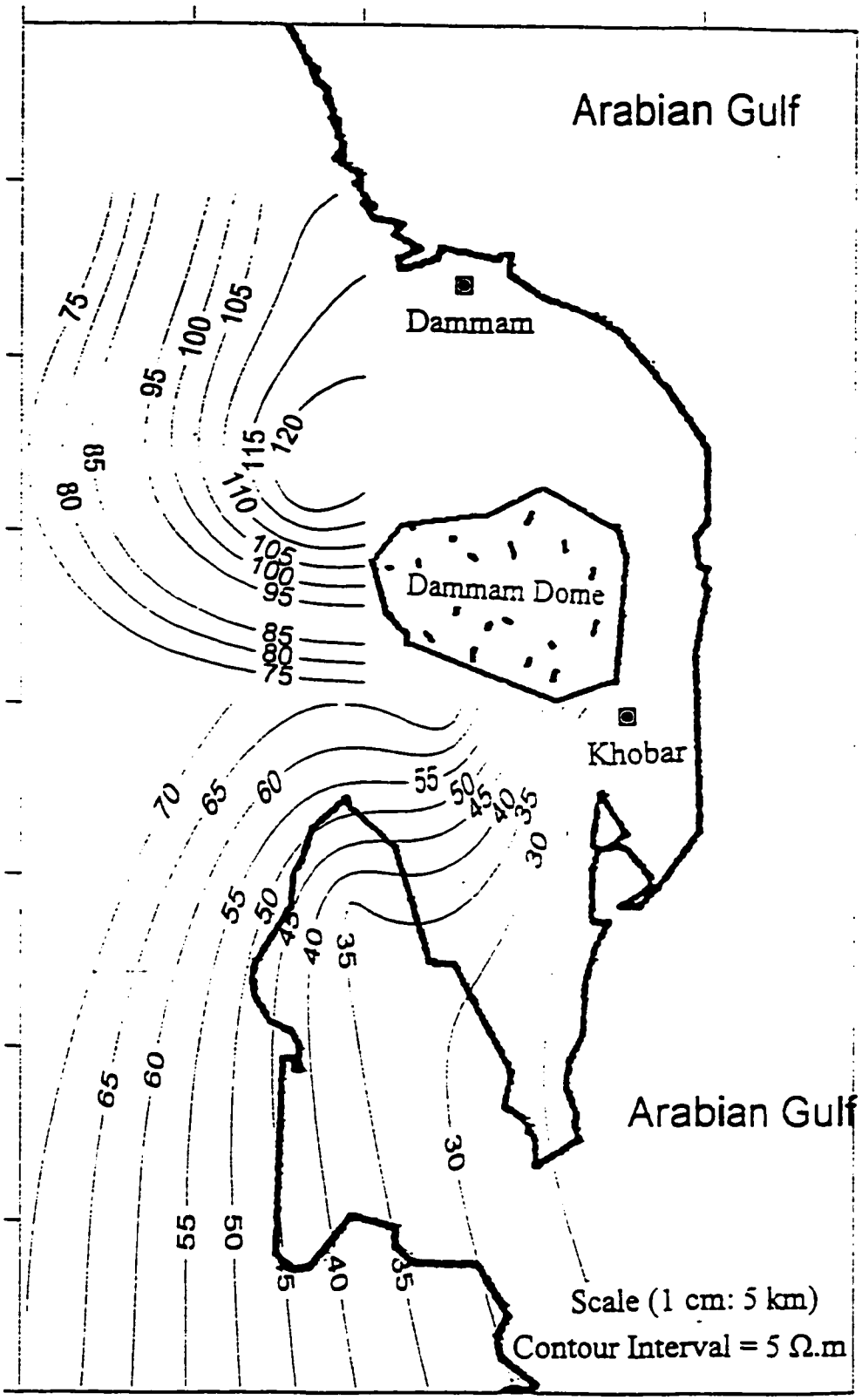

Figure 3.14: Isoresistivity map of the Khobar Aquifer.

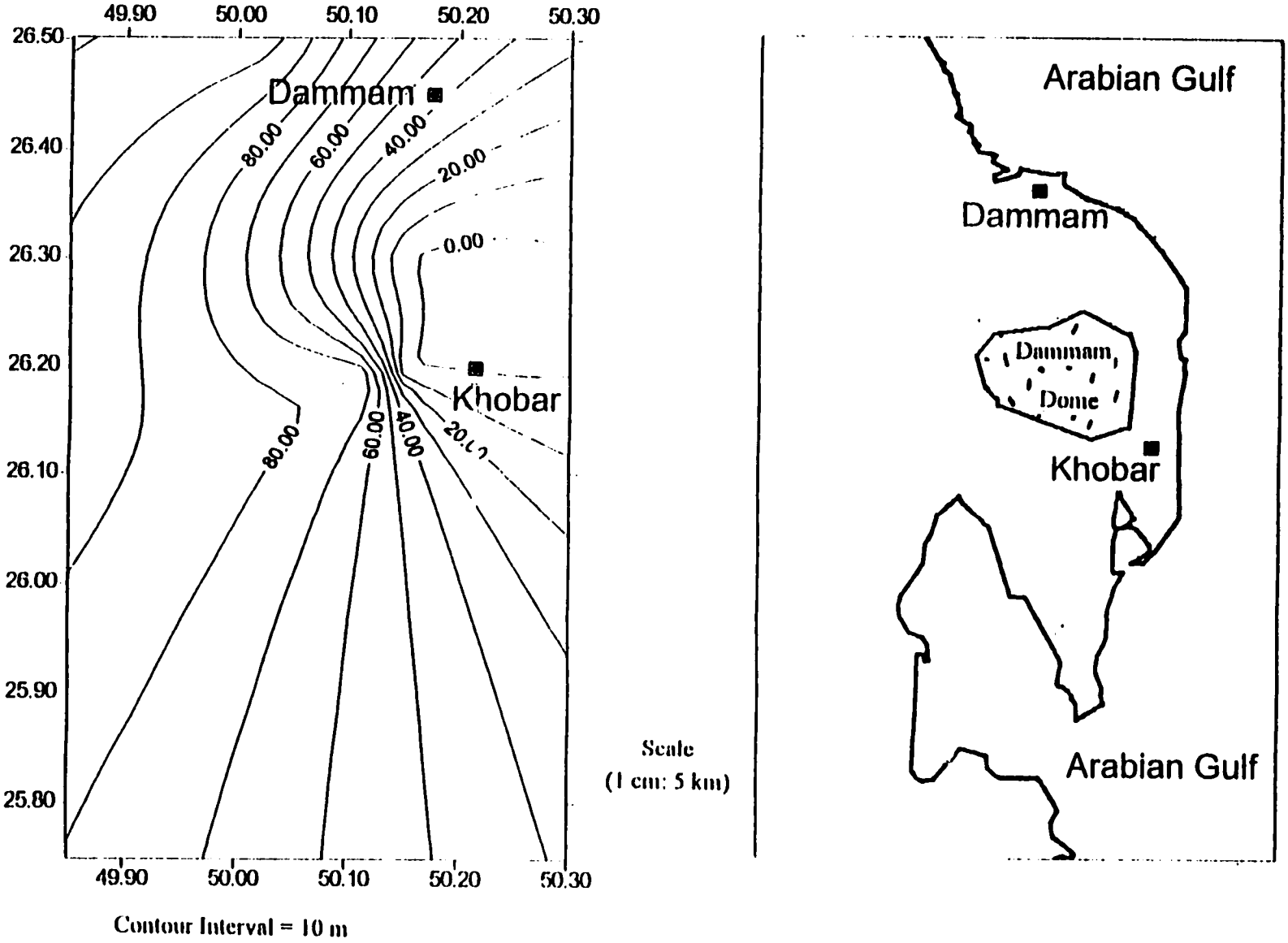

Figure 3.15: Contour map of depth to the Khobar Aquifer.

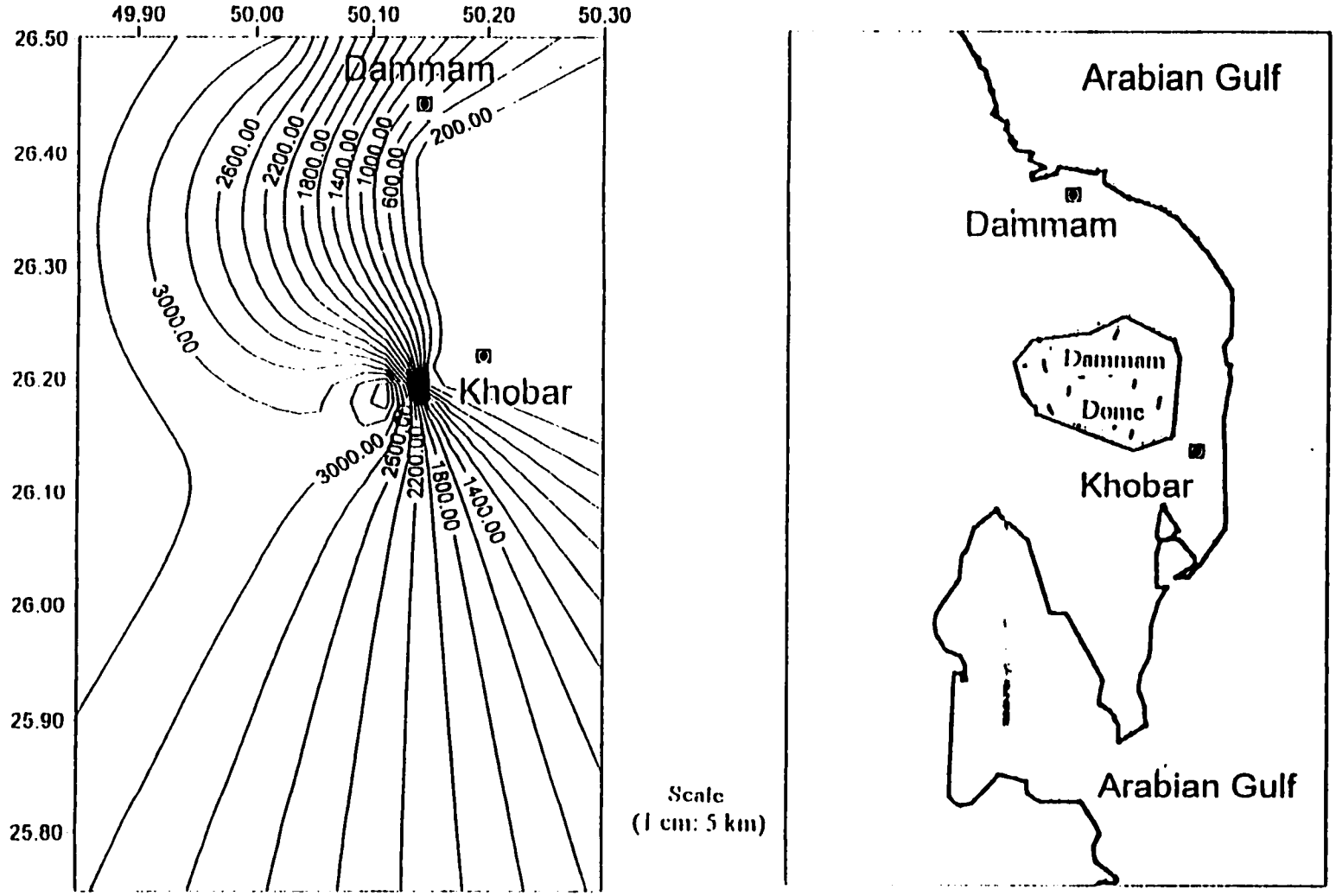

Contour Interval = 200 ppm

Figure 3.16: TDS contour map of the Khobar Aquifer (Layla and others, 1992)

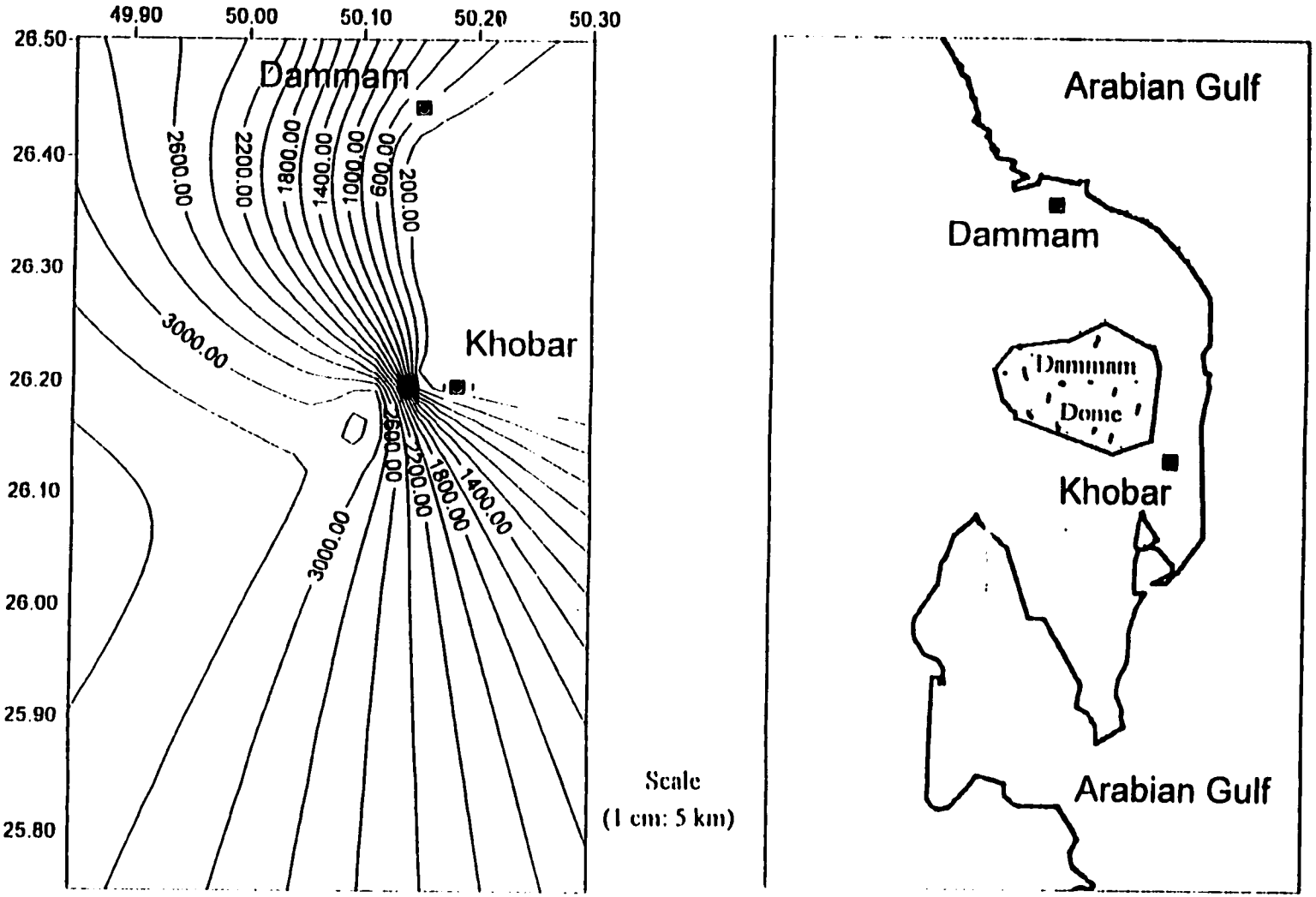

Contour Interval = 200 ppm

Figure 3.17: TDS contour map of the Khobar Aquifer (Rasheeduddin;1998)

Table 3.3: Comparing TDS maps and the isoresistivity map

VES Location	Resistivity (ohm.m) of The Khobar Aquifer (Mohammad, 2000)	TDS (ppm) of The Khobar Aquifer (Rasheeduddin,1998)	TDS (ppm) of the Khobar Aquifer (Layla and others,1992)
VES-1	24.1	3050	3100
VES-2	20.04	3150	3200
VES-3	33.99	3000	3000
VES-4	127.2	2500	2400
VES-5	106.6	2600	2850

CHAPTER FOUR

CONCLUSIONS

The conducted geophysical and geological studies of the Khobar Aquifer have provided the following conclusions:

1. The XRD and thin section analyses have shown that the Khobar Aquifer consists mainly of dolomite and limestone with a minor content of clay.
2. From the acoustic laboratory and field studies, it has been found that:
   - The Khobar aquifer velocity ranges generally between 2000 m/s to 4000 m/s in the field, and between 2000 m/s (for a dry dolomite sample with high porosity) to 6000 m/s (for a low porosity limestone sample saturated with saline water) according to the laboratory studies.
   - The dry samples have lower velocity values.
   - The saturated samples with fresh water have velocity lower than the ones saturated with saline or brackish water.
   - The obtained Porosity-Velocity relations are as follows:

A. Saline Saturated Samples:

$$\Phi = -0.003\ V + 21.703\ ;\ R = 0.467$$

B. Brackish Saturated Samples:

$$\Phi = -0.0069\ V + 30.0\ ;\ R = 0.258$$

C. Fresh Saturated Samples:

$$\Phi = -0.0072\ V + 36.199\ ;\ R = 0.785$$

D. Dry Saturated Samples:

$$\Phi = -0.013\ V + 38.25\ ;\ R = 0.5$$

where Φ is in percent and V in m/sec.

3. From the resistivity laboratory and field work, it has been concluded that:

- The core samples saturated with saline water have the lowest resistivity values.
- The resistivity values of the Khobar Aquifer range between 10 ohm-m to 500 Ω-m for different TDS values.
- The obtained Resistivity-Porosity relations are as follows:

A. Saline Saturated Samples:

$$\rho_c = 0.2041\ \Phi^{-1.9987}\ ;\ R = 0.97$$

B. Brackish Saturated Samples:

$$\rho_c = 0.9509\ \Phi^{-1.9993}\ ;\ R = 0.98$$

C. Fresh Saturated Samples:

$$\rho_c = 3.1558\ \Phi^{-1.9985}\ ;\ R = 0.96$$

where Φ is in fraction and ρ_c in ohm-m.

- As for the VES profiles, the higher the salinity of the groundwater, the lower the resistivity values.
- According to the VES profiles interpretations the TDS values increase from North to South in the study area, reflecting a decrease in the water quality in this direction.

References

Boggs, S. Jr., 1987, Principles of Sedimentology and Stratigraphy. Merrill Publishing Company, Ohio, 784 p.

BRGM, 1977, Appendix I-1: Geophysical Study. Groundwater Resources Study and Management Program. Al-Hassa Development Project, 19 p.

Core Sample Resistivity Measurement - Lab Experiment, 1995. Rock Properties Laboratory, Laboratory Manual, Petroleum Engineering Department, King Fahd University of Petroleum and Minerlas, 23-39.

Dabbagh, A.E and W.A. Abderrahman, 1997, Management of Groundwater Resources Under Various Irrigation Water Use Scenarios in Saudi Arabia. The Arabian Journal for Sciences and Engineering. Volume 22. Number 1 C. 47-64.

Dobrin, M.B. and C.H. Savit, 1988, Introduction to Geophysical Prospecting. 4th Edition, McGraw-Hill Book Company, Singapore, 867 p.

Doveton, J.H., 1986, Log Analysis of Subsurface Geology: Concepts and Computer Methods. John Wiley & Sons, New York. 273 p.

Edgell, H.S., 1997, Aquifers of Saudi Arabia and Their Geological Framework. The Arabian Journal for Sciences and Engineering, Volume 22, Number 1 C, 3-32.

Fetter, C.W., 1988, Applied Hydrogeology. 2nd Edition, Merrill Publishing Company, Ohio, 542 p.

Freeze, R.A. and J.A. Cherry, 1979, Groundwater. Prentice-Hall, Inc., Cliffs. N.J. 604 p.

Ghamdi, I., 1997, The Geology of the Dammam Dome. DGS Field Trip. December, 13 p.

Gueguen, Y. and V. Palciauskas, 1994, Introduction to the Physics of Rocks. Princeton University Press, Princeton, New Jersey, 294 p.

Hassan, A., 1995, Modeling of Groundwater Flow System in Wadi Al-Miyah Area, Eastern Saudi Arabia. M.Sc. Thesis, King Fahd University of Petroleum and Minerals, 248 p.

Hassan, H.M., 1992, Hydrogeochemistry of Alat and Khobar Aquifers in Eastern Saudi Arabia. M. Sc. Thesis, King Fahd University of Petroleum and Minerals. 156p.

Hassan, H.M., 1998, Major Ion Distribution in Khobar Aquifer, Eastern Saudi Arabia. The Arabian Journal for Sciences and Engineering, Vol. 23, No. 1C, 67-88.

Jado, A.R. and D.H. Johnson, 1983, Solution Caverns in the Dammam Dome, Dhahran, Saudi Arabia. The Arabian Journal for Sciences and Engineering, Volume 8, Number 1, 69-73.

Koefoed, O., 1979, Geosounding Principles-1: Resistivity Sounding Measurements. Elsevier, Amsterdam, 276 p.

Layla, R., H. Yazicigil, and R. de Jong, 1986, Numerical Modeling of the Dammam Aquifer in Eastern Saudi Arabia. The Arabian Journal for Sciences and Engineering, Vol. 11, No. 4, 349-362.

Layla, R., H. Yazicigil, and R. de Jong, 1992, Optimum Development of Dammam Aquifer in the Eastern Province of Saudi Arabia. General Directorate of Research Grants Programs-King Abdul Aziz City for Science & Technology. Riyadh, 246 p.

Mahmoud, M.J., 1987, Hydrogeology of the Al-Hassa Oasis. M. Sc. Thesis. King Fahd University of Petroleum and Minerals, 141 p.

Model ES-1225: Multichannel Signal Enhancement Seismograph. Operating Manual, 123 p.

Naggar, Z.R. and H.A. Al-Nakhal, 1989, Review of The Biostratigraphy of the Hasa Group (Palaeogene) in Saudi Arabia, Kuwait and Adjacent Regions. J. King Saud Univ., Vol. 1, Science (1,2), pp 73-99, Riyadh.

Parasnis, D.S., 1987, Principles of Applied Geophysics. 3th Edition. Chapman and Hall, London, 419 p.

Permeability Determination Using Liquid Permeameter Manual, 1995. Rock Properties Laboratory, Laboratory Manual, Petroleum Engineering Department. King Fahd University of Petroleum and Minerals, 40-51.

Porosity Determination Using Saturation Method Manual, 1995. Rock Properties Laboratory, Laboratory Manual, Petroleum Engineering Department. King Fahd University of Petroleum and Minerals, 1-18.

Powers, R.W., L.F. Ramirez, C.D. Redmond, and E.L. Elberg, Jr., 1963, Geology of the Arabian Peninsula: Sedimentary Geology of Saudi Arabia. U. S. Geological Survey Professional Paper 560-D, 147 p.

Rasheeduddin, M., 1988, Numerical Modeling of Alat, Khobar and Umm Er Radhuma Aquifers System in Eastern Saudi Arabia. M.Sc. Thesis, King Fahd University of Petroleum and Minerals, 219 p.

Rasheeduddin, M., 1998, Aquifers in Saudi Arabia. Geol 532 Seminar, Earth Sciences Department, King Fahd University of Petroleum and Minerals.

Resix-Ip User's Manual, 1988, Interpex Limited, 128 p.

Sander, N.J., 1962, A Percu Paleontologique et Stratigraphique du Paleogene en Arabie Saoudite Orientale. Revue Micropal, Vol. 5, No. 1, 3-40.

Sayari, S. and J. Zotl, 1978, Quaternary Period in Saudi Arabia 1: Sedimentological, Hydrogeological, Hydrochemical, Geomorphological, and Climatological Investigations in Central and Eastern Saudi Arabia. Springer - Verlag, Wien, New York, 334 p.

Scott, 1973, Seismic Refraction Modeling by Computer. Geophysics, Vol. 38, No. 2, 271-284.

Selley, R., 1985, Elements of Petroleum Geology. W.E. Freeman and Company, New York, 449 p.

Shirokoff, J., 1998, Analytical Service Report. The Central Analytical & Material Characterization Laboratories for XRD Analysis. Research Institute, King Fahd University of Petroleum and Minerals, Dhahran.

Syscal-R2 Operating Manual, V 3.1. BRGM, 31p.

Tamimi, M.H., 1985, Stratigraphical and Microfacies Analysis of the Early Palaeogene Succession in the Dammam Dome, Eastern Saudi Arabia. M.Sc. Thesis, King Fahd University of Petroleum and Minerals, 145 p.

Tarbuck, E.J. and F.K. Lutgens, 1992, The Earth: An Introduction to Physical Geology. 4th Edition, Macmillan Publishing Company, New York, 654 p.

Telford, W.M., L.P. Geldart, and R.E. Sheriff, 1990, Applied Geophysics. 2nd Edition, Cambridge University Press, Cambridge770 p.

The Seismic Refraction Interpretation Programs (SIP) Manual. Rimrock Geophysics, 229 p.

Tleel, J.W., 1972, Surface Geology of Dammam Dome, Eastern Province, Saudi Arabia. M.Sc. Thesis, Texas Christian University, 56 p.

Tleel, J.W., 1973, Surface Geology of Dammam Dome, Eastern Province, Saudi Arabia. AAPG, Vol. 57, No. 3, 558-576.

Ultrasonic Tester. User's Manual. Posso Ltd., 12 p.

Weijermars, R., 1999, Surface Geology, Lithostratigraphy and Tertiary Growth of the Dammam Dome, Saudi Arabia: A New Field Guide. GeoArabia, Vol. 4, No. 2, 199-226.

Willis, R.P., 1963, Geology of the Arabian Peninsula: Bahrain. U. S. Geological Survey Professional Paper 560-E, 5 p.

Wyllie, M.R.J., A.R. Gregory, and G.H.F. Gardner, 1958, An Experimental Investigation of factors Affecting Elastic Wave Velocities in Porous Media. Geophysics, Vol. 23, 459-493.

APPENDIX A

RESIX-IP PACKAGE INTERPRETATION OF THE VERTICAL ELECTRICAL SOUNDINGS (VES)

---------- VES-1 ---------- PAGE 1

DATA SET: VES-1

CLIENT: KFUPM
LOCATION: Dammam
COUNTY: Dammam
PROJECT: Thesis
ELEVATION: 0.00
DATE: 14/12/1999
SOUNDING: VES-2
AZIMUTH:
EQUIPMENT: Syscal-R2
SOUNDING COORDINATES: E: 50.1100 N: 26.1500

Schlumberger Configuration

FITTING ERROR: 22.077 PERCENT

L #	RESISTIVITY (ohm-m)	CHARGEABILITY (pfe)	THICKNESS (m)	ELEVATION (m)	CONDUCTANCE (Siemens)
				0.0	
1	0.377		30.07	-30.07	79.62
2	2.06		39.07	-69.14	18.95
3	24.10				

ALL PARAMETERS ARE FREE

No.	Spacing (m)	PA (ohm-m) DATA	SYNTHETIC	DIFFERENCE (percent)
1	26.00	0.300	0.418	-39.41
2	51.00	0.700	0.574	17.96
3	76.00	0.700	0.784	-12.05
4	101.0	0.800	1.00	-25.90
5	126.0	1.10	1.23	-12.04
6	151.0	1.10	1.45	-32.45
7	176.0	1.60	1.67	-4.96
8	201.0	1.80	1.89	-5.49
9	226.0	2.50	2.11	15.39
10	251.0	3.00	2.32	22.40
11	276.0	2.10	2.53	-20.82
12	301.0	3.60	2.74	23.79
13	326.0	2.80	2.94	-5.22

PARAMETER RESOLUTION MATRIX:
"F" INDICATES FIXED PARAMETER
P 1 1.00
P 2 0.00 0.10
P 3 0.00 0.05 0.29

* KFUPM *

```
T 1  0.00 -0.15  0.03  0.97
T 2  0.01 -0.19 -0.31  0.02  0.61
       P 1   P 2   P 3   T 1   T 2
```

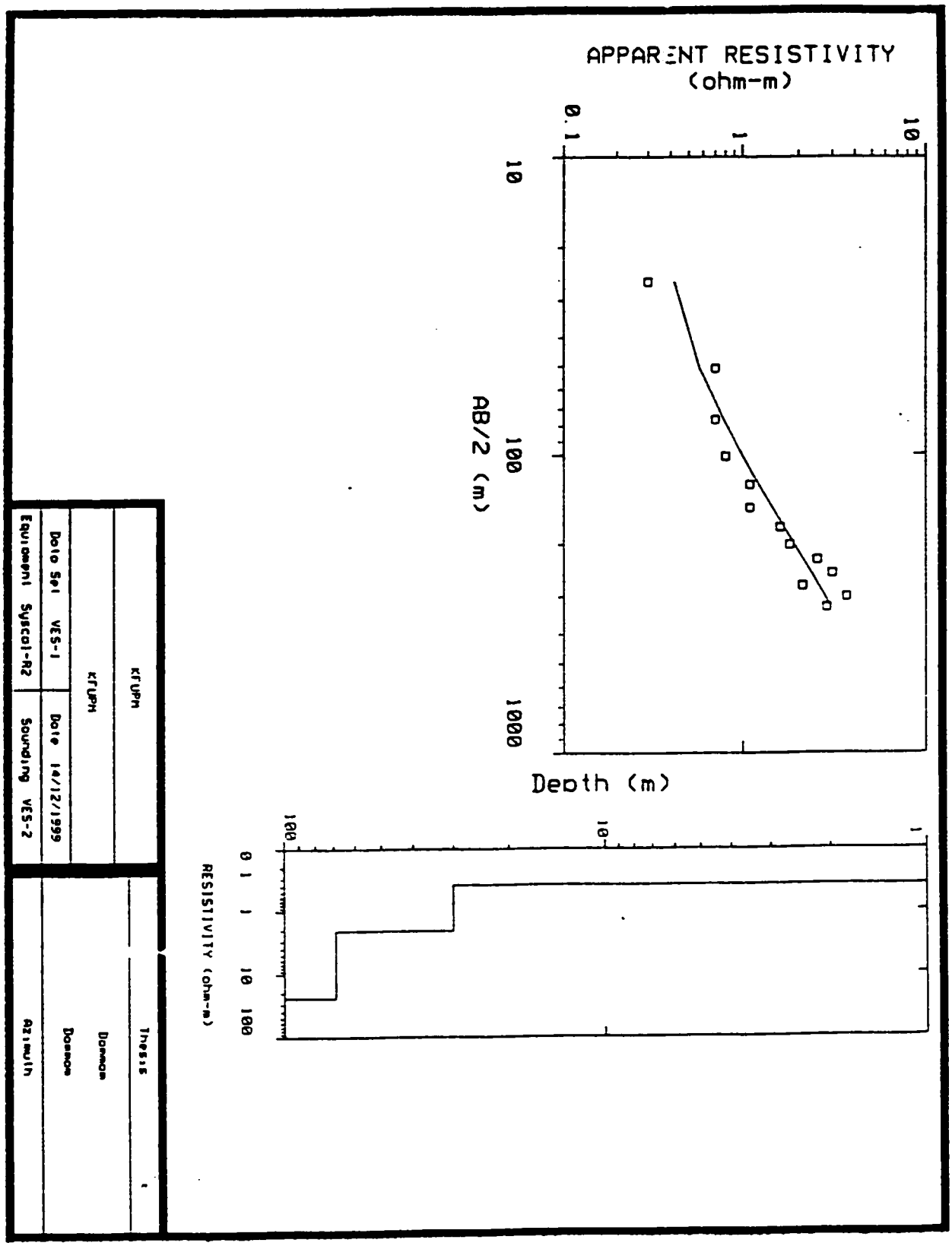

Resistivity Modeling for VES-1

DATA SET: VES-2

CLIENT: KFUPM
LOCATION: DAMMAM
COUNTY: DAMMAM
PROJECT: THESIS
ELEVATION: 0.00
DATE: 14/12/1999
SOUNDING: VES-2
AZIMUTH:
EQUIPMENT: Syscal-R2
SOUNDING COORDINATES: E: 50.1200 N: 26.1800

Schlumberger Configuration

FITTING ERROR: 15.976 PERCENT

L #	RESISTIVITY (ohm-m)	CHARGEABILITY (pfe)	THICKNESS (m)	ELEVATION (m)	CONDUCTANCE (Siemens)
				0.0	
1	0.212		20.09	-20.09	94.47
2	2.82		59.68	-79.78	21.12
3	20.04				

ALL PARAMETERS ARE FREE

No.	Spacing (m)	PA (ohm-m) DATA	SYNTHETIC	DIFFERENCE (percent)
1	11.00	0.200	0.220	-10.22
2	21.00	0.200	0.256	-28.45
3	31.00	0.300	0.320	-6.68
4	41.00	0.400	0.396	0.847
5	51.00	0.500	0.477	4.53
6	101.0	1.00	0.874	12.58
7	151.0	1.60	1.26	21.49
8	201.0	2.00	1.62	18.55
9	301.0	2.30	2.34	-1.90

CURRENT RESOLUTION MATRIX NOT AVAILABLE

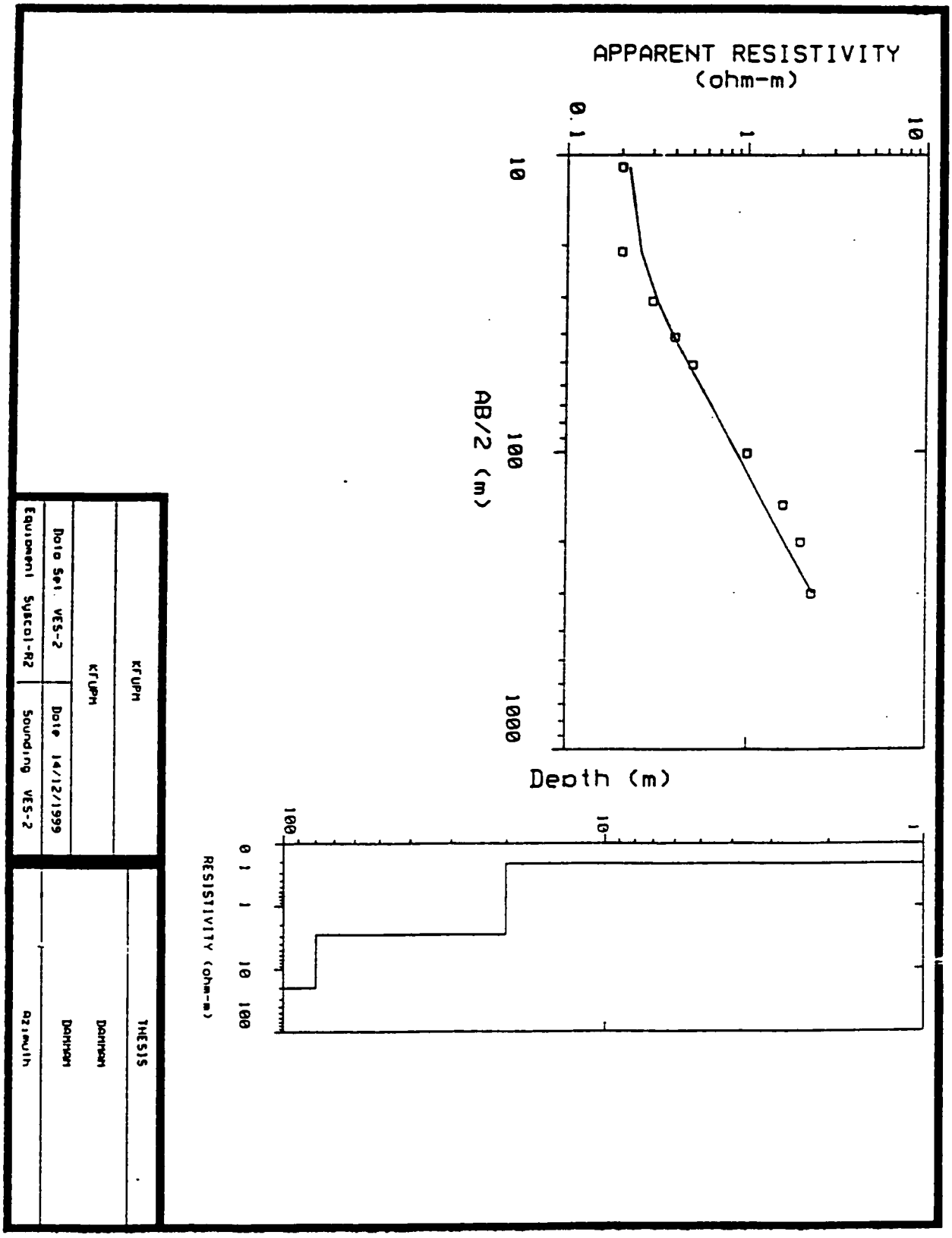

Resistivity Modeling for VES-2

DATA SET: VES-3

CLIENT: KFUPM
LOCATION: DAMMAM
COUNTY: DAMMAM
PROJECT: THESIS
ELEVATION: 0.00
SOUNDING COORDINATES: E: 50.0600 N: 26.1600

DATE: 14/12/1999
SOUNDING: VES-3
AZIMUTH:
EQUIPMENT: Syscal-R2

Schlumberger Configuration

FITTING ERROR: 10.120 PERCENT

L #	RESISTIVITY (ohm-m)	CHARGEABILITY (pfe)	THICKNESS (m)	ELEVATION (m)	CONDUCTANCE (Siemens)
				0.0	
1	0.282		39.11	-39.11	138.4
2	3.36		40.29	-79.40	11.96
3	33.99				

ALL PARAMETERS ARE FREE

No.	Spacing (m)	PA (ohm-m) DATA	SYNTHETIC	DIFFERENCE (percent)
1	11.00	0.300	0.284	5.31
2	21.00	0.300	0.292	2.47
3	31.00	0.300	0.312	-4.07
4	41.00	0.300	0.343	-14.53
5	51.00	0.400	0.385	3.69
6	101.0	0.700	0.668	4.46
7	151.0	1.10	0.980	10.85
8	201.0	1.40	1.29	7.77
9	301.0	2.30	1.89	17.44

CURRENT RESOLUTION MATRIX NOT AVAILABLE

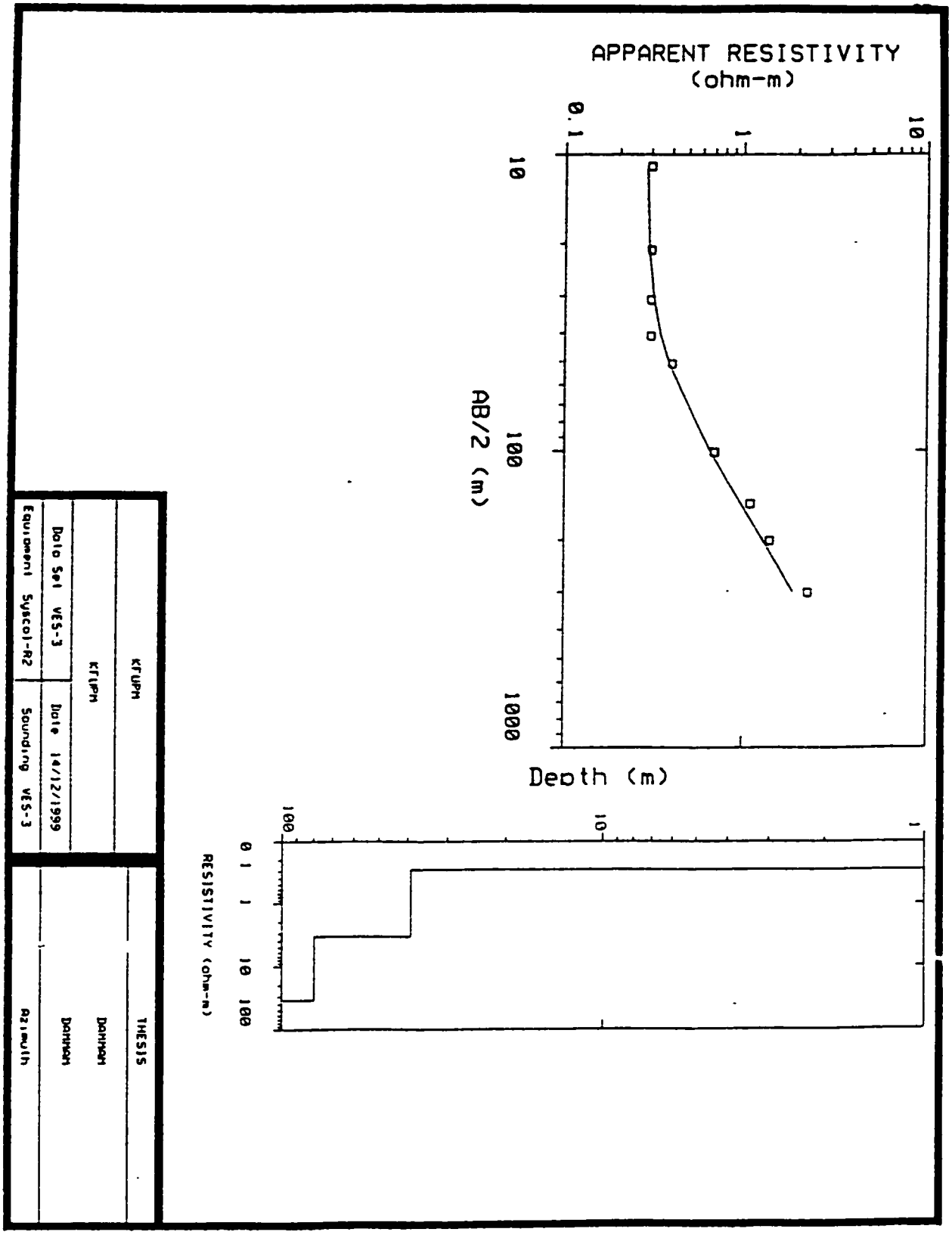

Resistivity Modeling for VES-3

DATA SET: VES-4

CLIENT: KFUPM
LOCATION: DAMMAM
COUNTY: DAMMAM
PROJECT: THESIS
ELEVATION: 0.00
SOUNDING COORDINATES: E: 26.5000 N: 50.2500

DATE: 14/12/1999
SOUNDING: VES-4
AZIMUTH:
EQUIPMENT: Syscal-R2

Schlumberger Configuration

FITTING ERROR: 13.295 PERCENT

L #	RESISTIVITY (ohm-m)	CHARGEABILITY (pfe)	THICKNESS (m)	ELEVATION (m)	CONDUCTANCE (Siemens)
1	2.90			0.0	
2	1.04		23.40	-23.40	8.05
3	127.2		38.73	-62.13	37.16

ALL PARAMETERS ARE FREE

No.	Spacing (m)	PA (ohm-m) DATA	SYNTHETIC	DIFFERENCE (percent)
1	11.00	3.40	2.87	15.37
2	21.00	2.80	2.74	1.85
3	71.00	1.60	2.05	-28.50
4	121.0	2.60	2.68	-3.28
5	171.0	3.50	3.68	-5.22
6	271.0	6.20	5.73	7.48
7	371.0	8.30	7.73	6.81
8	471.0	11.10	9.67	12.83

CURRENT RESOLUTION MATRIX NOT AVAILABLE

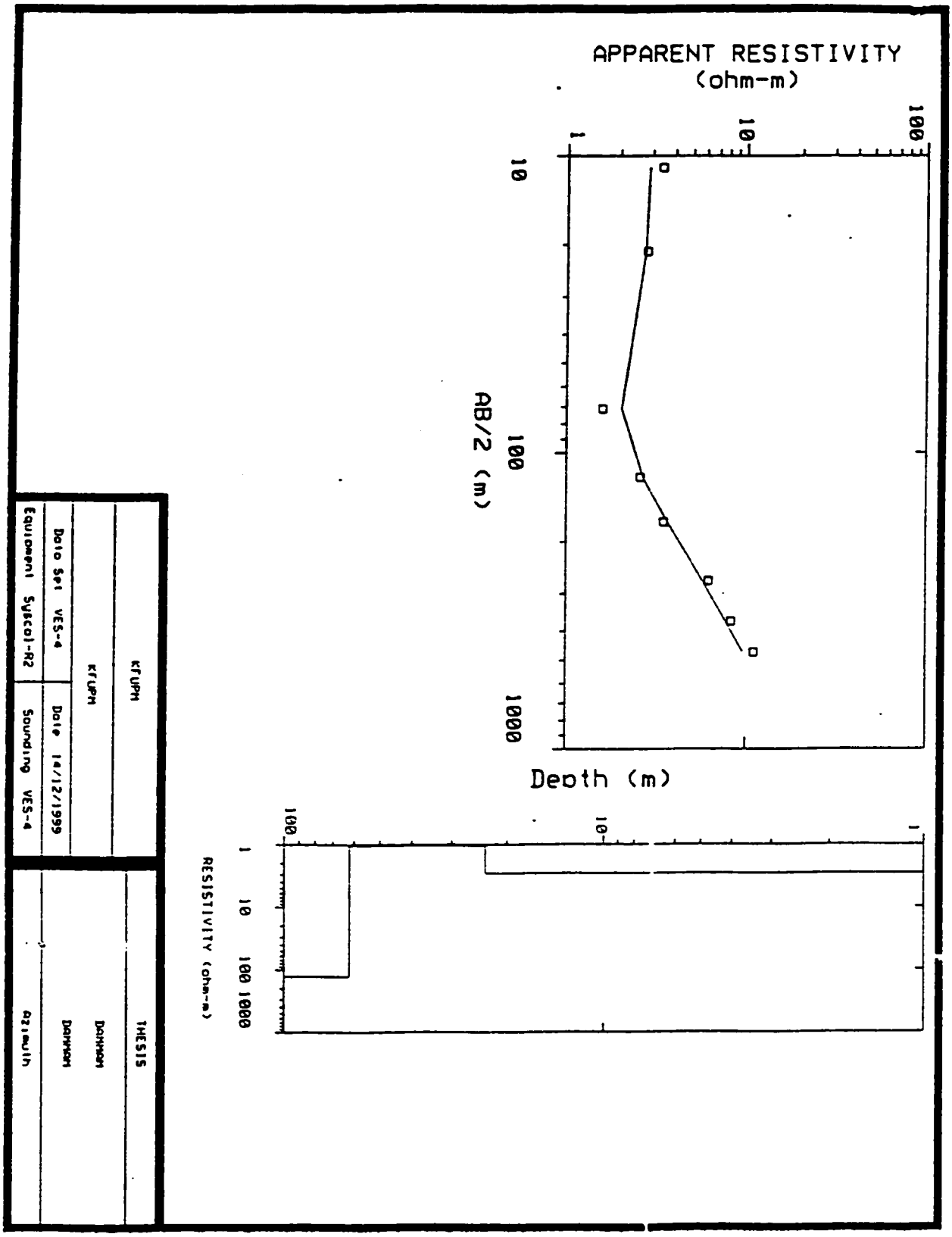

Resistivity Modeling for VES-4

DATA SET: VES-5

CLIENT: KFUPM
LOCATION: DAMMAM
COUNTY: DAMMAM
PROJECT: THESIS
ELEVATION: 0.00
SOUNDING COORDINATES: E: 50.0360 N: 26.2500

DATE: 14/12/1999
SOUNDING: VES-5
AZIMUTH:
EQUIPMENT: Syscal-R2

Schlumberger Configuration

FITTING ERROR: 15.826 PERCENT

L #	RESISTIVITY (ohm-m)	CHARGEABILITY (pfe)	THICKNESS (m)	ELEVATION (m)	CONDUCTANCE (Siemens)
				0.0	
1	0.247		27.79	-27.79	112.4
2	21.81		77.77	-105.5	3.56
3	106.6				

ALL PARAMETERS ARE FREE

No.	Spacing (m)	PA (ohm-m) DATA	SYNTHETIC	DIFFERENCE (percent)
1	21.00	0.300	0.273	8.96
2	41.00	0.300	0.380	-26.90
3	61.00	0.500	0.535	-7.15
4	81.00	0.600	0.703	-17.20
5	101.0	0.800	0.872	-9.06
6	121.0	1.10	1.04	5.32
7	141.0	1.30	1.20	6.93
8	161.0	1.80	1.37	23.46
9	201.0	2.10	1.71	18.47
10	301.0	2.50	2.54	-1.61
11	401.0	3.00	3.35	-11.92

CURRENT RESOLUTION MATRIX NOT AVAILABLE

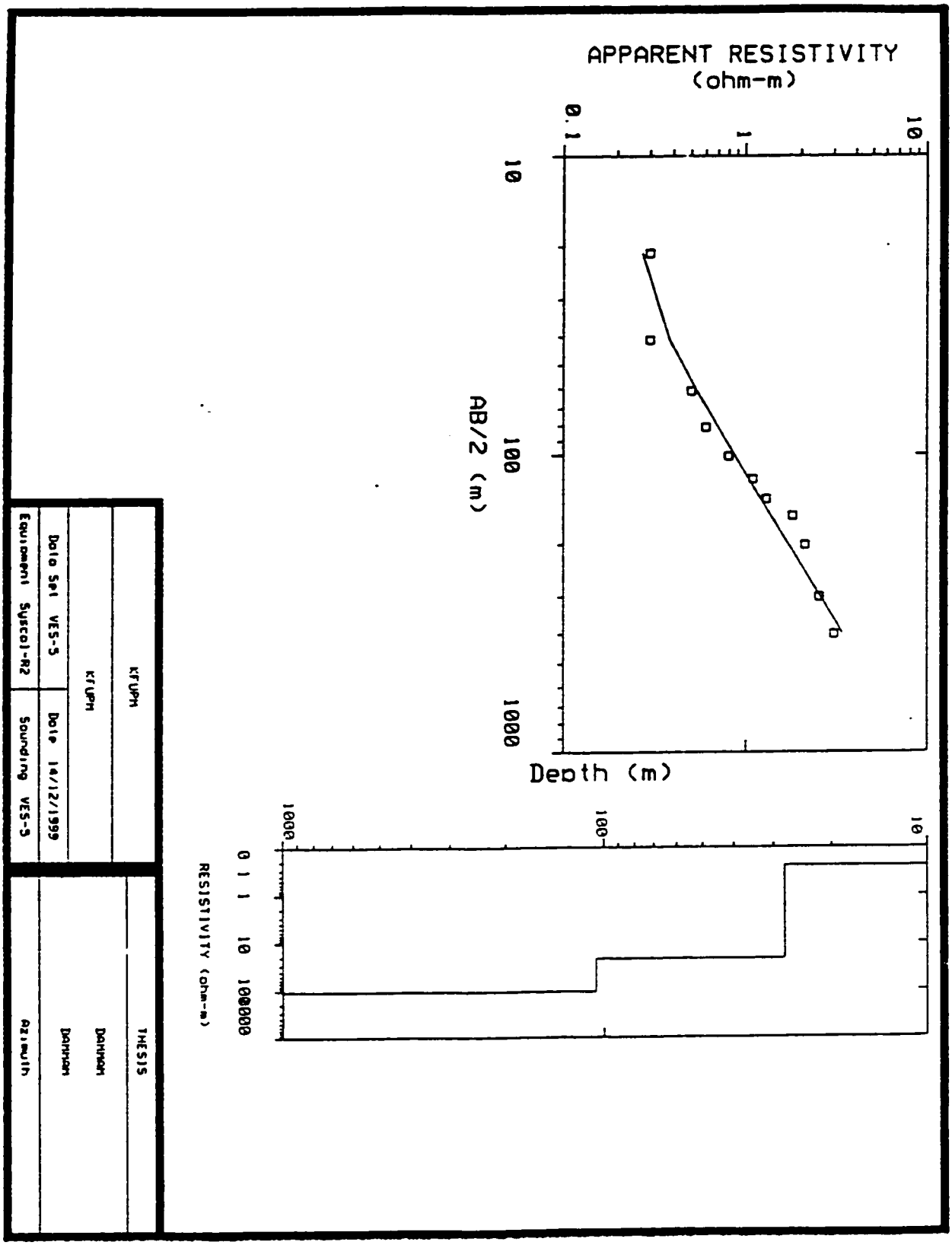

Resistivity Modeling for VES-5

APPENDIX B

X-RAY DIFFRACTOMETRY (XRD) ANALYSIS

Sample Name (MAM1): Loc. 1	Phase	Wt%	PDF#
$CaMg(CO_3)_2$ Dolomite	major	100	36-426

(Note: The peak at 2theta=6.46 degees could be a clay mineral of small amount i.e. <1 Wt%.)

Sample Name (MAM2): Loc. 3	Phase	Wt%	PDF#
$CaCO_3$ Calcite	major	100	5-586

(Note: The peaks at 2theta=6.28 degees and 8.52 degrees could be a clay mineral of small amount.)

Sample Name (MAM3): Loc. 5	Phase	Wt%	PDF#
$CaMg(CO_3)_2$ Dolomite	major	97	36-426
$(Mg,Al)_5(Si,Al)_8O_{20}(OH)_2$ Palygorskite	minor	2	21-550
$H_{18.9}Al_{18.9}Si_{173.1}O_{384}$ Hydrogen Aluminum Silicate	minor	1	42-18
		100	

Sample Name (MAM4): Loc. 2	Phase	Wt%	PDF#
$CaCO_3$ Calcite	major	100	5-586

(Note: The peak at 2theta=6.25 degees could be a clay mineral of small amount.)

Sample Name (MAM5): Loc. 4	Phase	Wt%	PDF#
$Ca(Fe,Mg)(CO_3)_2$ Ankerite	major	100	41-586

(Note: The peaks at 2theta=6.54 degees, 8.41 degrees and 10.49 degrees could be a clay mineral of small amount.)

Sample Name (MAM6): Loc. 5	Phase	Wt%	PDF#
$CaMg(CO_3)_2$ Dolomite	major	99	36-426
$CaSO_4.2H_2O$ Gypsum	minor	1	21-816
		100	

(Note: The peaks at 2theta=6.59 degees and 8.43 degrees could be a clay mineral of small amount.)

Sample Name (MAM7): Loc. 9	Phase	Wt%	PDF#
$CaCO_3$ Calcite	major	100	5-586

(Note: The peaks at 2theta=6.14 degees and 8.99 degrees could be a clay mineral of small amount.)

Sample Name (MAM8): Loc. 11	Phase	Wt%	PDF#
$Ca(Mg_{0.67}Fe_{0.33})(CO_3)_2$ Ankerite	major	95	12-88
$CaCO_3$ Calcite	major	5 100	24-27

(Note: The peak at 2theta=6.53 degees could be a clay mineral of small amount.)

Sample Name (MAM9): Loc. 12	Phase	Wt%	PDF#
$CaMg(CO_3)_2$ Dolomite	major	100	36-426

(Note: The peak at 2theta=6.56 degees and 8.45 degrees could be a clay mineral of small amount. Also, the peak at 2theta=27.94 degrees could be an Albite or Anorthite mineral of small amount.)

Checked by : _____ Approved by : _____

Group Coordinator
Dr. H.M. Tawancy

Section Manager
Dr. N.M. Abbas

X-ray diffractogram showing peak search for sample from Location # 1.

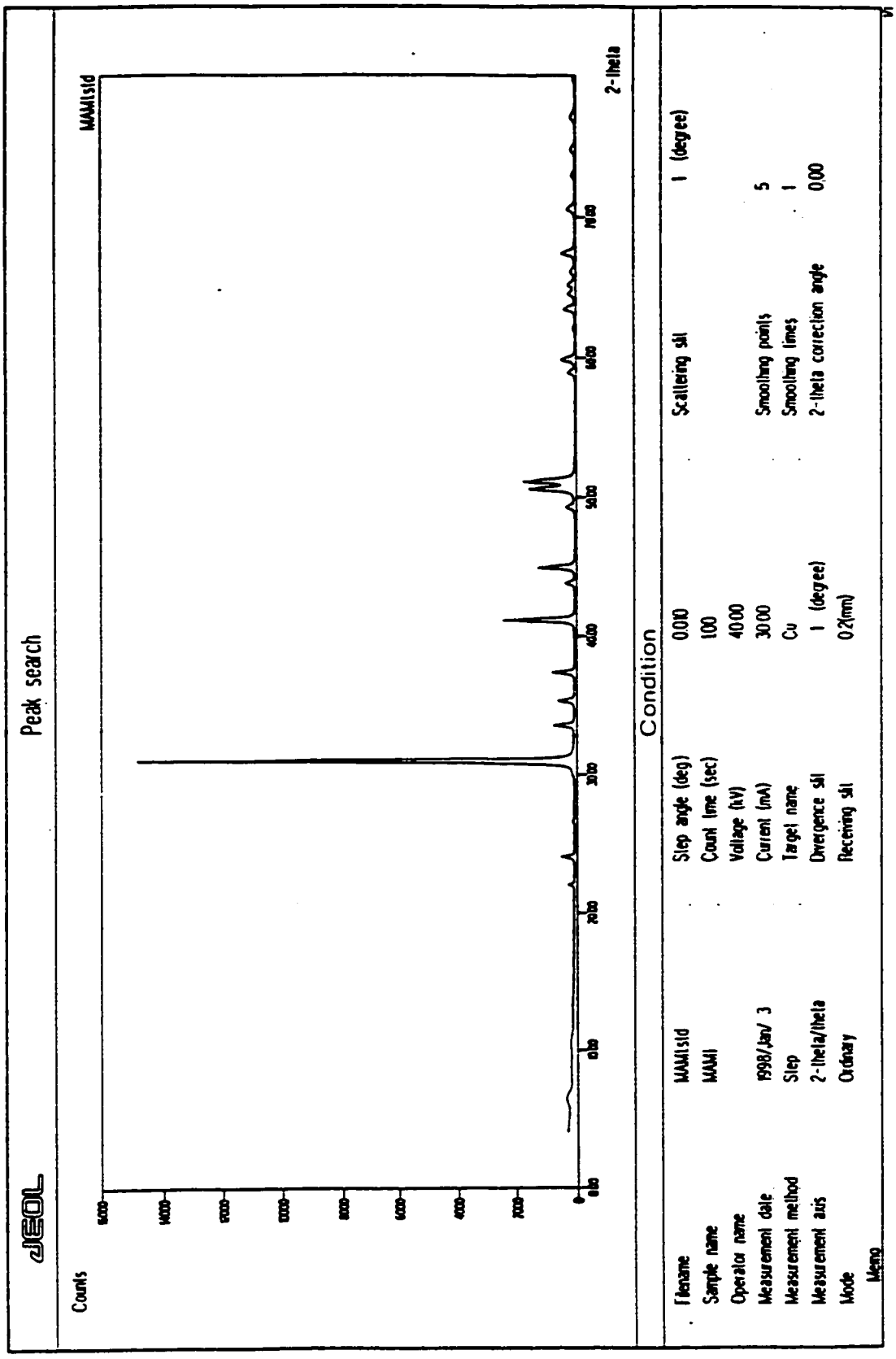

X-ray diffractogram showing search match for sample from Location # 1.

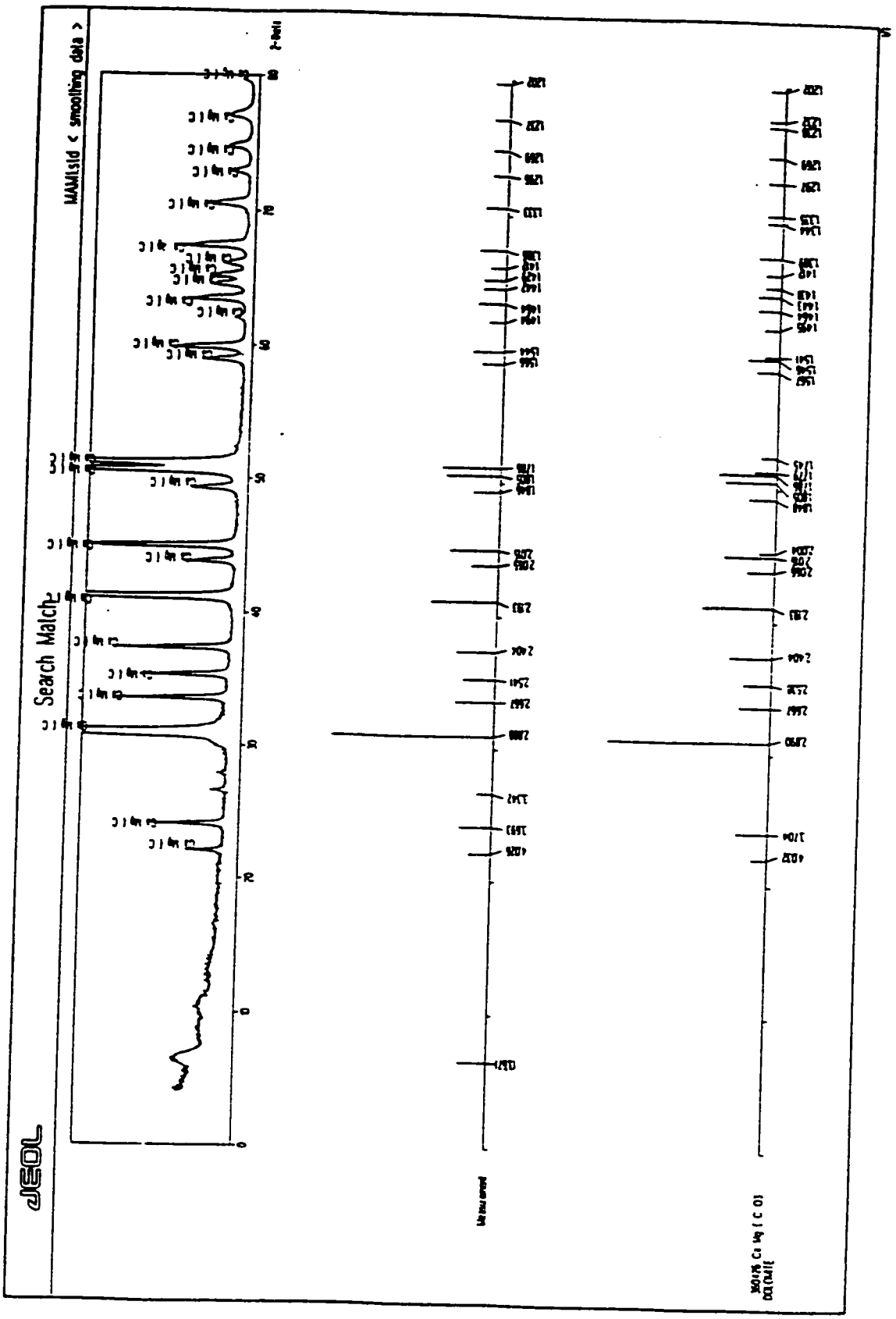

X-ray diffractogram showing peak search for sample from Location # 3.

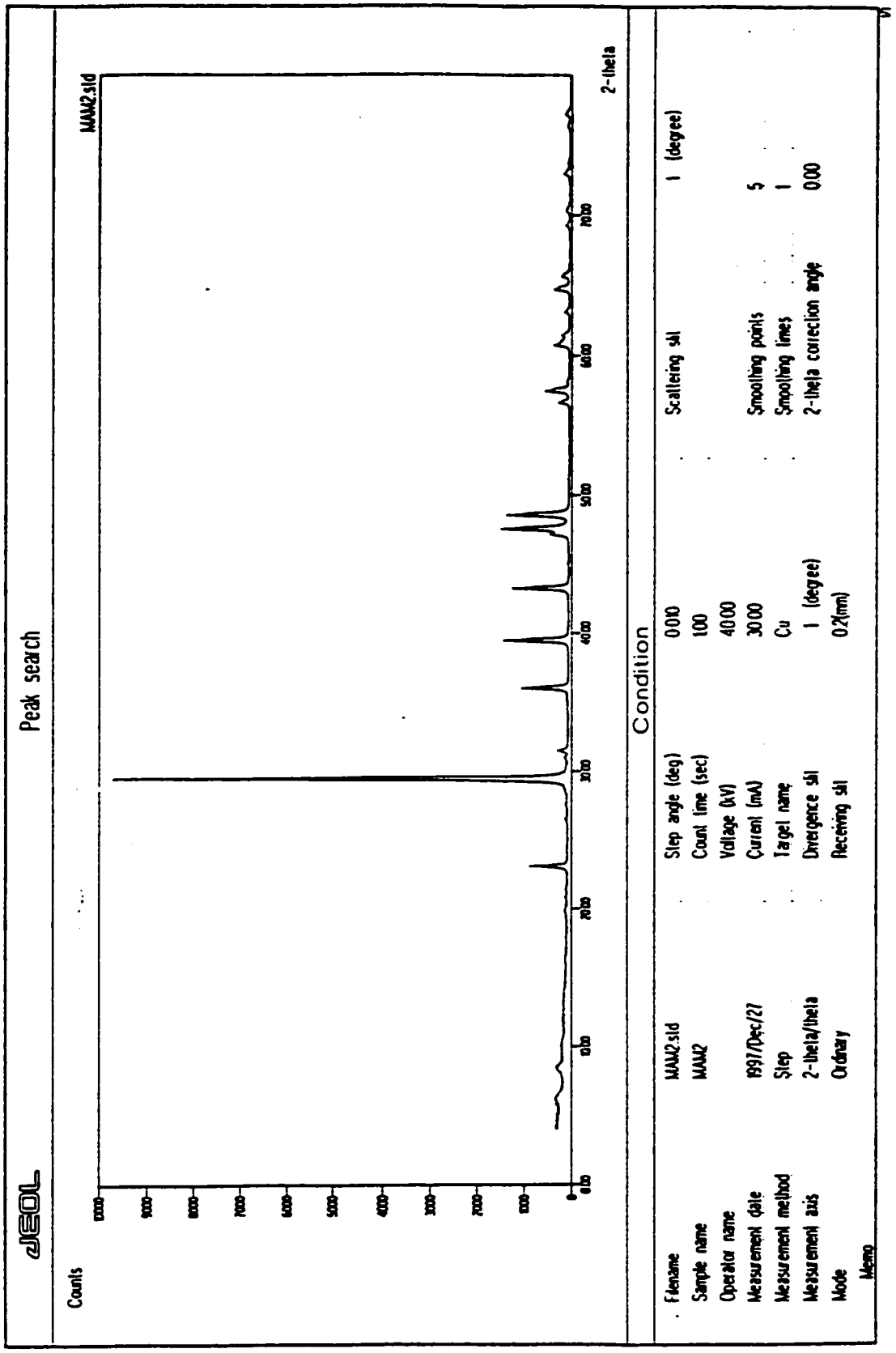

X-ray diffractogram showing search match for sample from Location # 3.

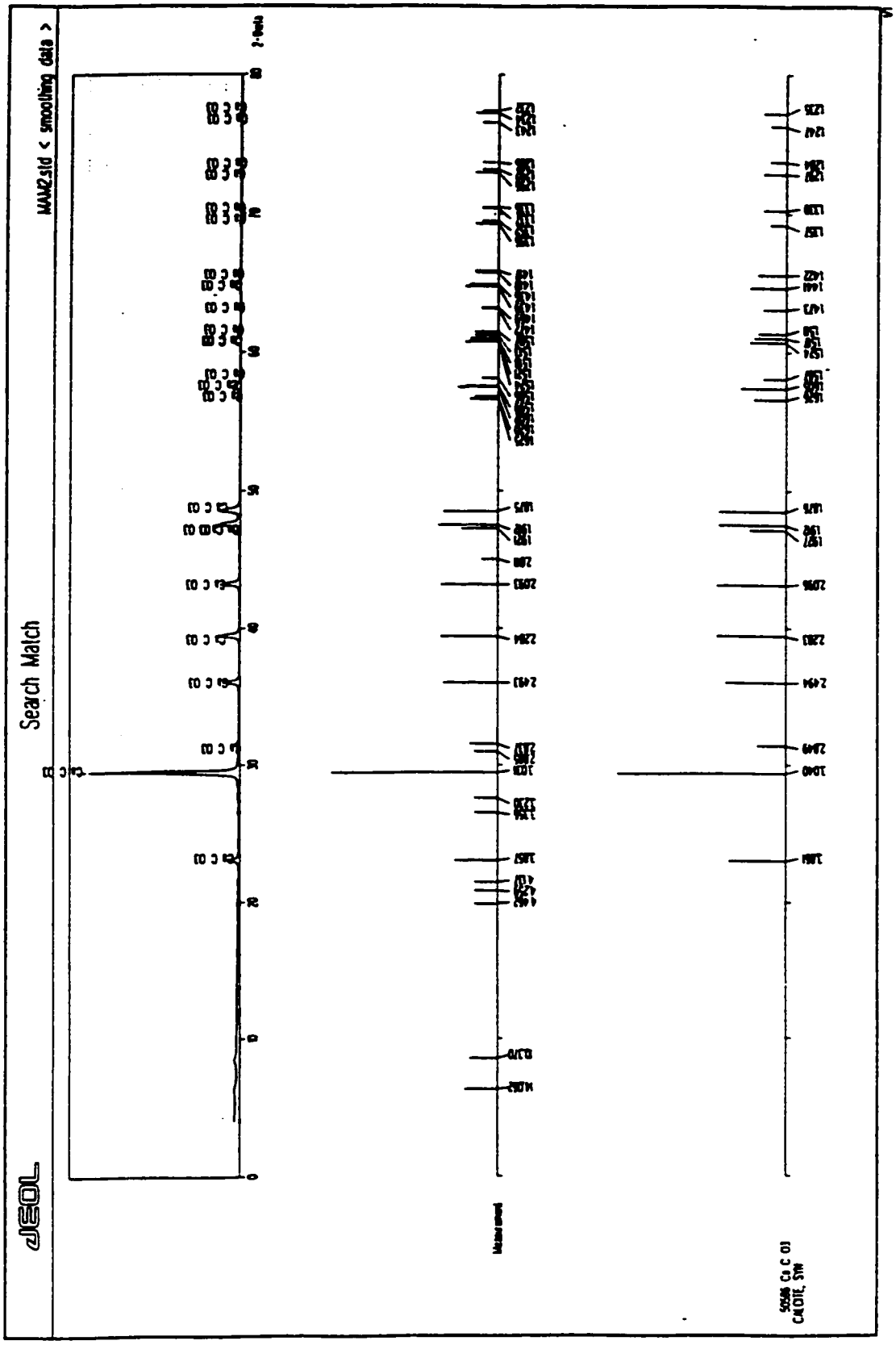

X-ray diffractogram showing peak search for sample from Location # 5.

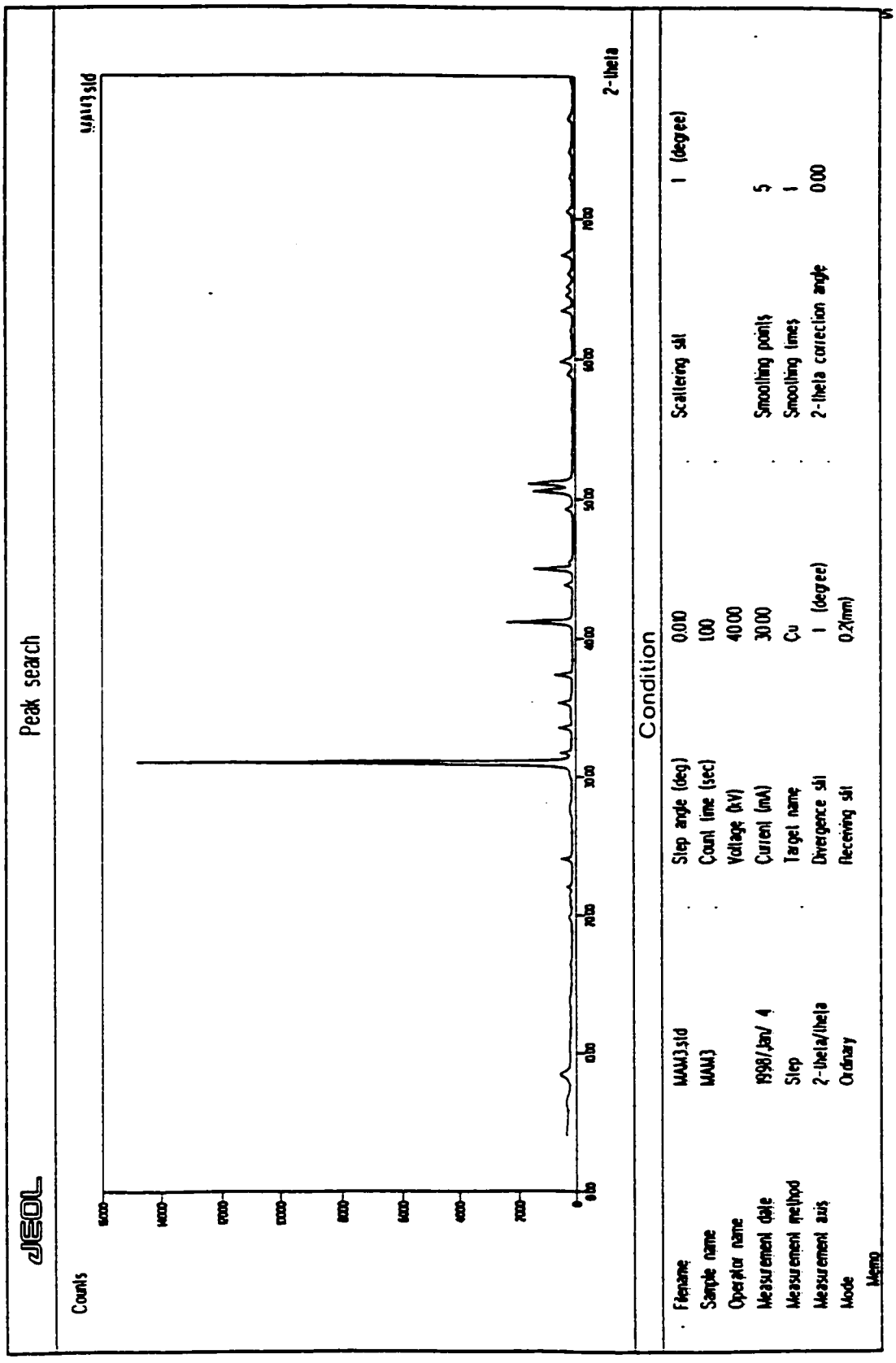

X-ray diffractogram showing search match for sample from Location # 5.

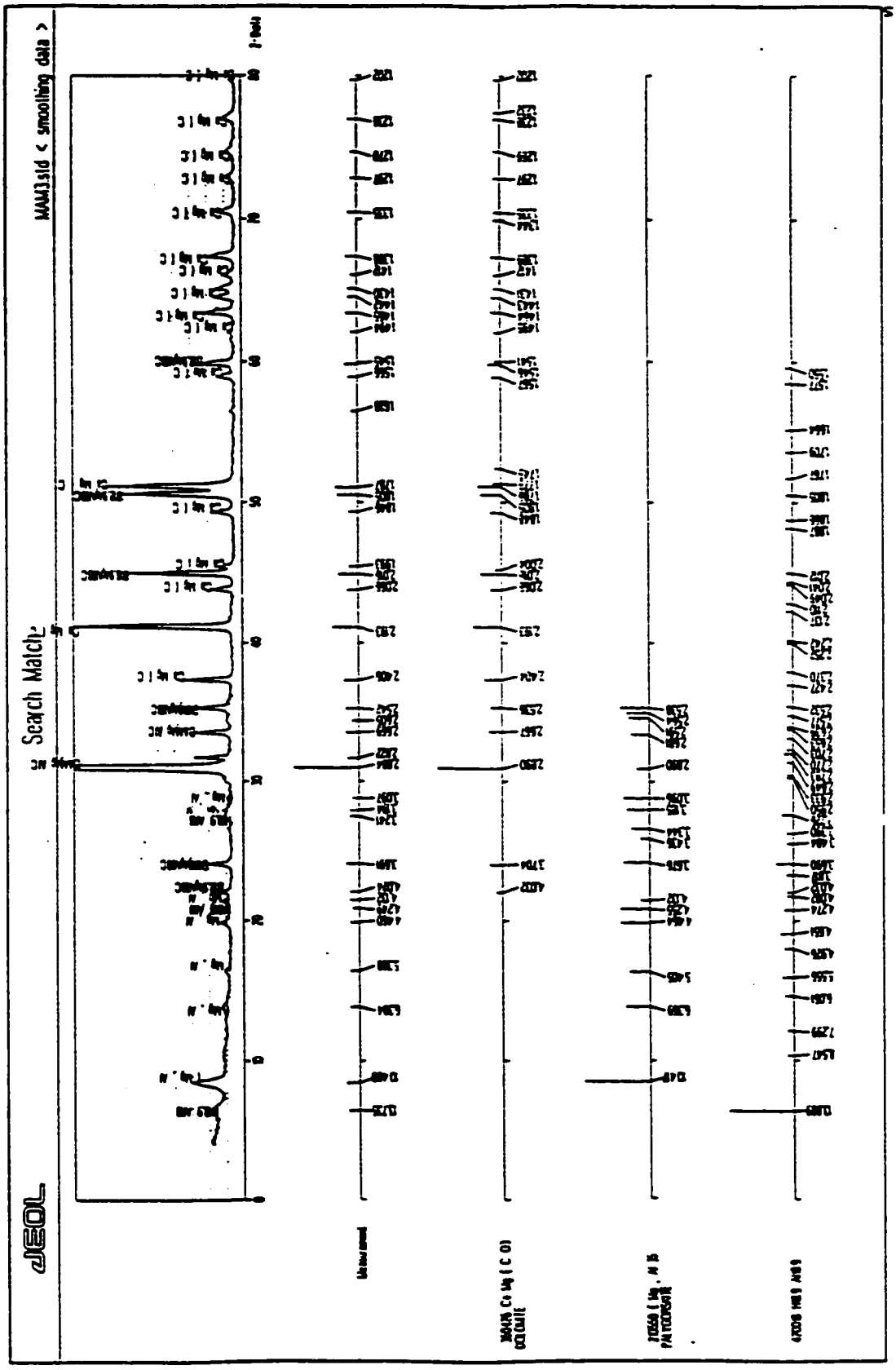

X-ray diffractogram showing peak search for sample from Location # 2.

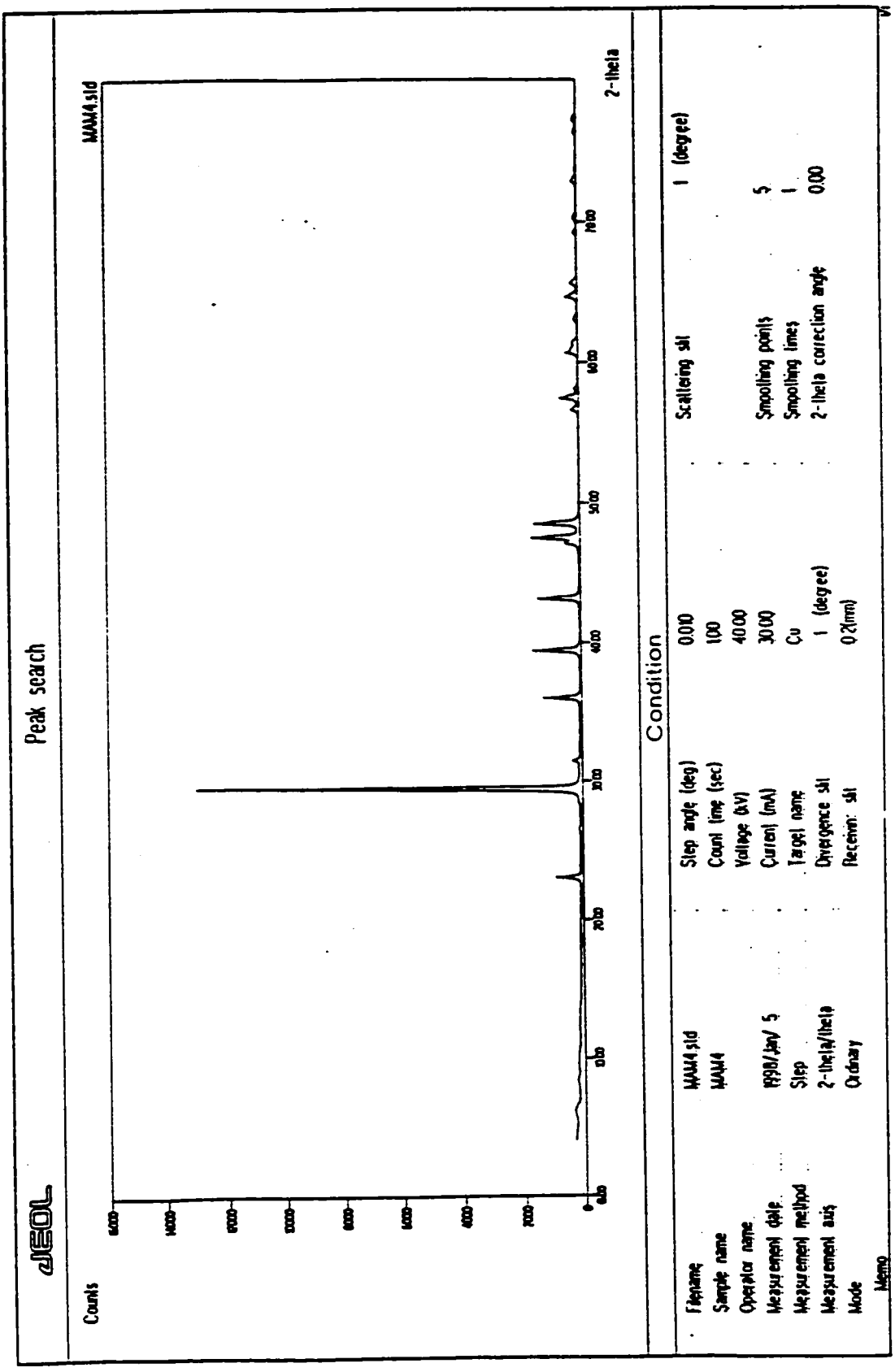

X-ray diffractogram showing search match for sample from Location # 2.

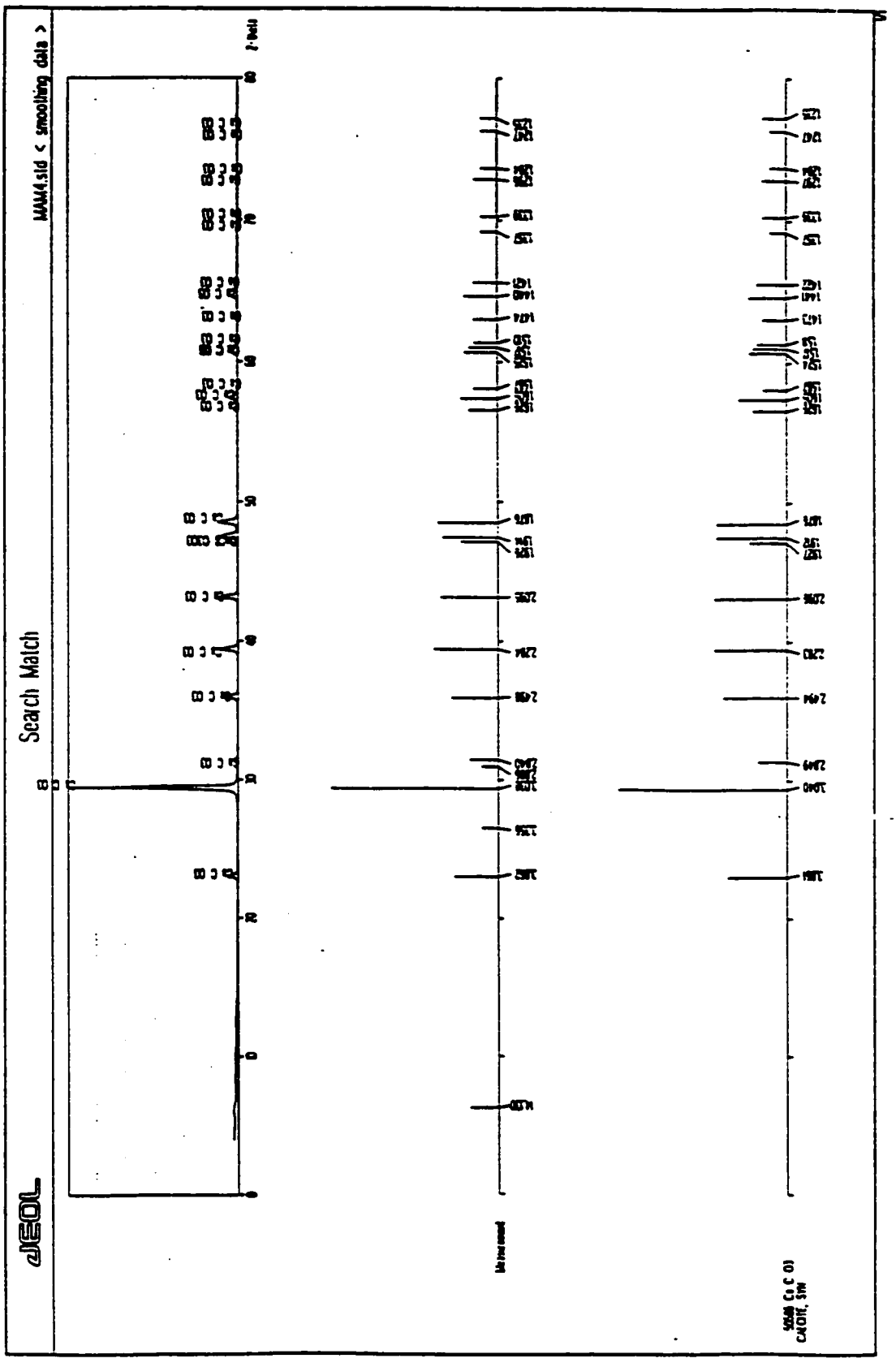

X-ray diffractogram showing peak search for sample from Location # 4.

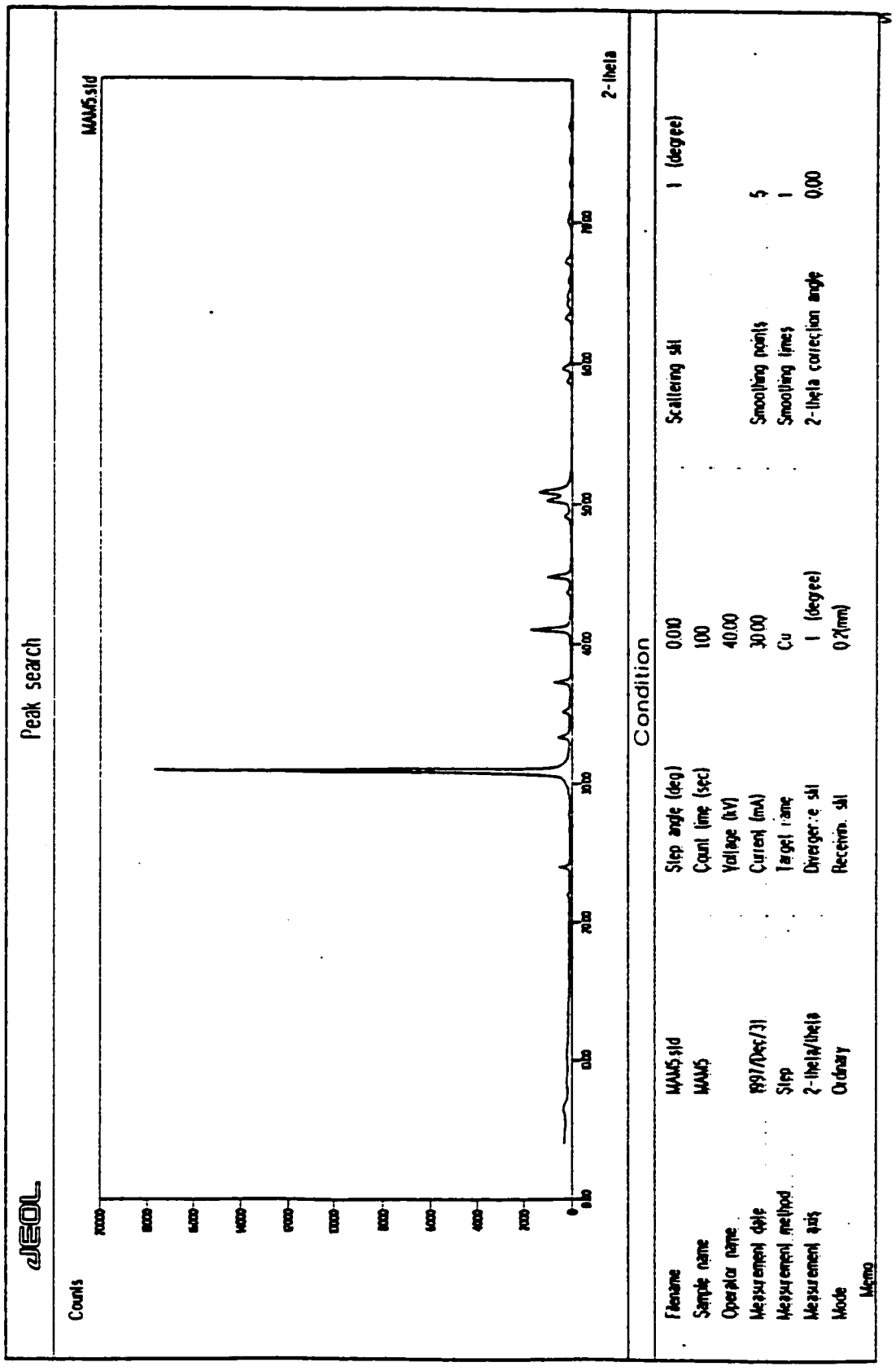

X-ray diffractogram showing search match for sample from Location # 4.

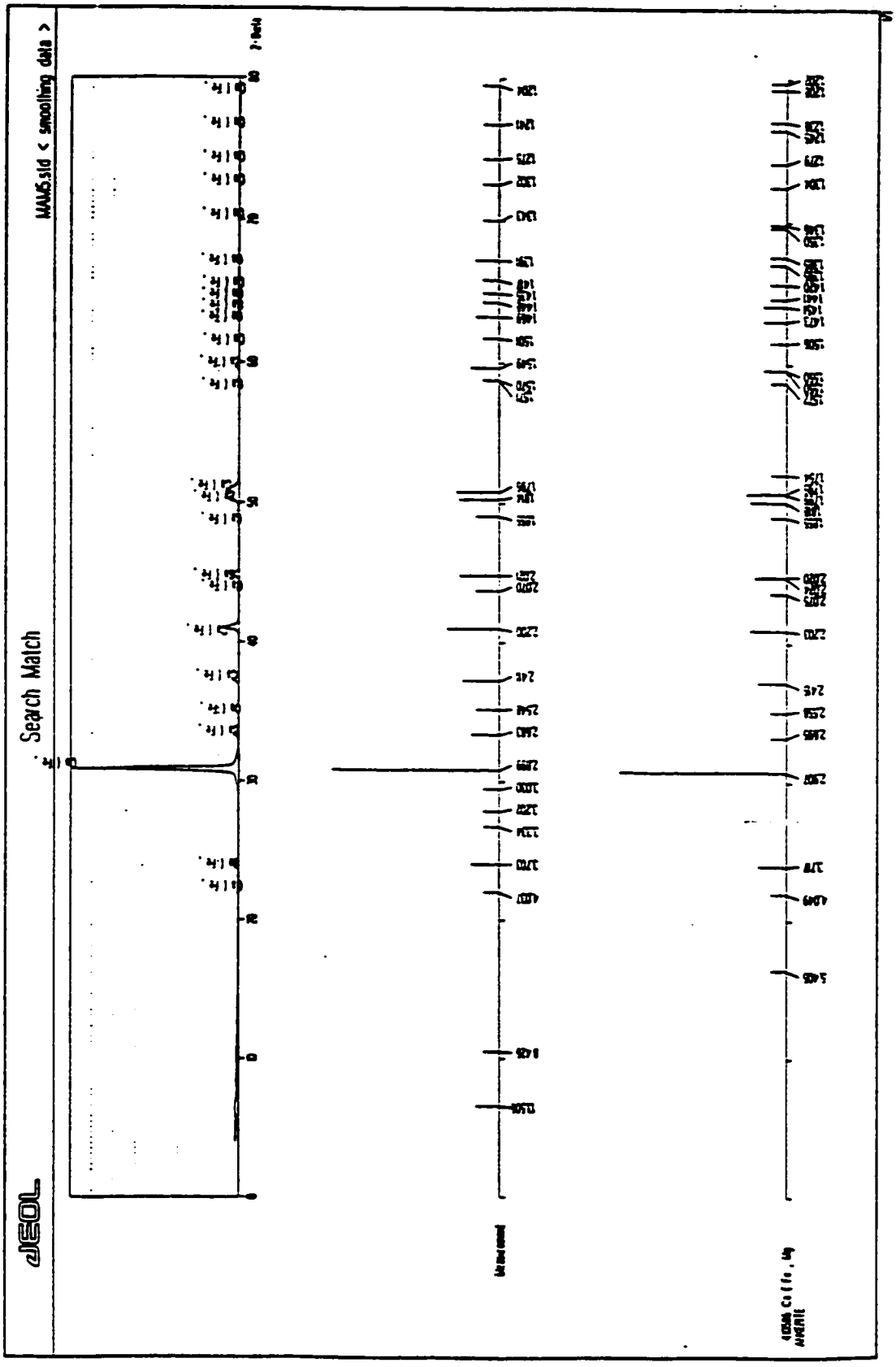

X-ray diffractogram showing peak search for sample from Location # 5.

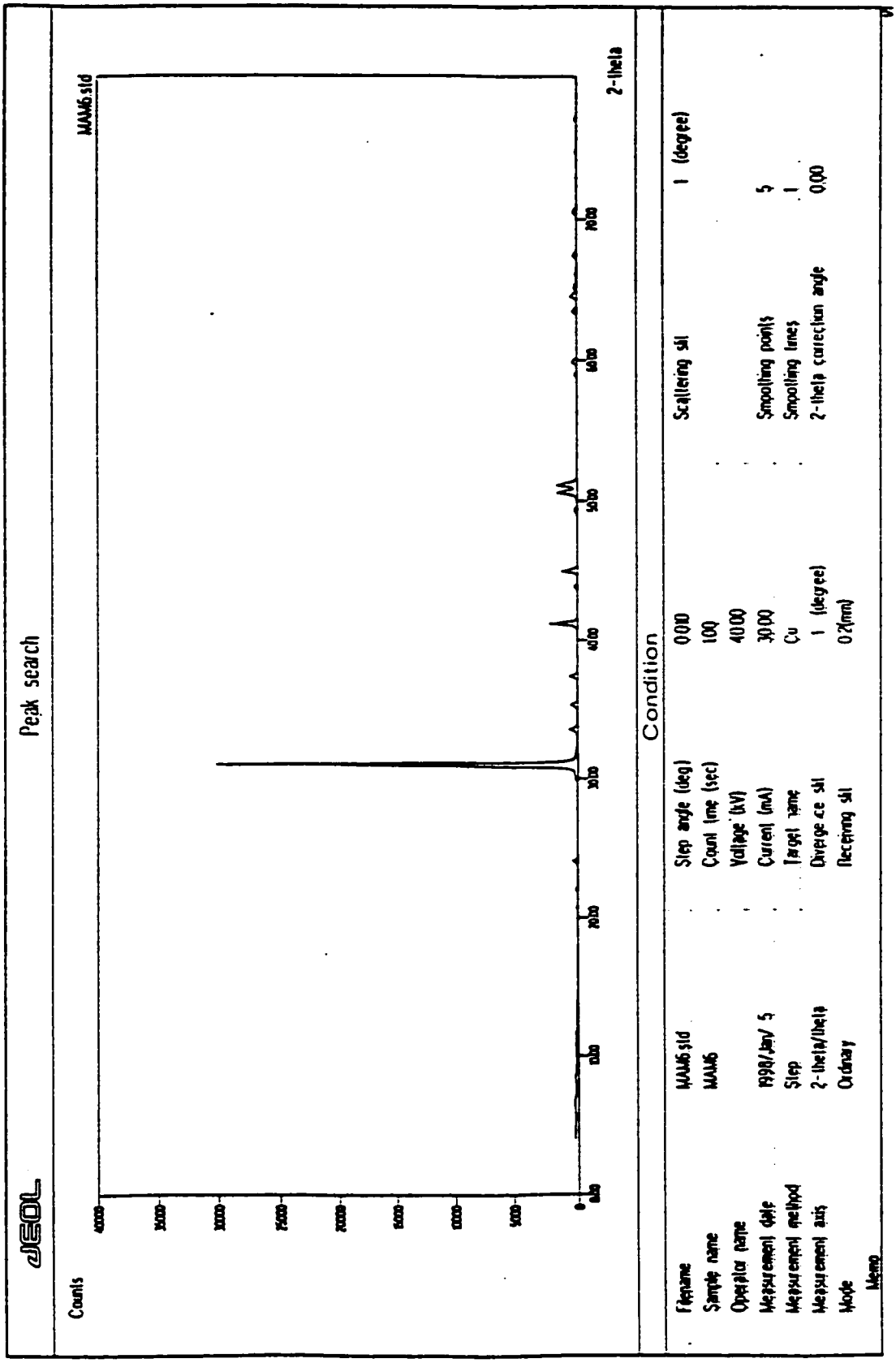

X-ray diffractogram showing search match for sample from Location # 5.

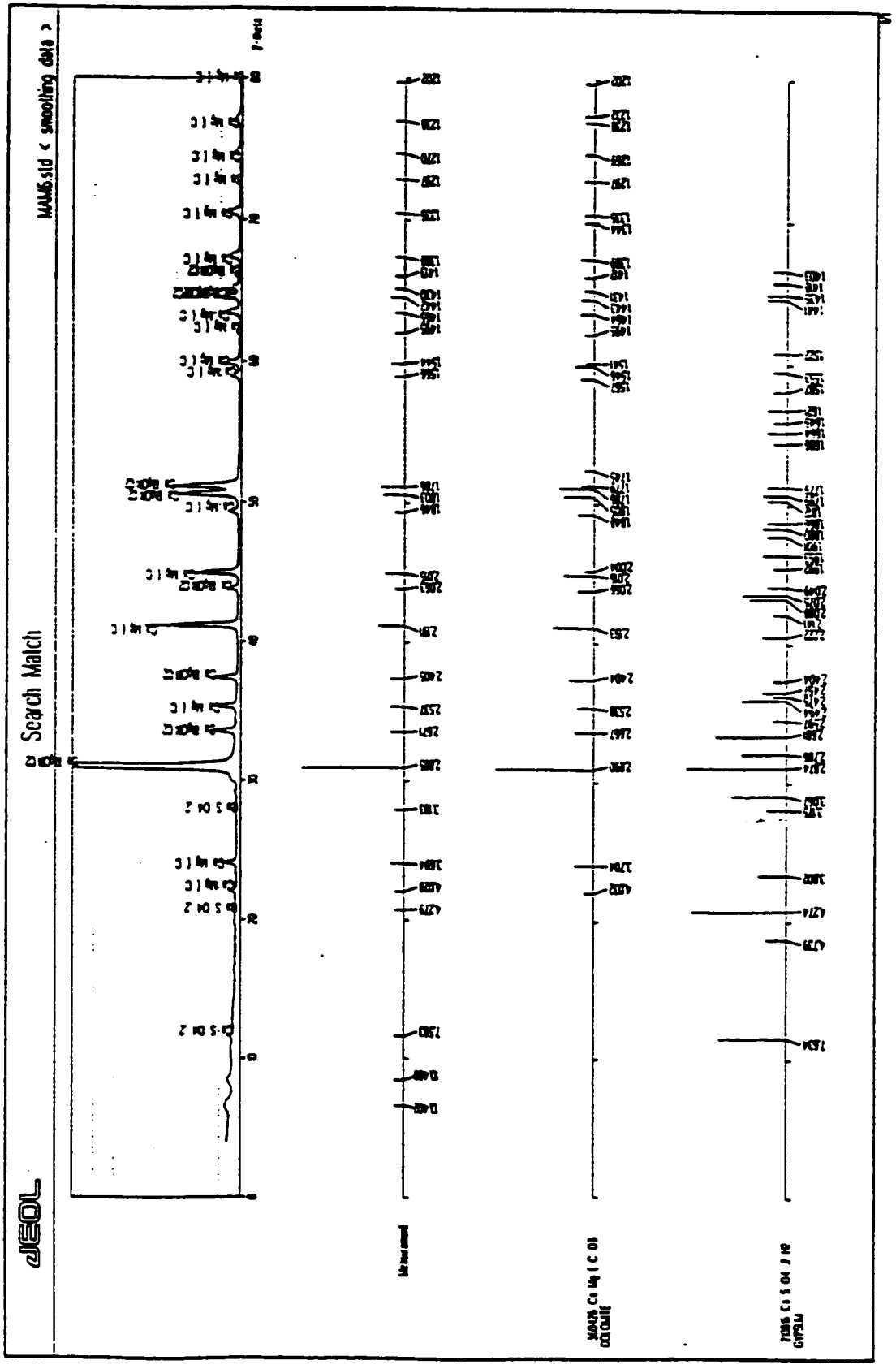

X-ray diffractogram showing peak search for sample from Location # 9.

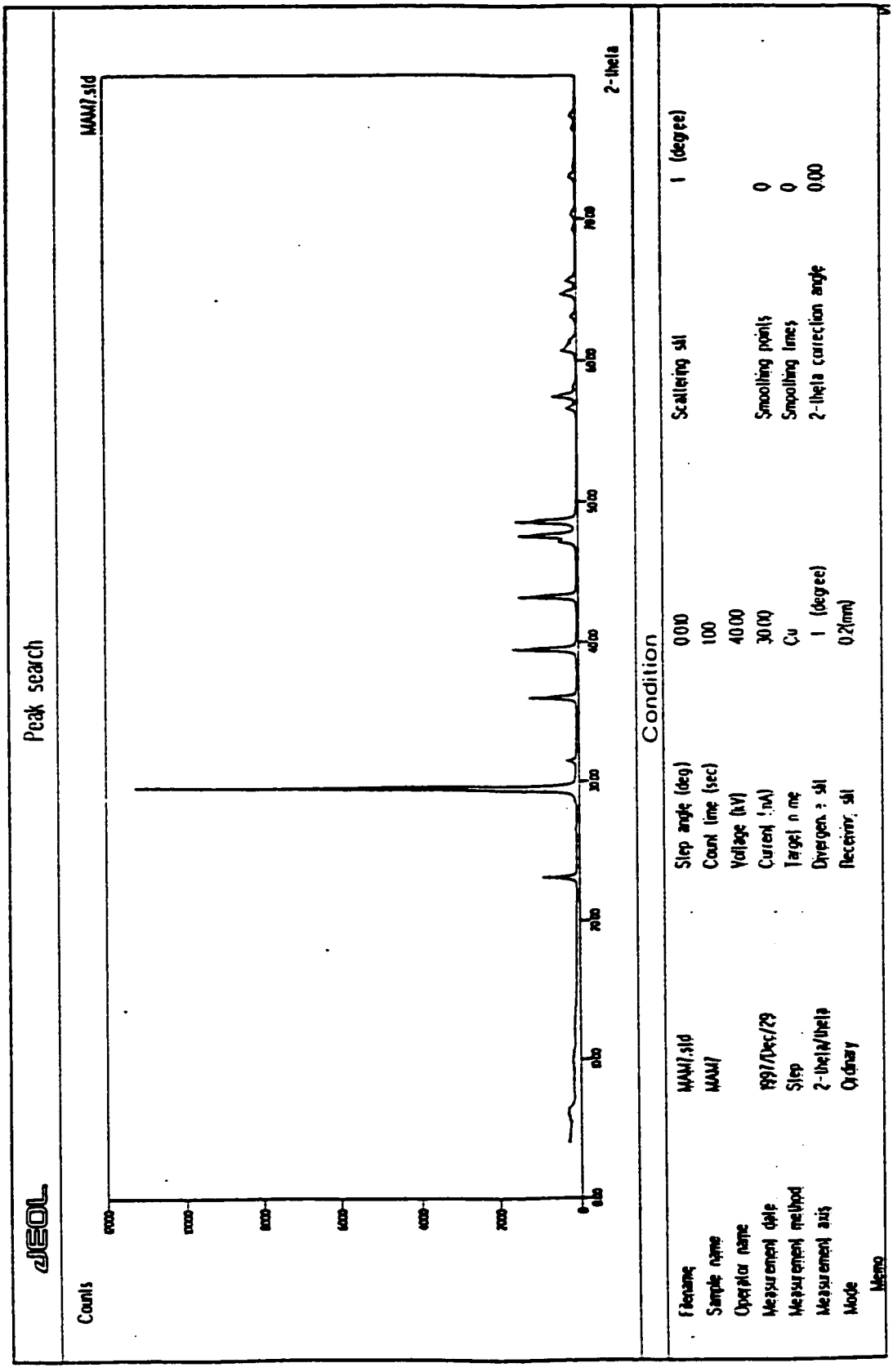

X-ray diffractogram showing search match for sample from Location # 9.

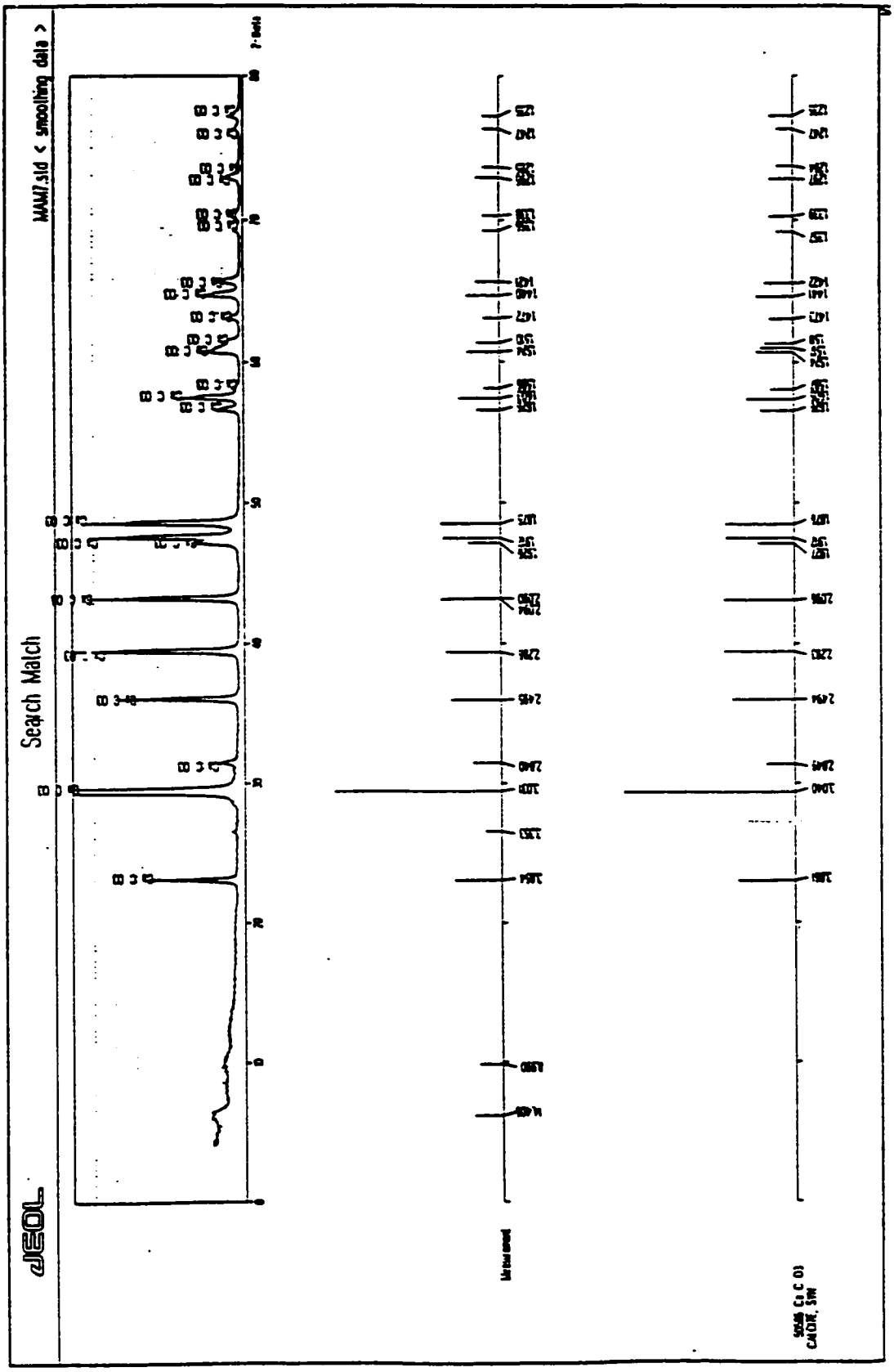

X-ray diffractogram showing peak search for sample from Location # 11.

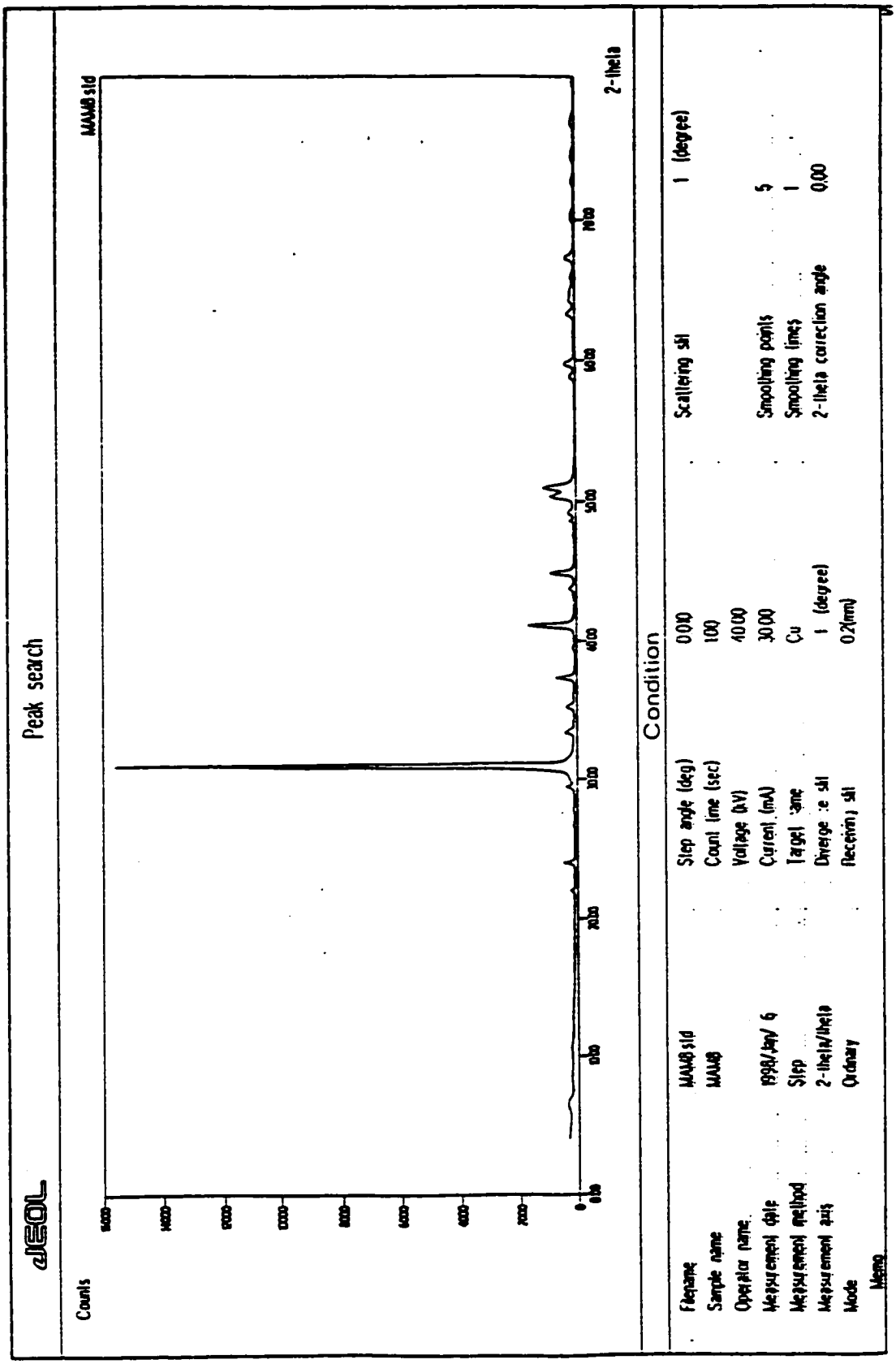

X-ray diffractogram showing search match for sample from Location # 11.

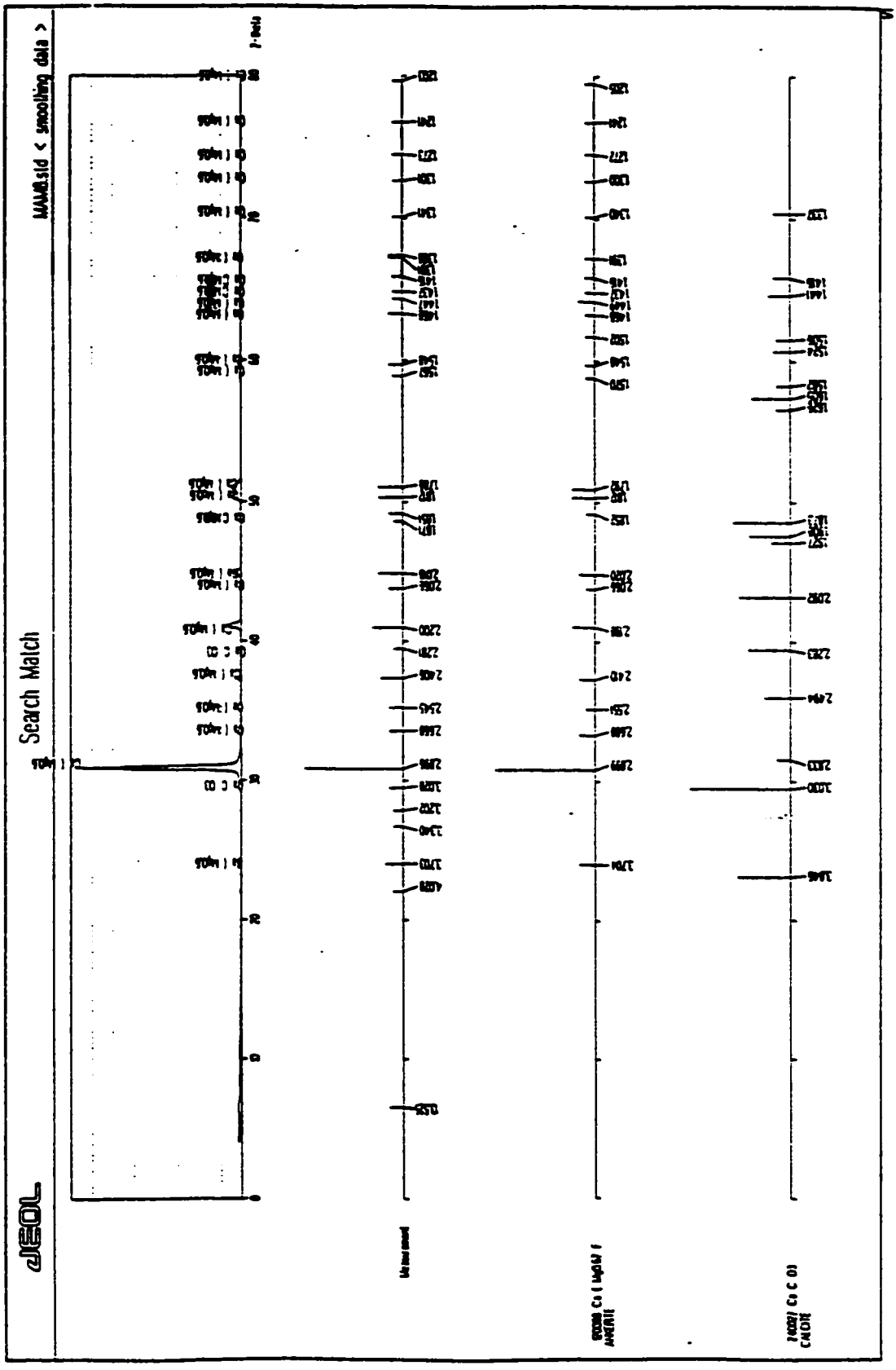

X-ray diffractogram showing peak search for sample from Location # 12.

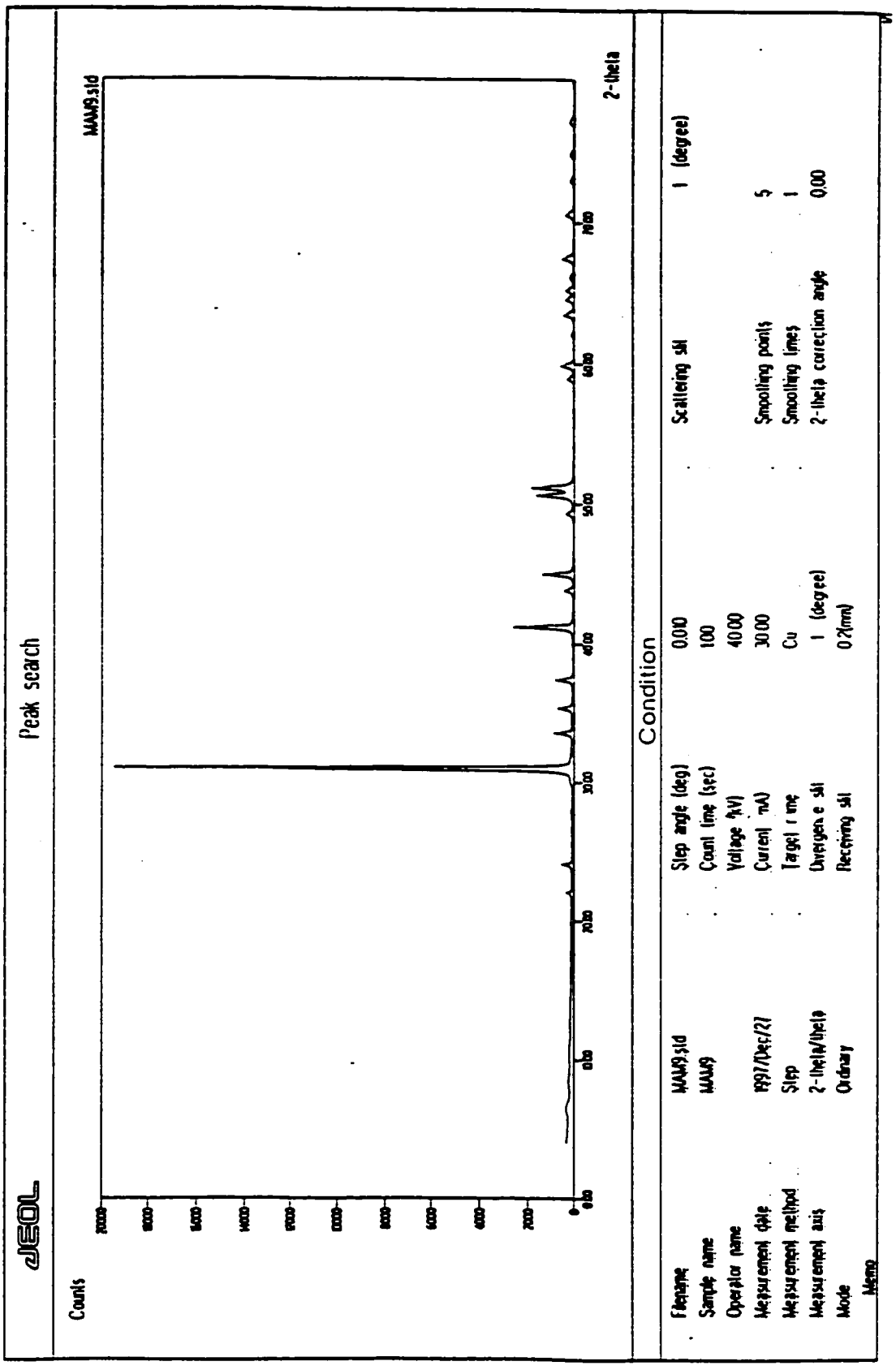

X-ray diffractogram showing search match for sample from Location # 12.

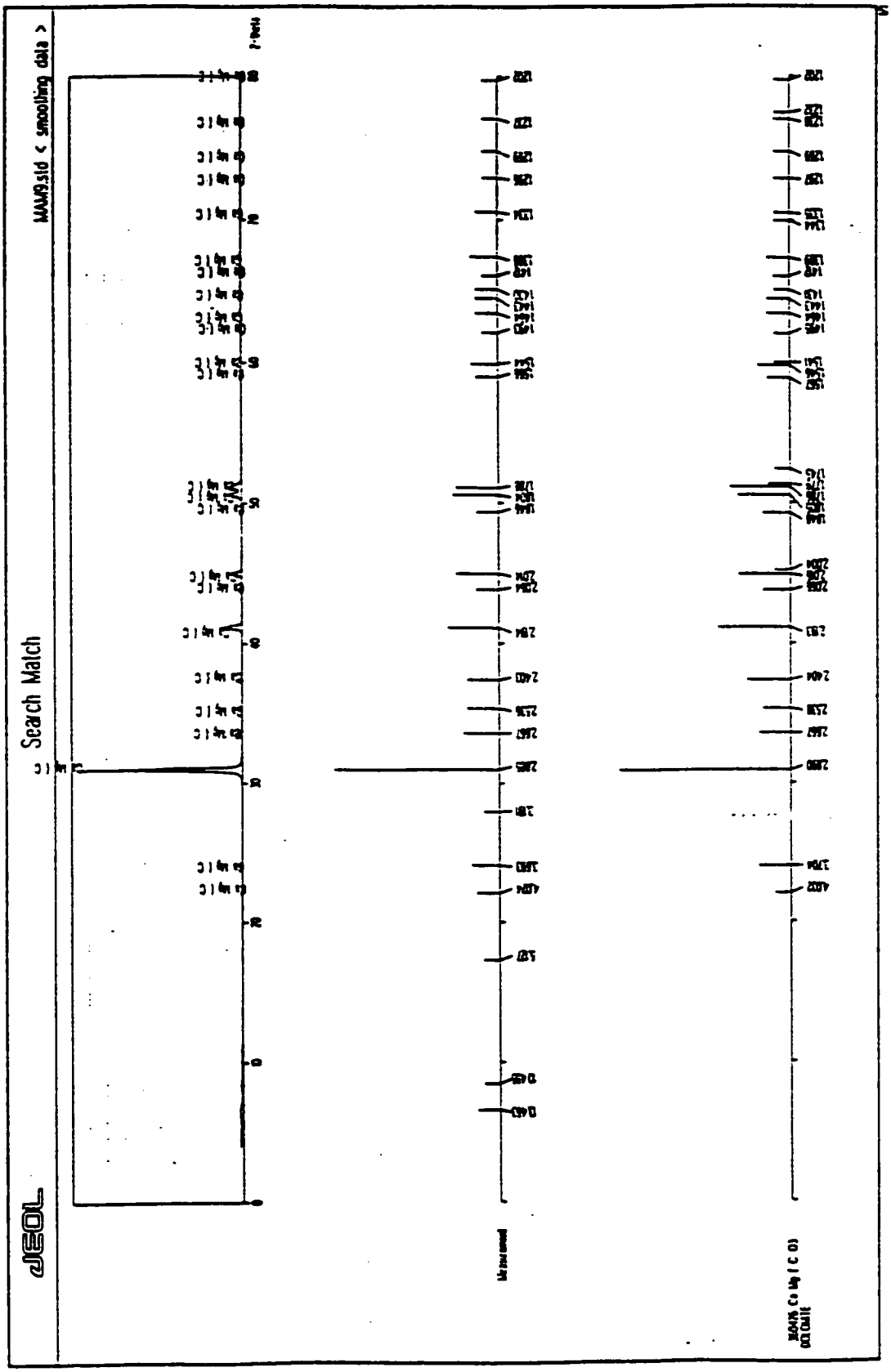

APPENDIX C

THIN SECTION DESCRIPTIONS

Petrographic description of thin sections texture and porosity is as follow:

Thin Section No. 1: A wackestone sample with low porosity (less than 2 %). This poor porosity is represented mainly by small irregular vuggy pores. Some of the Nummulites, consisting 10 to 15 percent of the sample, are replaced by microsparite calcite cement with 5 to 10 percent of the sample. The groundmass is a fine-grained micrite (80-85 %).

Thin Section No. 2: A crystalline dolomite sample with low porosity (2-3 %), with microsparite calcite cement. This poor porosity is represented mainly by small irregular vuggy pores. The complete dolomitization is observed, by where most of the organic remains and the original fabric of the rock are almost compeletely destoryed.

Thin Section No. 3: A grainstone sample, with low porosity (2-3 %), emdedded in a fine-grained micritic groundmass. This poor porosity is represented mainly by small irregular vuggy pores. The Nummulites are filled with microsparite calcite cement with 5 to 10 percent of the sample. The grain percentage is 70 to 80, and the matrix percentage is 10 to 15.

Thin Section No. 4: A packstone sample, with low porosity (5 %). The gorundmass is a fine-grained micrite (20-30 %). Intercrystalline and intraparticle porosities are observed. The sparite cement probably come of a latter stage, with 5 to 10 percent of the sample. It is observed in replacing the morphological structure of the Nummulites grains. Nummulites, with 40 to 50 percent of the sample, are abundant, but there are some other forms of forraminifera.

Thin Section No. 5: A crystalline dolomite sample with high porosity (Interparticle porosity - 20 %) with some microsparite calcite cements. No fossils are observed. Dolomite rhombs are abundant with 60 to to 65 percent of the sample.

Thin Section No. 6: A crystalline dolomite sample with high porosity (25 %). Intercrystalline and intraparticle porosities are observed. The cement is microsparite calcite. The groundmass is a fine-grained micrite. The grain percentage is 65 to 70.

Thin Section No. 7: A crystalline dolomite sample with high porosity (Interparticle porosity -25 %) with microsparite calcite cement. The groundmass is a fine-grained micrite. The Dolomitization is affecting the cement also.

Thin Section No. 8: A crystalline dolomite sample with porosity (Intercrystalline porosity) of less than 10 %. Bioclasts make about 5 % by volume. The groundmass is a fine-grained micrite.

Thin Section No. 9: A crystalline dolomite sample with high porosity (20-25 %), with uncompleted (undeveloped) grains. The microsparite calcite cement is dominant.Interparticle and intracrystalline porosities are observed. But most of the high porosity is mouldic porosity due to dissolution of bioclasts of different forms of foraminifera. However, some fossil forms are not dissolved; and are filled by carbonate.

Thin Section No. 10: A crystalline dolomite sample with high porosity (Interparticle porosity - 20 %). The grains are fine to medium in size. The cement is microsparite calcite cement. Many dolomite rhombs are coarser in size.

Thin Section No. 11: A wackestone sample with low porosity (less than 1 %). Some of the calcite grains replacing the Nummulites. The groundmass is a fine-grained micrite (80-85 %). The grain percentage is 10 to 15 of the sample. The cement percentage is 5 to 10.There is a variety of microfossils in addition to Nummulites. Thin veinlets are filled by sparry calcite. Fenestrae (3 %) are present.

Thin Section # 11 - Location # 3

Thin Section # 4 - Location # 4

Thin Section # 3 - Location # 4

Photomicrographs showing microfossils in some of the thin sections (mag. X 11.25).

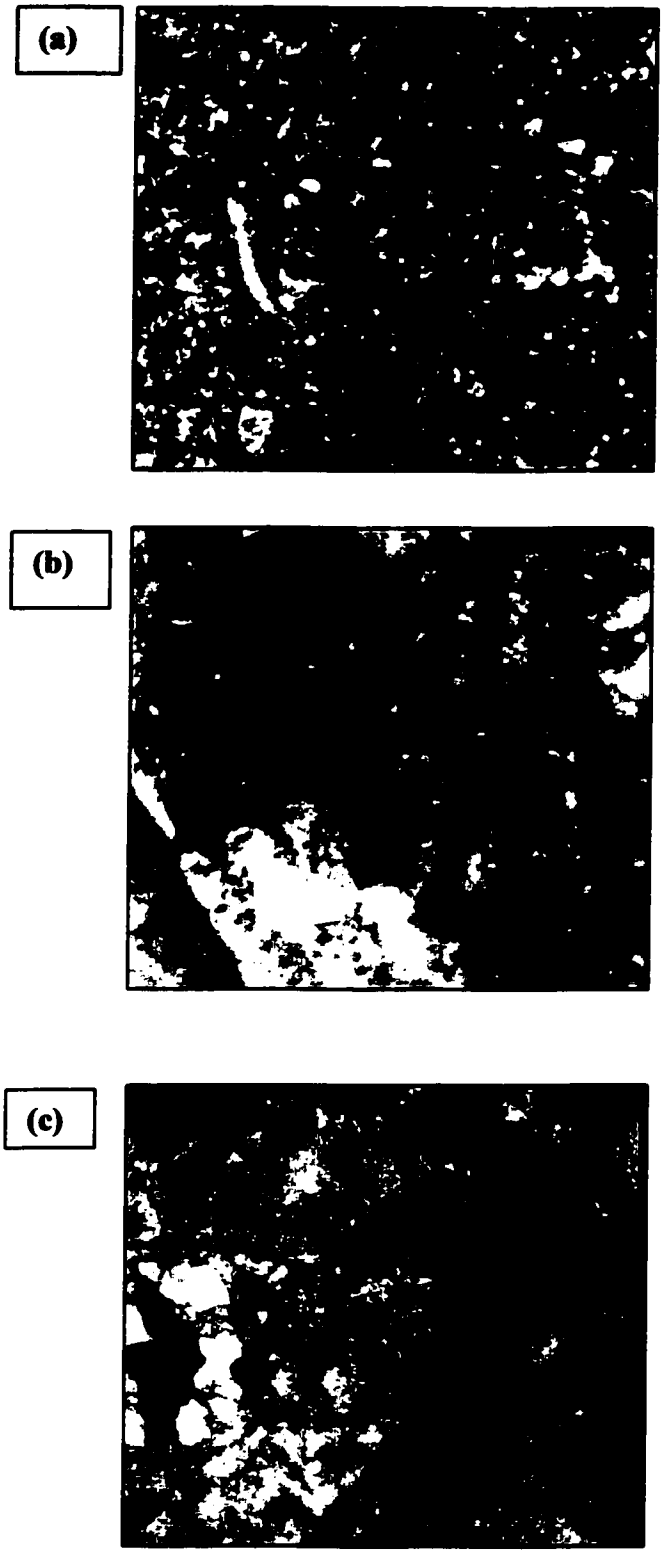

Photomicrographs showing: (a) A wackestone sample (Location # 3 – Thin Section #1). (b) A packstone sample (Location # 4 – Thin Secion # 4). (c) A grainstone sample (Location # 4 – Thin Section # 3) (mag. X 11.25).

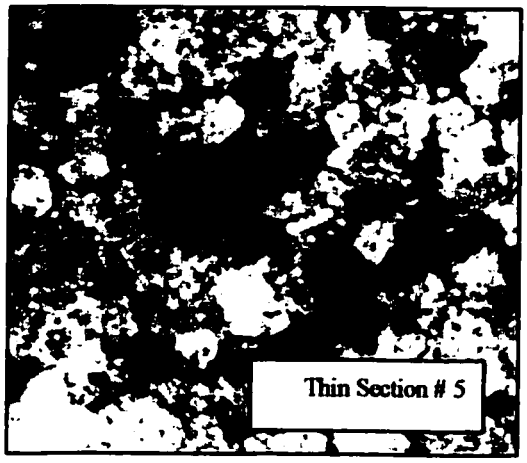

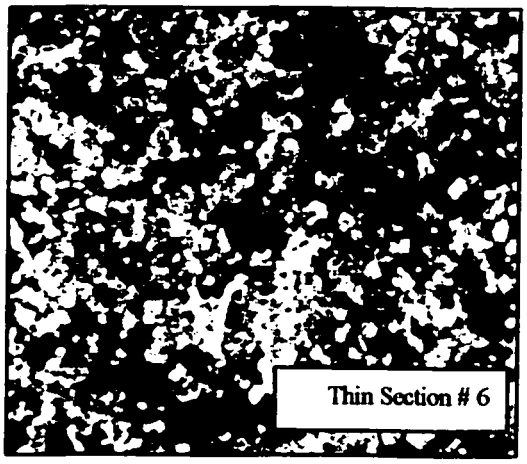

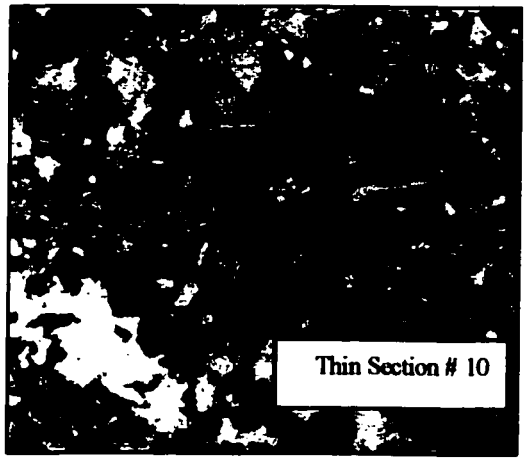

Photomicrographs showing crystalline samples (Location # 5 – Thin Section # 5,6, and 10) with high porosity (mag. X 11.25).

APPENDIX D

THE SEISMIC REFRACTION INTER PRETATION PROGRAMS (SIP) RESULTS AND REFRACTION SEISMOGRAMS

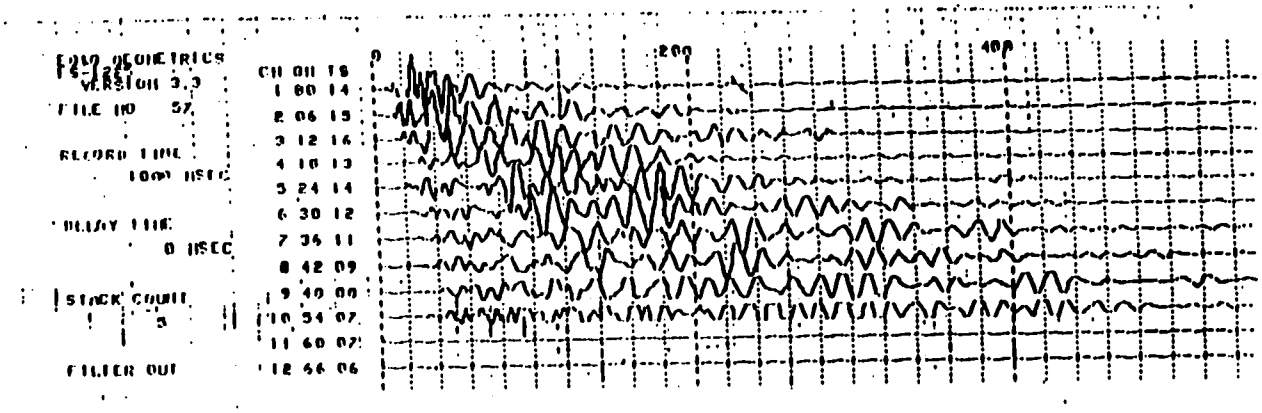

Seismic Refraction Seismogram - Profile ' SP 1000'

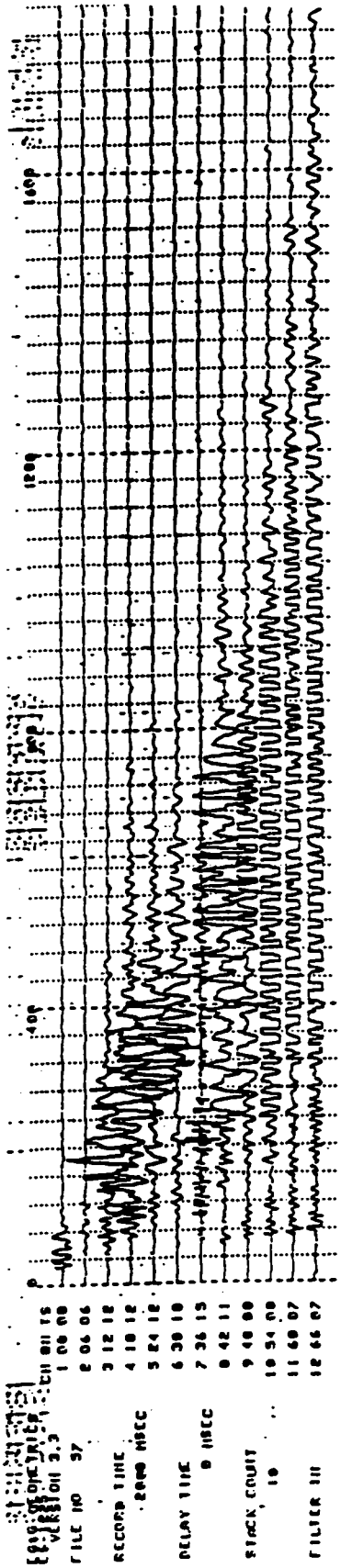

Seismic Refraction Seismogram - Profile ' SP 2000'

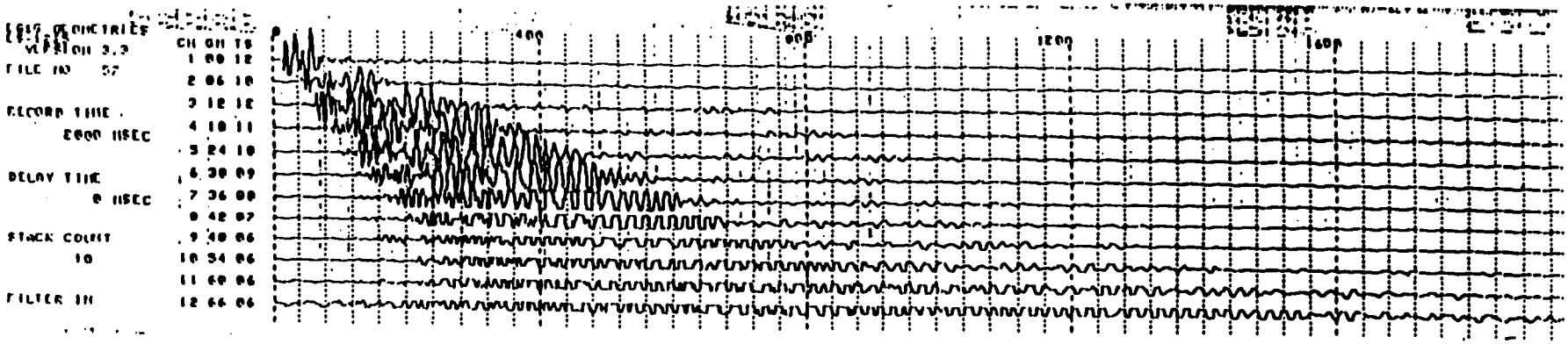

Seismic Refraction Seismogram - Profile ' SP 3000'

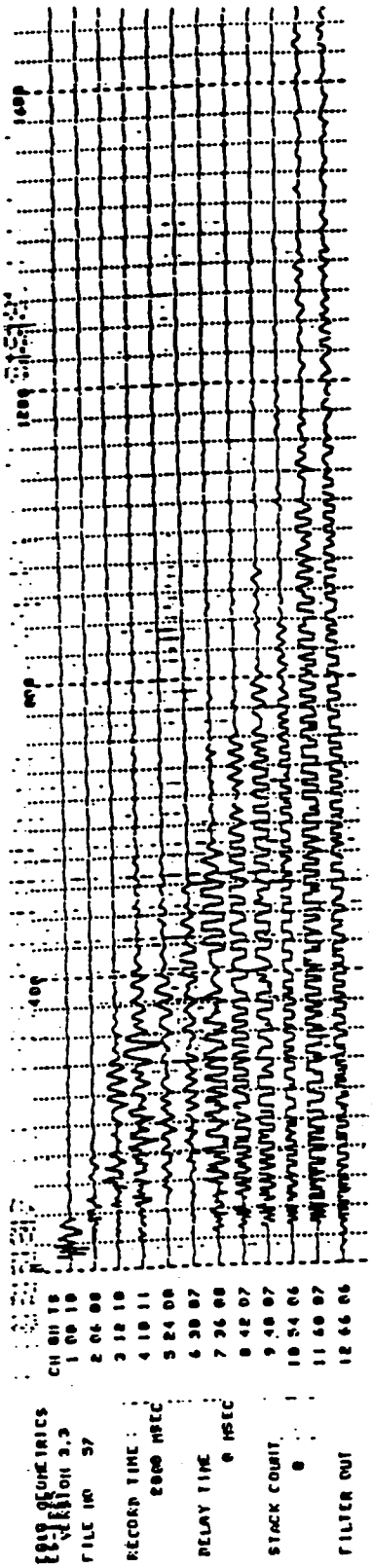

Seismic Refraction Seismogram - Profile ' SP 4000'

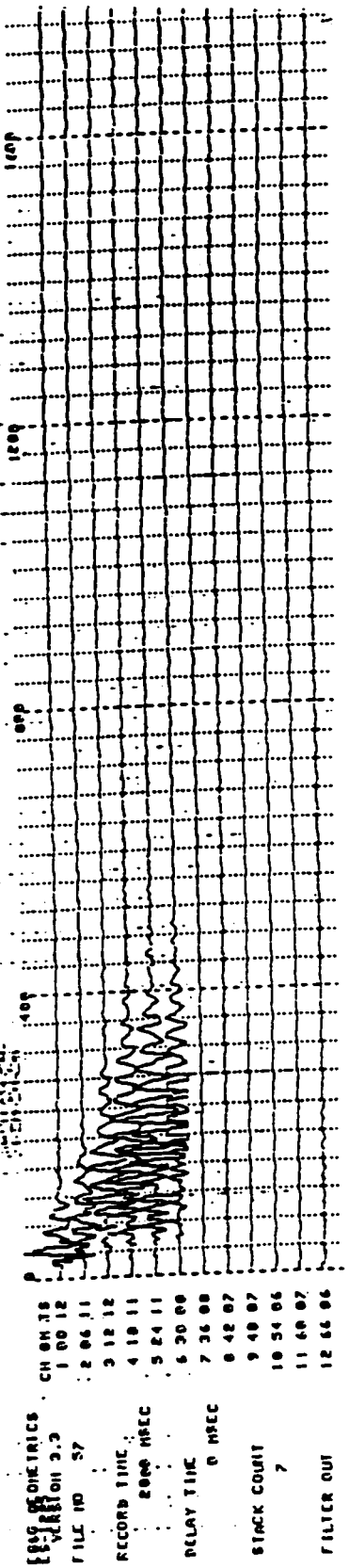

Seismic Refraction Seismogram - Profile ' SP 5000'

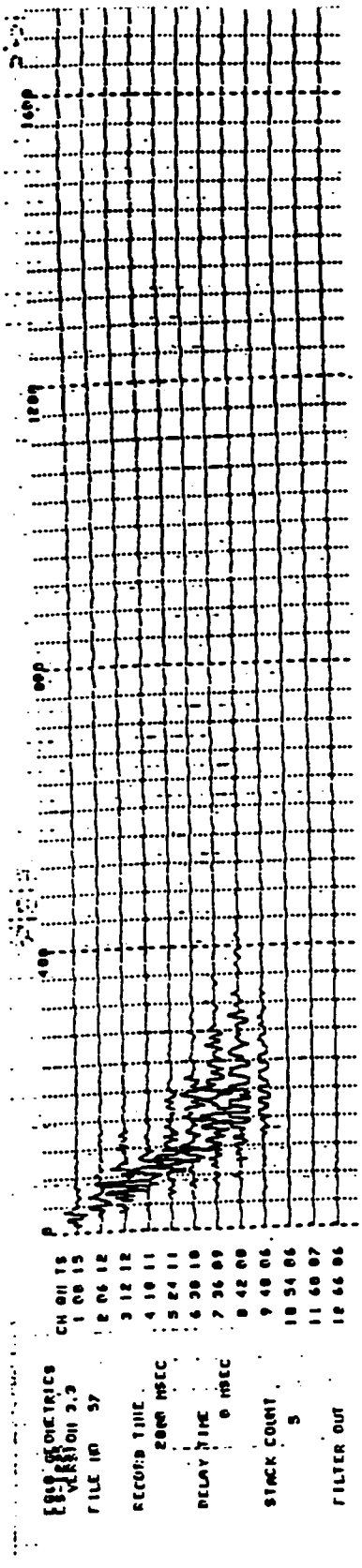

Seismic Refraction Seismogram - Profile ' SP 6000'

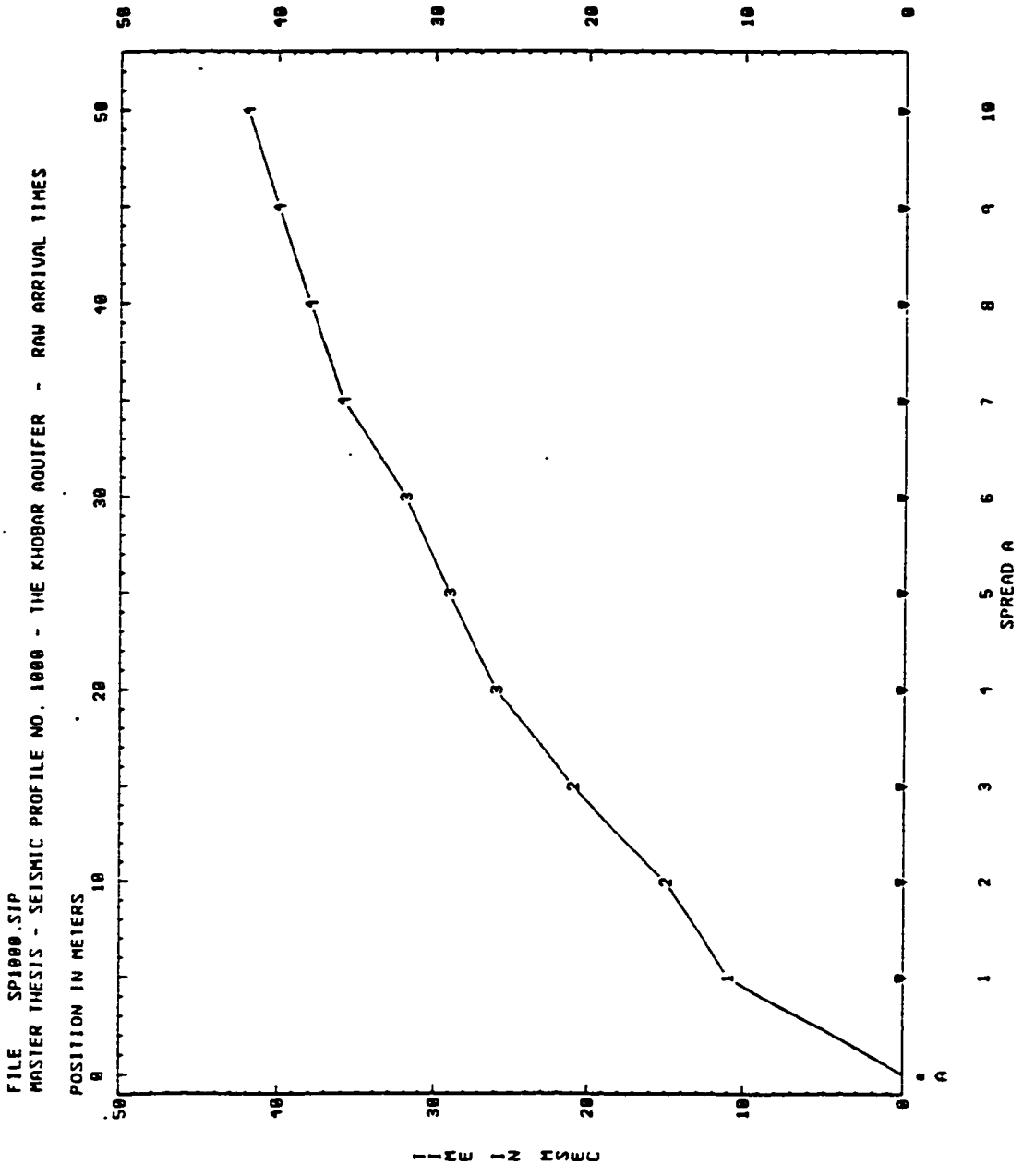
FILE SP1000.SIP
MASTER THESIS - SEISMIC PROFILE NO. 1000 - THE KHOBAR AQUIFER - RAW ARRIVAL TIMES
POSITION IN METERS
TIME IN MSEC
SPREAD A

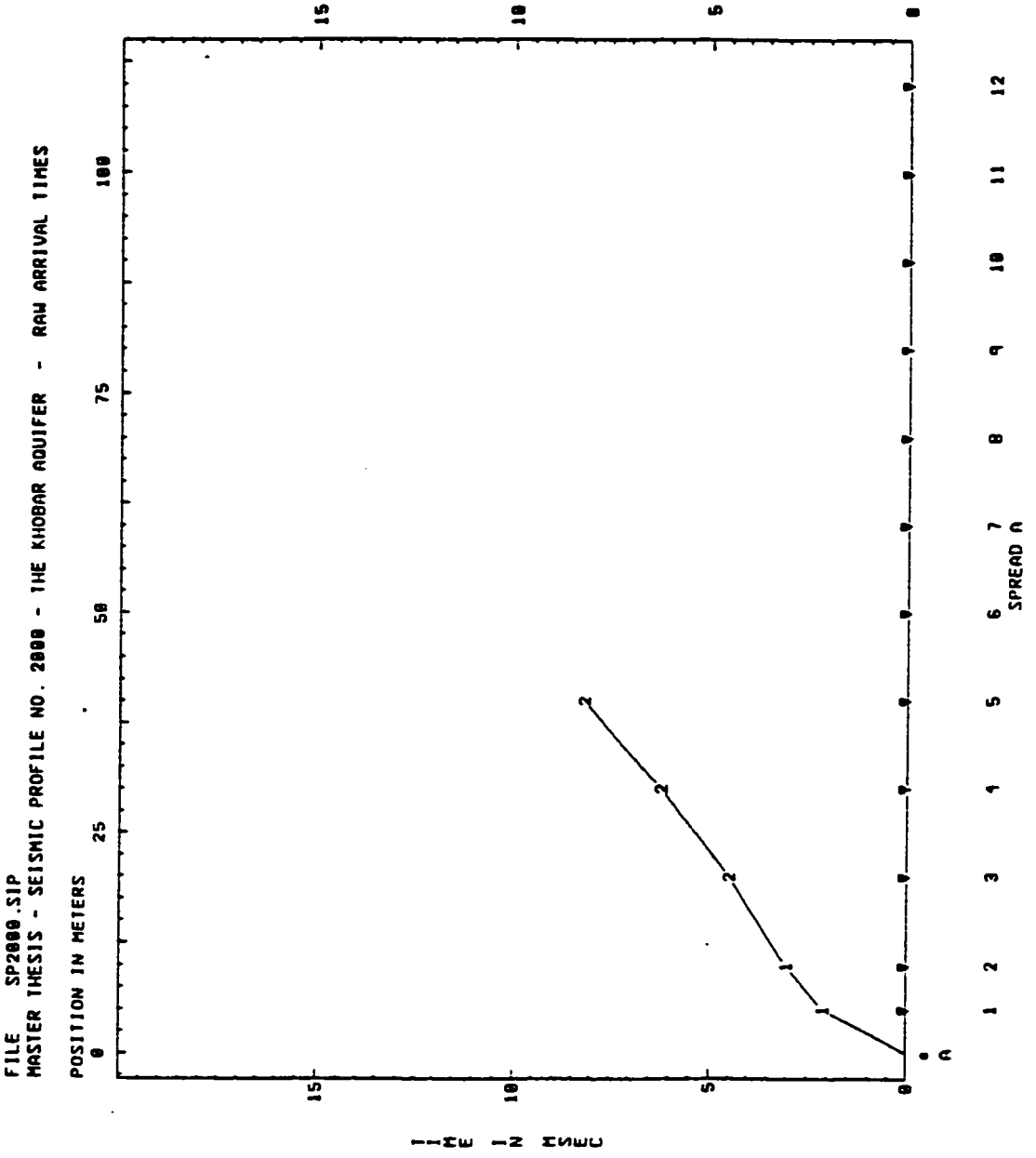
FILE SP2000.SIP
MASTER THESIS - SEISMIC PROFILE NO. 2000 - THE KHOBAR AQUIFER - RAW ARRIVAL TIMES
POSITION IN METERS
0
25
50
75
100
15
10
5
0
TIME IN MSEC
SPREAD A
1 2 3 4 5 6 7 8 9 10 11 12

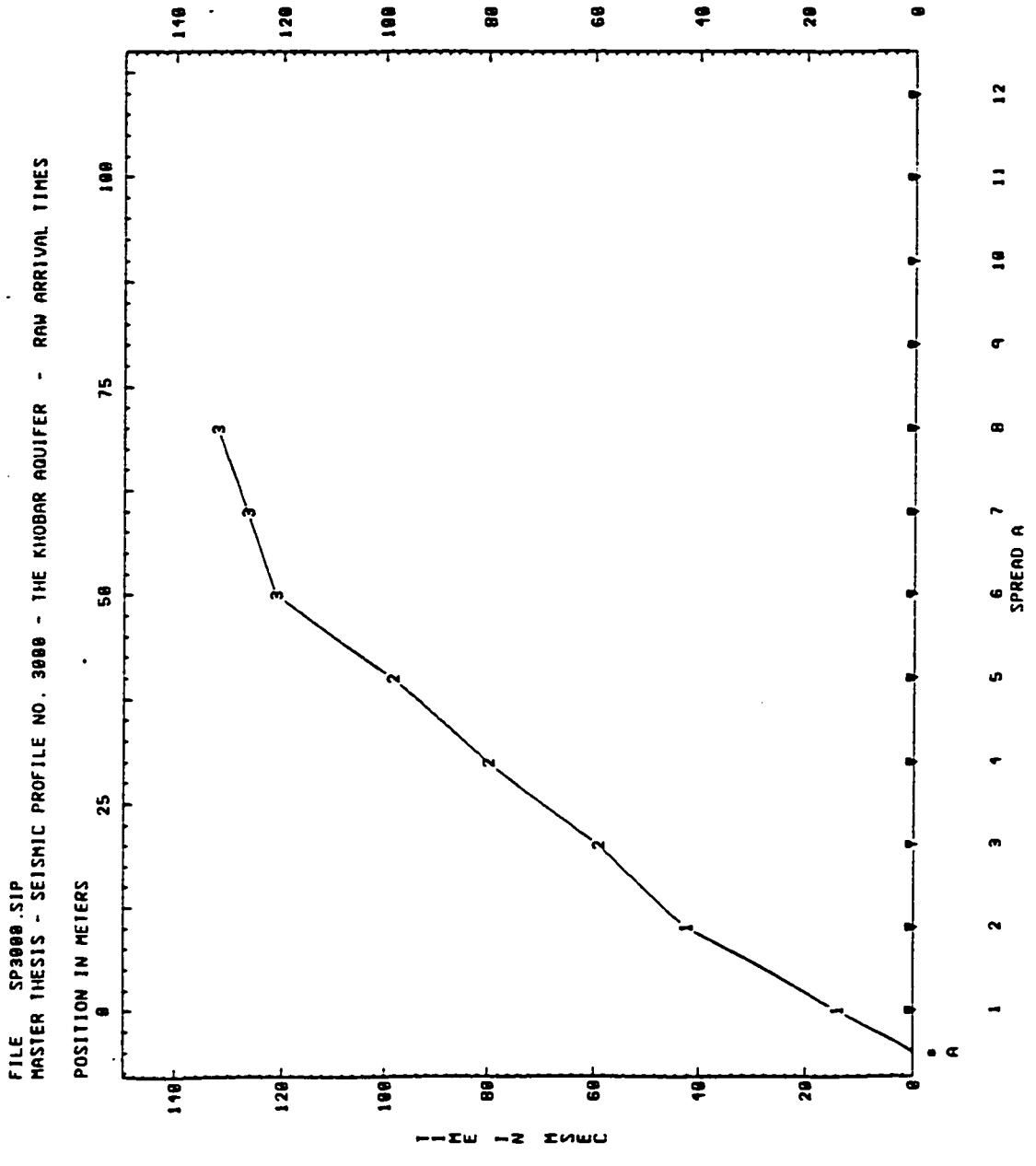
FILE SP3000.SIP
MASTER THESIS - SEISMIC PROFILE NO. 3000 - THE KNOBAR AQUIFER - RAW ARRIVAL TIMES
POSITION IN METERS
0
25
50
75
100
TIME IN MSEC
110
120
100
80
60
40
20
0
A
1 2 3 4 5 6 7 8 9 10 11 12
SPREAD A

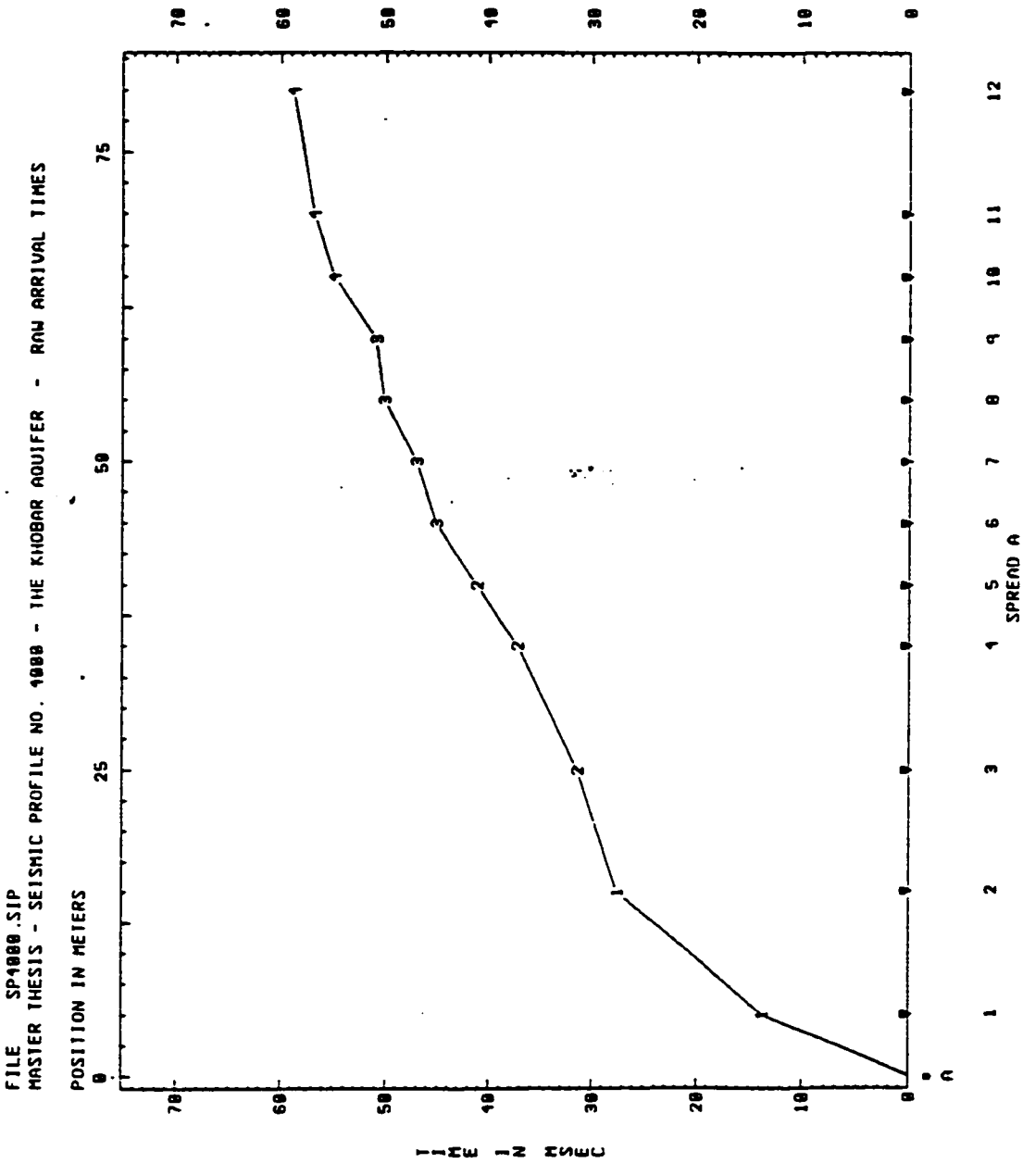
FILE SP1000.SIP
MASTER THESIS - SEISMIC PROFILE NO. 1000 - THE KHOBAR AQUIFER - RAW ARRIVAL TIMES
POSITION IN METERS
0
25
50
75
TIME IN MSEC
SPREAD A
1
2
3
4
5
6
7
8
9
10
11
12

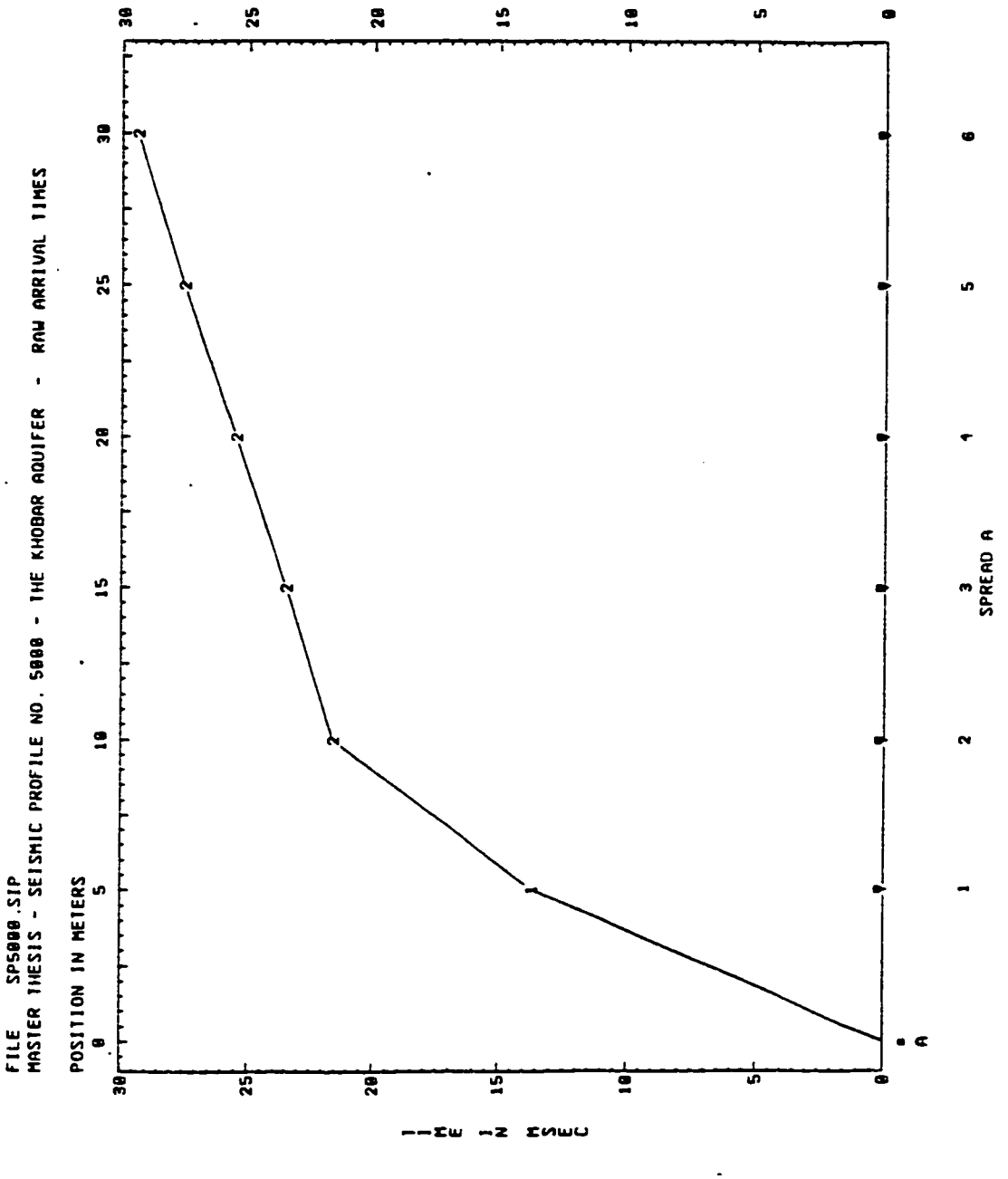
FILE SP5000.SIP
MASTER THESIS - SEISMIC PROFILE NO. 5000 - THE KHOBAR AQUIFER - RAW ARRIVAL TIMES
POSITION IN METERS
0
5
10
15
20
25
30
TIME IN MSEC
SPREAD A
A
1
2
3
5
6

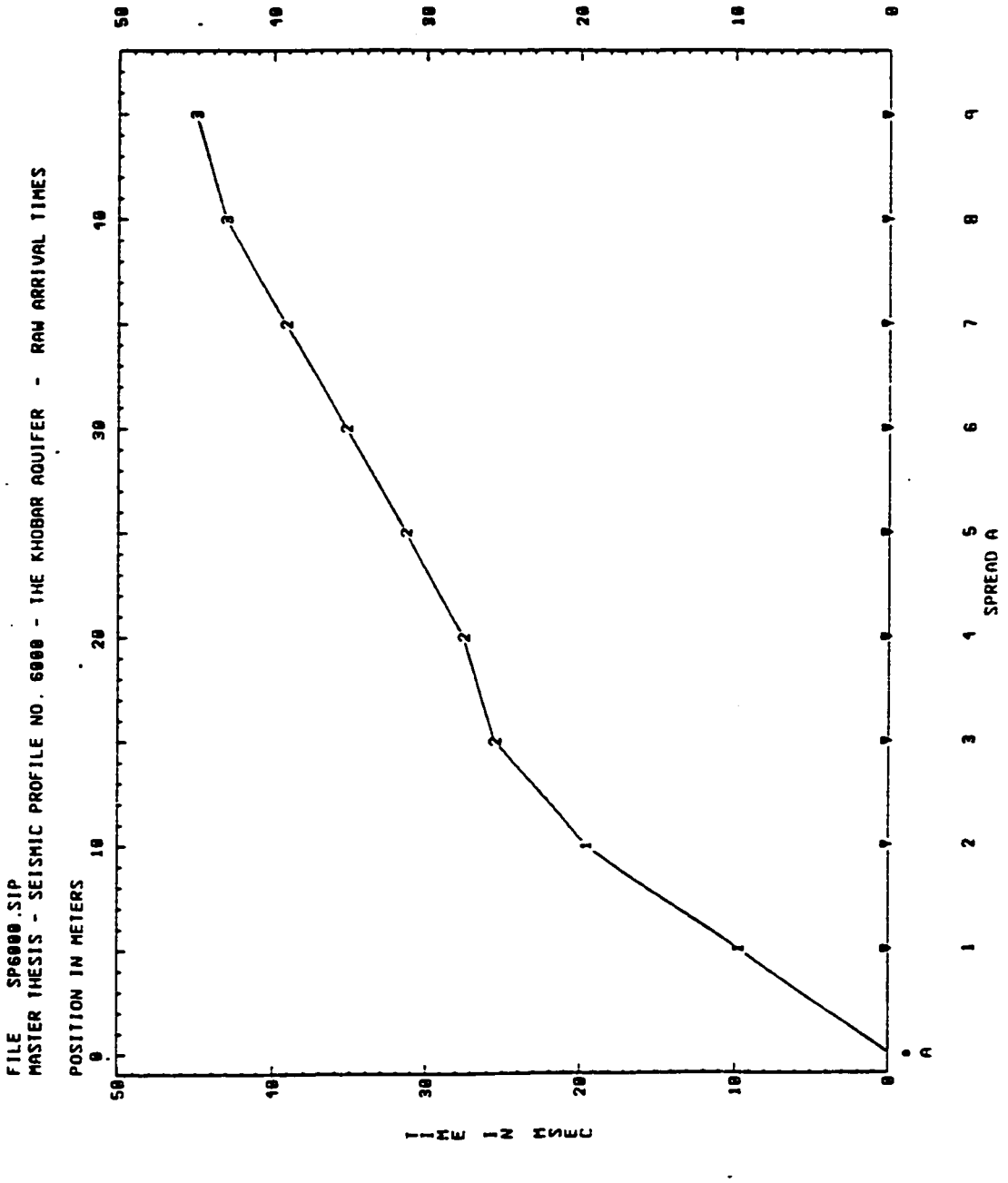
FILE SP6000.SIP
MASTER THESIS - SEISMIC PROFILE NO. 6000 - THE KHOBAR AQUIFER - RAW ARRIVAL TIMES
POSITION IN METERS
0
10
20
30
40
50
TIME IN MSEC
SPREAD A
A

INPUT DATA FILE for SP1000.SIP

TITLE FOR SIPT2/SIPLUS INPUT DATA SET for SP1000.SIP

Master Thesis - Seismic Profile No. 1000 - The Khobar Aquifer

PROGRAM CONTROL DATA

Sprds	Exist	Lays	Over	PRINTER PLOT SCALES Elev m/col	Horiz m/row	Time ms/col	DATUM Pt 1 Elev/X	CONTROL Pt 2 Elev/X	PLOT CONTROL Elevations Top	Bottom	B
1	6	4	0	0.0	0.0	0.0	0.0 0.0	0.0 0.0	0	0	-

SHOTPOINT AND GEOPHONE DATA

Spread A, 1 SP, 10 Geo's, X-Shift = 0.0, X-True = 0, Units: M

SP	Elev	X-Loc	Y-Loc	Depth	Uphole T	Fudge T	End SP
A	0.0	0.0	0.0	0.0	0.0	0.0	1

ARRIVAL TIMES AND LAYERS REPRESENTED

Geo	Elev	X-Loc	Y	SP A	L
1	0.0	5.0	0.0	11.0	1
2	0.0	10.0	0.0	15.0	2
3	0.0	15.0	0.0	21.0	2
4	0.0	20.0	0.0	26.0	3
5	0.0	25.0	0.0	29.0	3
6	0.0	30.0	0.0	32.0	3
7	0.0	35.0	0.0	36.0	4
8	0.0	40.0	0.0	38.0	4
9	0.0	45.0	0.0	40.0	4
10	0.0	50.0	0.0	42.0	4

VELOCITY ANALYSIS TABLES for SP1000.SIP

Layer 1 Velocity from direct arrivals

Spread A	SP	Geo	DD	V	Avg V
	A	1	5.0	455	
					455

Wtd Avg Velocity computed for Layer 1 = 455

Layer 2 Velocity computed by regression of raw uncorrected arrivals

Spread A V	Ti	Geos	<-SP->	Geos	Ti	V	Avg V	Avg T
			A	2 3	3.0	833	833	3.
						Avg =	833	for

Layer 2 Velocity computed by Hobson-Overton method

Not enough points.

Wtd Avg Velocity computed for Layer 2 = 833

Layer 3 Velocity computed by regression of raw uncorrected arrivals

Spread A V	Ti	Geos	<-SP->	Geos	Ti	V	Avg V	Avg T
			A	4 6	14.0	1667	1667	14.
						Avg =	1667	for

Layer 3 Velocity computed by Hobson-Overton method

Not enough points.

Wtd Avg Velocity computed for Layer 3 = 1667

Layer 4 Velocity computed by regression of raw uncorrected arrivals

Spread A V	Ti	Geos	<-SP->	Geos	Ti	V	Avg V	Avg T
			A	7 10	22.0	2500	2500	22.
						Avg =	2500	for

Layer 4 Velocity computed by Hobson-Overton method

Not enough points.

Wtd Avg Velocity computed for Layer 4 = 2500

DEPTH MODEL TABLES for SP1000.SIP

Spread A Depth and Elev of layers directly beneath SPs and Geos

SP	Surface X-Loc	Surface Elev	Layer 2 Depth	Layer 2 Elev	Layer 3 Depth	Layer 3 Elev	Layer 4 Depth	Layer 4 Elev
A	0.0	0.0	0.8	-0.8	5.9	-5.9	13.7	-13.7

Geo	Surface X-Loc	Surface Elev	Layer 2 Depth	Layer 2 Elev	Layer 3 Depth	Layer 3 Elev	Layer 4 Depth	Layer 4 Elev
1	5.0	0.0	0.8	-0.8	5.9	-5.9	13.7	-13.7
2	10.0	0.0	0.8	-0.8	5.9	-5.9	13.7	-13.7
3	15.0	0.0	0.8	-0.8	5.9	-5.9	13.7	-13.7
4	20.0	0.0	0.8	-0.8	5.9	-5.9	13.7	-13.7
5	25.0	0.0	0.8	-0.8	5.9	-5.9	13.7	-13.7
6	30.0	0.0	0.8	-0.8	5.9	-5.9	13.7	-13.7
7	35.0	0.0	0.8	-0.8	5.9	-5.9	13.7	-13.7
8	40.0	0.0	0.8	-0.8	5.9	-5.9	13.7	-13.7
9	45.	0.0	0.8	-0.8	5.9	-5.9	13.7	-13.7
10	50.0	0.0	0.8	-0.8	5.9	-5.9	13.7	-13.7

Velocities used to formulate the Depth Model

Spread A	Layer 1	Layer 2	Layer 3	Layer 4
Vertical	455	833	1667	
Horizontal		833	1667	2500

INPUT DATA FILE for SP2000.SIP

TITLE FOR SIPT2/SIPLUS INPUT DATA SET for SP2000.SIP

Master Thesis - Seismic Profile No. 2000 - The Khobar Aquifer

PROGRAM CONTROL DATA

Sprds	Ext	Lays	Ovr	PRINTER PLOT SCALES Elev m/col	Horiz m/row	Time ms/col	DATUM Pt 1 Elev/X	CONTROL Pt 2 Elev/X	PLOT CONTROL Elevations Top	Bottom	BLi
1	6	2	0	0.0	0.0	0.0	0.0 0.0	0.0 0.0	0	0	0.

SHOTPOINT AND GEOPHONE DATA

Spread A, 1 SP, 12 Geo's, X-Shift = 0.0, X-True = 0, Units: Met

SP	Elev	X-Loc	Y-Loc	Depth	Uphole T	Fudge T	End SP
A	0.0	0.0	0.0	0.0	0.0	0.0	1

ARRIVAL TIMES AND LAYERS REPRESENTED

Geo	Elev	X-Loc	Y	SP A	L
1	0.0	5.0	0.0	2.14	1
2	0.0	10.0	0.0	3.00	1
3	0.0	20.0	0.0	4.50	2
4	0.0	30.0	0.0	6.19	2
5	0.0	40.0	0.0	8.16	2
6	0.0	50.0	0.0	0.00	0
7	0.0	60.0	0.0	0.00	0
8	0.0	70.0	0.0	0.00	0
9	0.0	80.0	0.0	0.00	0
10	0.0	90.0	0.0	0.00	0
11	0.0	100.0	0.0	0.00	0
12	0.0	110.0	0.0	0.00	0

VELOCITY ANALYSIS TABLES for SP2000.SIP

Layer 1 Velocity from direct arrivals

Spread A	SP	Geo	DD	V	Avg V
	A	1	5.0	2336	
	A	2	10.0	3333	
					2835

Wtd Avg Velocity computed for Layer 1 = 2835

Layer 2 Velocity computed by regression of raw uncorrected arrivals

Spread A V	Ti	Geos	<-SP->	Geos	Ti	V	Avg V	Avg Ti
			A	3 5	0.8	5464	5464	0.8
						Avg =	5464	for

Layer 2 Velocity computed by Hobson-Overton method

Not enough points.

Wtd Avg Velocity computed for Layer 2 = 5464

DEPTH MODEL TABLES for SP2000.SIP

Spread A Depth and Elev of layers directly beneath SPs and Geos

SP	Surface X-Loc	Surface Elev	Layer 2 Depth	Layer 2 Elev
A	0.0	0.0	1.4	-1.4

Geo	Surface X-Loc	Surface Elev	Layer 2 Depth	Layer 2 Elev
1	5.0	0.0	1.4	-1.4
2	10.0	0.0	1.4	-1.4
3	20.0	0.0	1.4	-1.4
4	30.0	0.0	1.1	-1.1
5	40.0	0.0	1.4	-1.4
6	50.0	0.0	1.4	-1.4
7	60.0	0.0	1.4	-1.4
8	70.0	0.0	1.3	-1.3
9	80.0	0.0	1.3	-1.3
10	90.0	0.0	1.3	-1.3
11	100.0	0.0	1.3	-1.3
12	110.0	0.0	1.3	-1.3

Velocities used to formulate the Depth Model

Spread A	Layer 1	Layer 2
Vertical	2835	
Horizontal		5464

INPUT DATA FILE for SP3000.SIP

TITLE FOR SIPT2/SIPLUS INPUT DATA SET for SP3000.SIP

Master Thesis - Seismic Profile No. 3000 - The Khobar Aquifer

PROGRAM CONTROL DATA

Sprds	Exist	Layrs	Overr	PRINTER PLOT SCALES Elev m/col	Horiz m/row	Time ms/col	DATUM CONTROL Pt 1 Elev/X	Pt 2 Elev/X	PLOT CONTROL Elevations Top	Bottom	BL
1	6	3	0	0.0	0.0	0.0	0.0 0.0	0.0 0.0	0	0	0

SHOTPOINT AND GEOPHONE DATA

Spread A, 1 SP, 12 Geo's, X-Shift = 0.0, X-True = 0, Units: Me

SP	Elev	X-Loc	Y-Loc	Depth	Uphole T	Fudge T	End SP
A	0.0	-5.0	0.0	0.0	0.0	0.0	1

ARRIVAL TIMES AND LAYERS REPRESENTED

Geo	Elev	X-Loc	Y	SP A	L
1	0.0	0.0	0.0	14.08	1
2	0.0	10.0	0.0	42.25	1
3	0.0	20.0	0.0	59.15	2
4	0.0	30.0	0.0	80.00	2
5	0.0	40.0	0.0	98.59	2
6	0.0	50.0	0.0	121.20	3
7	0.0	60.0	0.0	126.70	3
8	0.0	70.0	0.0	132.30	3
9	0.0	80.0	0.0	0.00	0
10	0.0	90.0	0.0	0.00	0
11	0.0	100.0	0.0	0.00	0
12	0.0	110.0	0.0	0.00	0

VELOCITY ANALYSIS TABLES for SP3000.SIP

Layer 1 Velocity from direct arrivals

Spread A	SP	Geo	DD	V	Avg V
	A	1	5.0	355	
	A	2	15.0	355	
					355

Wtd Avg Velocity computed for Layer 1 = 355

Layer 2 Velocity computed by regression of raw uncorrected arrivals

Spread A V	Ti	Geos	<-SP->	Geos	Ti	V	Avg V	Avg Ti
			A	3 5	10.2	507	507	10.2
						Avg =	507	for

Layer 2 Velocity computed by Hobson-Overton method

Not enough points.

Wtd Avg Velocity computed for Layer 2 = 507

Layer 3 Velocity computed by regression of raw uncorrected arrivals

Spread A V	Ti	Geos	<-SP->	Geos	Ti	V	Avg V	Avg T
			A	6 8	90.7	1802	1802	90.
						Avg =	1802	for

Layer 3 Velocity computed by Hobson-Overton method

Not enough points.

Wtd Avg Velocity computed for Layer 3 = 1802

DEPTH MODEL TABLES for SP3000.SIP

Spread A Depth and Elev of layers directly beneath SPs and Geos

SP	Surface X-Loc	Surface Elev	Layer 2 Depth	Layer 2 Elev	Layer 3 Depth	Layer 3 Elev
A	-5.0	0.0	2.5	-2.5	22.8	-22.8

Geo	Surface X-Loc	Surface Elev	Layer 2 Depth	Layer 2 Elev	Layer 3 Depth	Layer 3 Elev
1	0.0	0.0	2.5	-2.5	22.8	-22.8
2	10.0	0.0	2.5	-2.5	22.8	-22.8
3	20.0	0.0	2.6	-2.6	22.8	-22.8
4	30.0	0.0	2.6	-2.6	22.8	-22.8
5	40.0	0.0	2.5	-2.5	22.8	-22.8
6	50.0	0.0	2.5	-2.5	22.8	-22.8
7	60.0	0.0	2.5	-2.5	22.8	-22.8
8	70.0	0.0	2.5	-2.5	22.8	-22.8
9	80.0	0.0	2.5	-2.5	22.8	-22.8
10	90.0	0.0	2.5	-2.5	22.8	-22.8
11	100.0	0.0	2.5	-2.5	22.8	-22.8
12	110.0	0.0	2.5	-2.5	22.8	-22.8

Velocities used to formulate the Depth Model

Spread A	Layer 1	Layer 2	Layer 3
Vertical	355	507	
Horizontal		507	1802

INPUT DATA FILE for SP4000.SIP

TITLE FOR SIPT2/SIPLUS INPUT DATA SET for SP4000.SIP

Master Thesis - Seismic Profile No. 4000 - The Khobar Aquifer

PROGRAM CONTROL DATA

Sprds	Extis	Lays	Over	PRINTER PLOT SCALES Elev m/col	Horiz m/row	Time ms/col	DATUM CONTROL Pt 1 Elev/X	Pt 2 Elev/X	PLOT CONTROL Elevations Top	Bottom	BI
1	6	4	0	0.0	0.0	0.0	0.0 0.0	0.0 0.0	0	0	(

SHOTPOINT AND GEOPHONE DATA

Spread A, 1 SP, 12 Geo's, X-Shift = 0.0, X-True = 0, Units: Me

SP	Elev	X-Loc	Y-Loc	Depth	Uphole T	Fudge T	End SP
A	0.0	0.0	0.0	0.0	0.0	0.0	1

ARRIVAL TIMES AND LAYERS REPRESENTED

Geo	Elev	X-Loc	Y	SP A	L
1	0.0	5.0	0.0	13.72	1
2	0.0	15.0	0.0	27.45	1
3	0.0	25.0	0.0	31.37	2
4	0.0	35.0	0.0	37.25	2
5	0.0	40.0	0.0	41.17	2
6	0.0	45.0	0.0	45.09	3
7	0.0	50.0	0.0	47.05	3
8	0.0	55.0	0.0	50.19	3
9	0.0	60.0	0.0	50.98	3
10	0.0	65.0	0.0	54.90	4
11	0.0	70.0	0.0	56.86	4
12	0.0	80.0	0.0	58.82	4

VELOCITY ANALYSIS TABLES for SP4000.SIP

Layer 1 Velocity from direct arrivals

Spread A	SP	Geo	DD	V	Avg V
	A	1	5.0	364	
	A	2	15.0	546	
					455

Wtd Avg Velocity computed for Layer 1 = 455

Layer 2 Velocity computed by regression of raw uncorrected arrival

Spread A V	Ti	Geos	<-SP->	Geos	Ti	V	Avg V	Avg
			A	3 5	15.1	1553	1553	15
						Avg =	1553	fo

Layer 2 Velocity computed by Hobson-Overton method

Not enough points.

Wtd Avg Velocity computed for Layer 2 = 1553

Layer 3 Velocity computed by regression of raw uncorrected arrival

Spread A V	Ti	Geos	<-SP->	Geos	Ti	V	Avg V	Avg
			A	6 9	26.5	2403	2403	26
						Avg =	2403	fo

Layer 3 Velocity computed by Hobson-Overton method

Not enough points.

Wtd Avg Velocity computed for Layer 3 = 2403

Layer 4 Velocity computed by regression of raw uncorrected arrival

Spread A V	Ti	Geos	<-SP->	Geos	Ti	V	Avg V	Avg
			A	10 12	38.8	3968	3968	38
						Avg =	3968	fo

Layer 4 Velocity computed by Hobson-Overton method

Not enough points.

Wtd Avg Velocity computed for Layer 4 = 3968

VELOCITY ANALYSIS TABLES for SP4000.SIP

Layer 1 Velocity from direct arrivals

Spread A	SP	Geo	DD	V	Avg V
	A	1	5.0	364	
	A	2	15.0	546	
					455

Wtd Avg Velocity computed for Layer 1 = 455

Layer 2 Velocity computed by regression of raw uncorrected arrival

Spread A V	Ti	Geos	<-SP->	Geos	Ti	V	Avg V	Avg
			A	3 5	15.1	1553	1553	15
						Avg =	1553	fo

Layer 2 Velocity computed by Hobson-Overton method

Not enough points.

Wtd Avg Velocity computed for Layer 2 = 1553

Layer 3 Velocity computed by regression of raw uncorrected arrival

Spread A V	Ti	Geos	<-SP->	Geos	Ti	V	Avg V	Avg
			A	6 9	26.5	2403	2403	26
						Avg =	2403	fo

Layer 3 Velocity computed by Hobson-Overton method

Not enough points.

Wtd Avg Velocity computed for Layer 3 = 2403

Layer 4 Velocity computed by regression of raw uncorrected arrival

Spread A V	Ti	Geos	<-SP->	Geos	Ti	V	Avg V	Avg
			A	10 12	38.8	3968	3968	38
						Avg =	3968	fo

Layer 4 Velocity computed by Hobson-Overton method

Not enough points.

Wtd Avg Velocity computed for Layer 4 = 3968

DEPTH MODEL TABLES for SP4000.SIP

Spread A Depth and Elev of layers directly beneath SPs and Geos

SP	Surface X-Loc	Surface Elev	Layer 2 Depth	Layer 2 Elev	Layer 3 Depth	Layer 3 Elev	Layer 4 Depth	Layer 4 Elev
A	0.0	0.0	3.6	-3.6	14.7	-14.7	29.4	-29.4

Geo	Surface X-Loc	Surface Elev	Layer 2 Depth	Layer 2 Elev	Layer 3 Depth	Layer 3 Elev	Layer 4 Depth	Layer 4 Elev
1	5.0	0.0	3.6	-3.6	14.7	-14.7	29.4	-29.4
2	15.0	0.0	3.6	-3.6	14.6	-14.6	29.4	-29.4
3	25.0	0.0	3.6	-3.6	14.6	-14.6	29.5	-29.5
4	35.0	0.0	3.6	-3.6	14.5	-14.5	29.6	-29.6
5	40.0	0.0	3.6	-3.6	14.7	-14.7	29.7	-29.7
6	45.0	0.0	3.6	-3.6	14.7	-14.7	29.7	-29.7
7	50.0	0.0	3.6	-3.6	14.2	-14.2	30.2	-30.2
8	55.0	0.0	3.6	-3.6	14.2	-14.2	30.4	-30.4
9	60.0	0.0	3.6	-3.6	14.2	-14.2	30.2	-30.2
10	65.0	0.0	3.6	-3.6	14.2	-14.2	30.2	-30.2
11	70.0	0.0	3.6	-3.6	14.2	-14.2	30.2	-30.2
12	80.0	0.0	3.6	-3.6	14.2	-14.2	30.2	-30.2

Velocities used to formulate the Depth Model

Spread A	Layer 1	Layer 2	Layer 3	Layer 4
Vertical	455	1553	2403	
Horizontal		1553	2403	3968

INPUT DATA FILE for SP5000.SIP

TITLE FOR SIPT2/SIPLUS INPUT DATA SET for SP5000.SIP

Master Thesis - Seismic Profile No. 5000 - The Khobar Aquifer

PROGRAM CONTROL DATA

Sprds	Exit	Lays	Over	PRINTER PLOT SCALES Elev m/col	Horiz m/row	Time ms/col	DATUM CONTROL Pt 1 Elev/X	Pt 2 Elev/X	PLOT CONTROL Elevations Top	Bottom	BI
1	6	2	0	0.0	0.0	0.0	0.0 0.0	0.0 0.0	0	0	(

SHOTPOINT AND GEOPHONE DATA

Spread A, 1 SP, 6 Geo's, X-Shift = 0.0, X-True = 0, Units: Met

SP	Elev	X-Loc	Y-Loc	Depth	Uphole T	Fudge T	End SP
A	0.0	0.0	0.0	0.0	0.0	0.0	1

ARRIVAL TIMES AND LAYERS REPRESENTED

Geo	Elev	X-Loc	Y	SP A	L
1	0.0	5.0	0.0	13.72	1
2	0.0	10.0	0.0	21.56	2
3	0.0	15.0	0.0	23.52	2
4	0.0	20.0	0.0	25.49	2
5	0.0	25.0	0.0	27.45	2
6	0.0	30.0	0.0	29.41	2

VELOCITY ANALYSIS TABLES for SP5000.SIP

Layer 1 Velocity from direct arrivals

Spread A	SP	Geo	DD	V	Avg V
	A	1	5.0	364	
					364

Wtd Avg Velocity computed for Layer 1 = 364

Layer 2 Velocity computed by regression of raw uncorrected arriva

Spread A V	Ti	Geos	<-SP->	Geos	Ti	V	Avg V	Avg
			A	2 6	17.6	2547	2547	1
						Avg =	2547	fc

Layer 2 Velocity computed by Hobson-Overton method

Not enough points.

Wtd Avg Velocity computed for Layer 2 = 2547

DEPTH MODEL TABLES for SP5000.SIP

Spread A Depth and Elev of layers directly beneath SPs and Geos

SP	Surface X-Loc	Surface Elev	Layer 2 Depth	Layer 2 Elev
A	0.0	0.0	3.2	-3.2

Geo	Surface X-Loc	Surface Elev	Layer 2 Depth	Layer 2 Elev
1	5.0	0.0	3.2	-3.2
2	10.0	0.0	3.2	-3.2
3	15.0	0.0	3.2	-3.2
4	20.0	0.0	3.2	-3.2
5	25.0	0.0	3.2	-3.2
6	30.0	0.0	3.2	-3.2

Velocities used to formulate the Depth Model

Spread A	Layer 1	Layer 2
Vertical	364	
Horizontal		2547

INPUT DATA FILE for SP6000.SIP

TITLE FOR SIPT2/SIPLUS INPUT DATA SET for SP6000.SIP

Master Thesis - Seismic Profile No. 6000 - The Khobar Aquifer

PROGRAM CONTROL DATA

Sprds	Expt	Lays	VOver	PRINTER PLOT SCALES Elev m/col	Horiz m/row	Time ms/col	DATUM CONTROL Pt 1 Elev/X	Pt 2 Elev/X	PLOT CONTROL Elevations Top	Bottom	BLim
1	6	3	0	0.0	0.0	0.0	0.0 0.0	0.0 0.0	0	0	0.5

SHOTPOINT AND GEOPHONE DATA

Spread A, 1 SP, 9 Geo's, X-Shift = 0.0, X-True = 0, Units: Meter

SP	Elev	X-Loc	Y-Loc	Depth	Uphole T	Fudge T	End SP
A	0.0	0.0	0.0	0.0	0.0	0.0	1

ARRIVAL TIMES AND LAYERS REPRESENTED

Geo	Elev	X-Loc	Y	SP A	L
1	0.0	5.0	0.0	9.80	1
2	0.0	10.0	0.0	19.60	1
3	0.0	15.0	0.0	25.49	2
4	0.0	20.0	0.0	27.47	2
5	0.0	25.0	0.0	31.37	2
6	0.0	30.0	0.0	35.29	2
7	0.0	35.0	0.0	39.21	2
8	0.0	40.0	0.0	43.13	3
9	0.0	45.0	0.0	45.09	3

VELOCITY ANALYSIS TABLES for SP6000.SIP

Layer 1 Velocity from direct arrivals

Spread A	SP	Geo	DD	V	Avg V
	A	1	5.0	510	
	A	2	10.0	510	
					510

Wtd Avg Velocity computed for Layer 1 = 510

Layer 2 Velocity computed by regression of raw uncorrected arrivals

Spread A V	Ti	Geos	<-SP->	Geos	Ti	V	Avg V	Avg Ti
			A	3 7	14.1	1418	1418	14.1
						Avg =	1418	for

Layer 2 Velocity computed by Hobson-Overton method

Not enough points.

Wtd Avg Velocity computed for Layer 2 = 1418

Layer 3 Velocity computed by regression of raw uncorrected arrivals

Spread A V	Ti	Geos	<-SP->	Geos	Ti	V	Avg V	Avg Ti
			A	8 9	27.5	2551	2551	27.5
						Avg =	2551	for

Layer 3 Velocity computed by Hobson-Overton method

Not enough points.

Wtd Avg Velocity computed for Layer 3 = 2551

DEPTH MODEL TABLES for SP6000.SIP

Spread A Depth and Elev of layers directly beneath SPs and Geos

SP	Surface X-Loc	Surface Elev	Layer 2 Depth	Layer 2 Elev	Layer 3 Depth	Layer 3 Elev
A	0.0	0.0	4.0	-4.0	14.2	-14.2

Geo	Surface X-Loc	Surface Elev	Layer 2 Depth	Layer 2 Elev	Layer 3 Depth	Layer 3 Elev
1	5.0	0.0	4.0	-4.0	14.2	-14.2
2	10.0	0.0	3.9	-3.9	14.2	-14.2
3	15.0	0.0	3.9	-3.9	14.2	-14.2
4	20.0	0.0	3.7	-3.7	14.3	-14.3
5	25.0	0.0	3.7	-3.7	14.3	-14.3
6	30.0	0.0	3.9	-3.9	14.3	-14.3
7	35.0	0.0	4.0	-4.0	14.3	-14.3
8	40.0	0.0	4.0	-4.0	14.3	-14.3
9	45.0	0.0	4.0	-4.0	14.3	-14.3

Velocities used to formulate the Depth Model

Spread A	Layer 1	Layer 2	Layer 3
Vertical	510	1418	
Horizontal		1418	2551

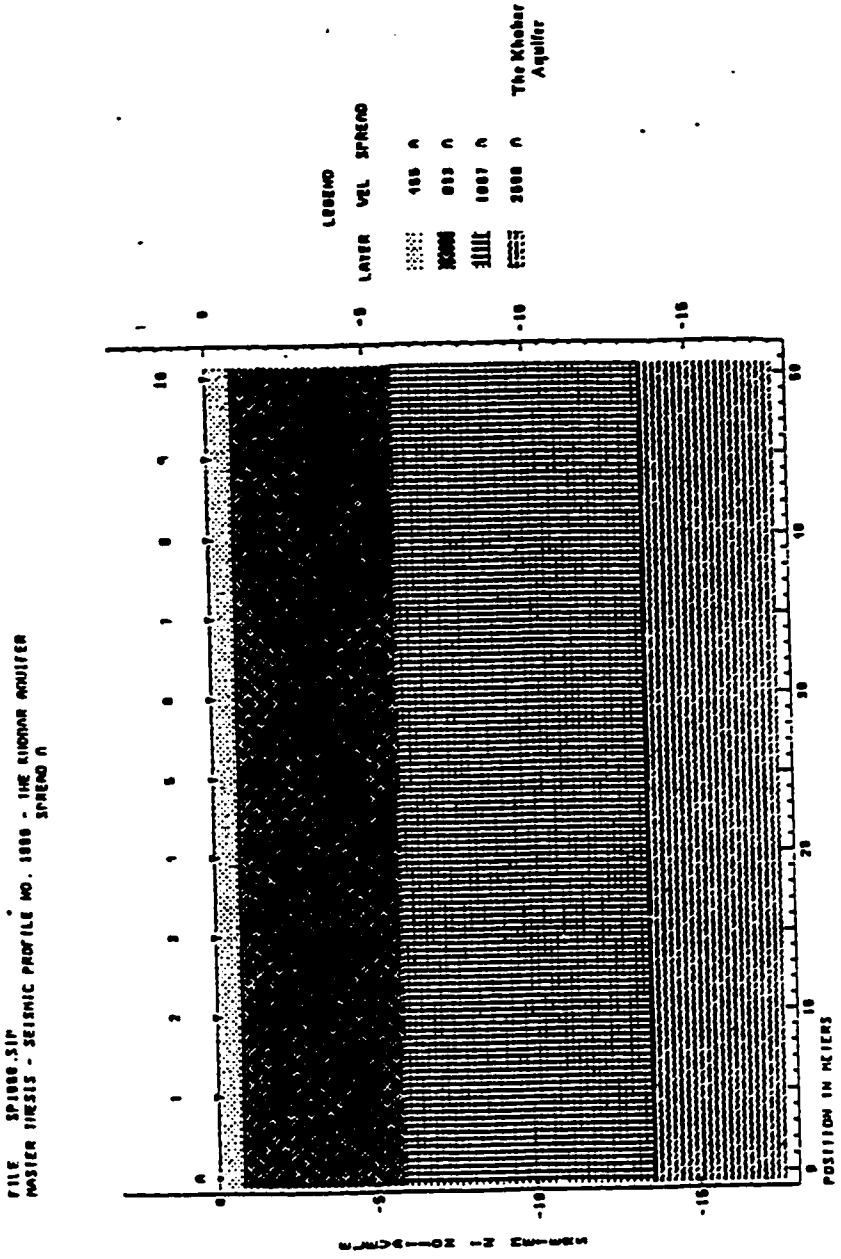
FILE SP1000.SIP
MASTER THESIS - SEISMIC PROFILE NO. 1000 - THE KHOSAR AQUIFER
SPREAD A
LEGEND
LAYER VEL SPREAD
The Khobar Aquifer
POSITION IN METERS
DEPTH IN METERS

FILE SP2000.SIP
MASTER THESIS - SEISMIC PROFILE NO. 2000 - THE KHOBAR AQUIFER
SPREAD A

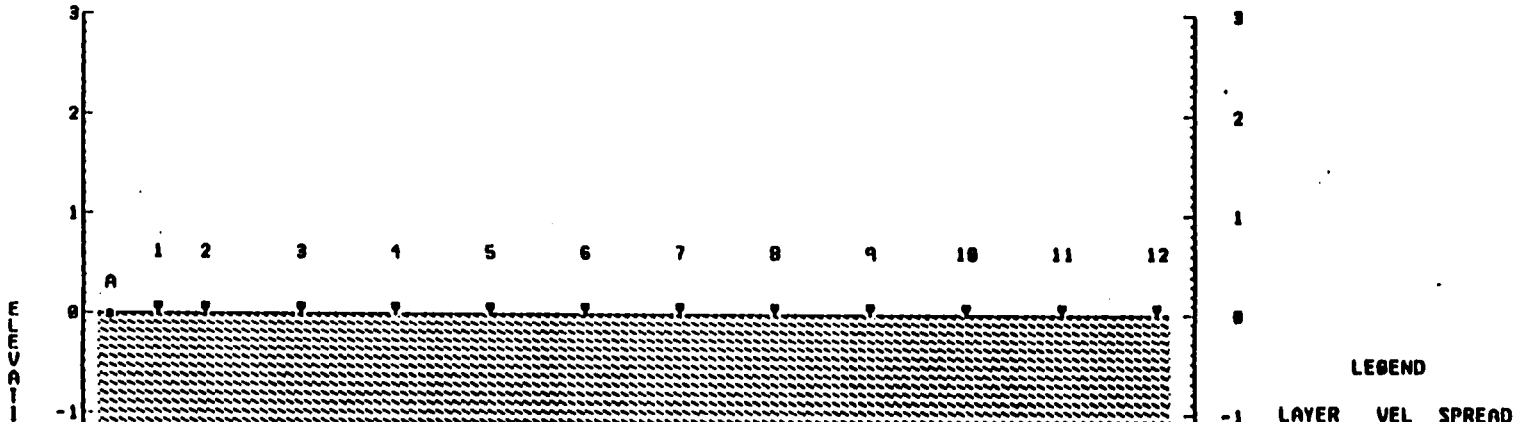

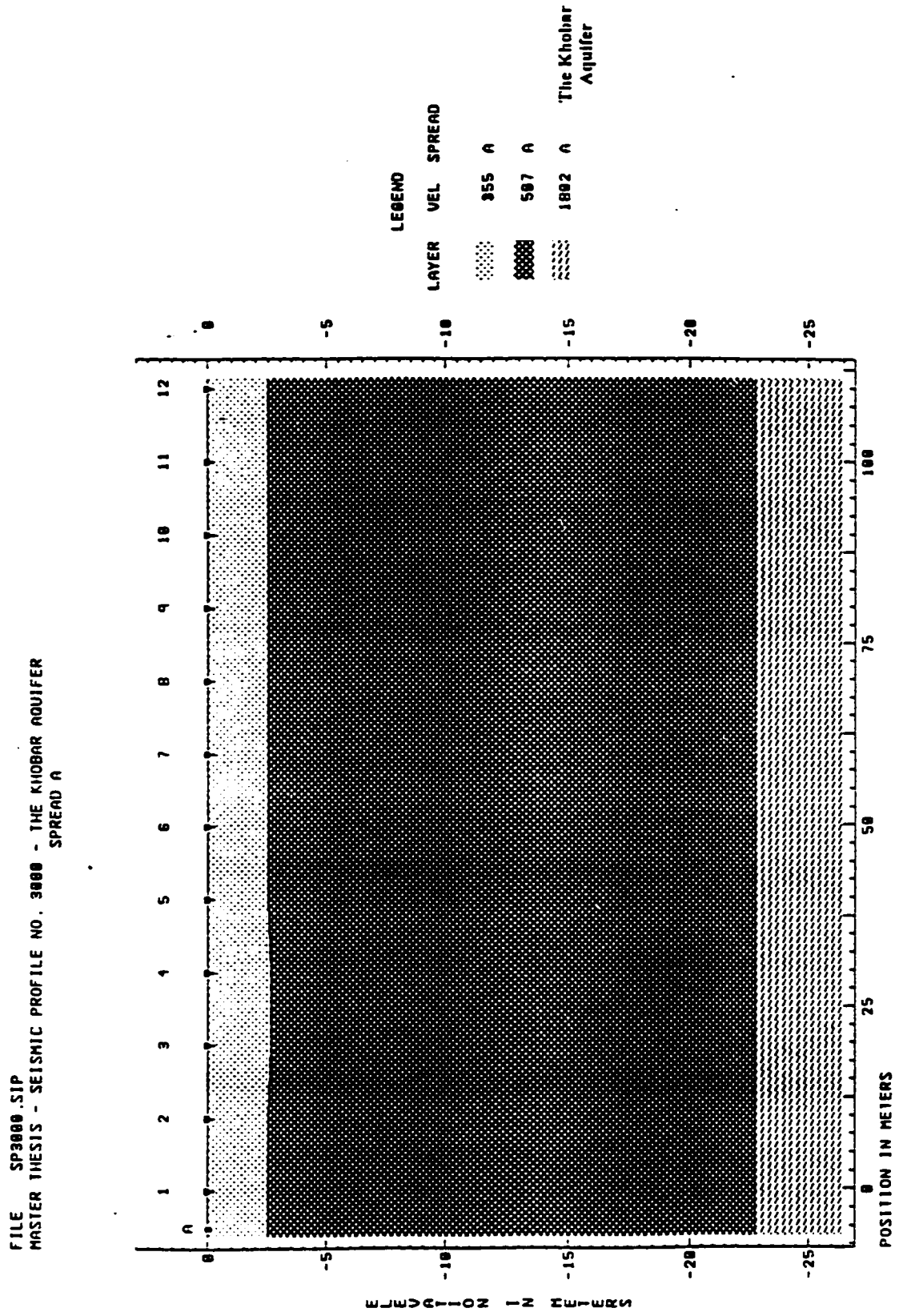
FILE SP3000.SIP
MASTER THESIS - SEISMIC PROFILE NO. 3000 - THE KHOBAR AQUIFER
SPREAD A
LEGEND
LAYER VEL SPREAD
355 A
587 A
1882 A
The Khobar Aquifer
ELEVATION IN METERS
POSITION IN METERS

FILE SP1000.SIP
MASTER THESIS - SEISMIC PROFILE NO. 1000 - THE KHOBAR AQUIFER
SPREAD A

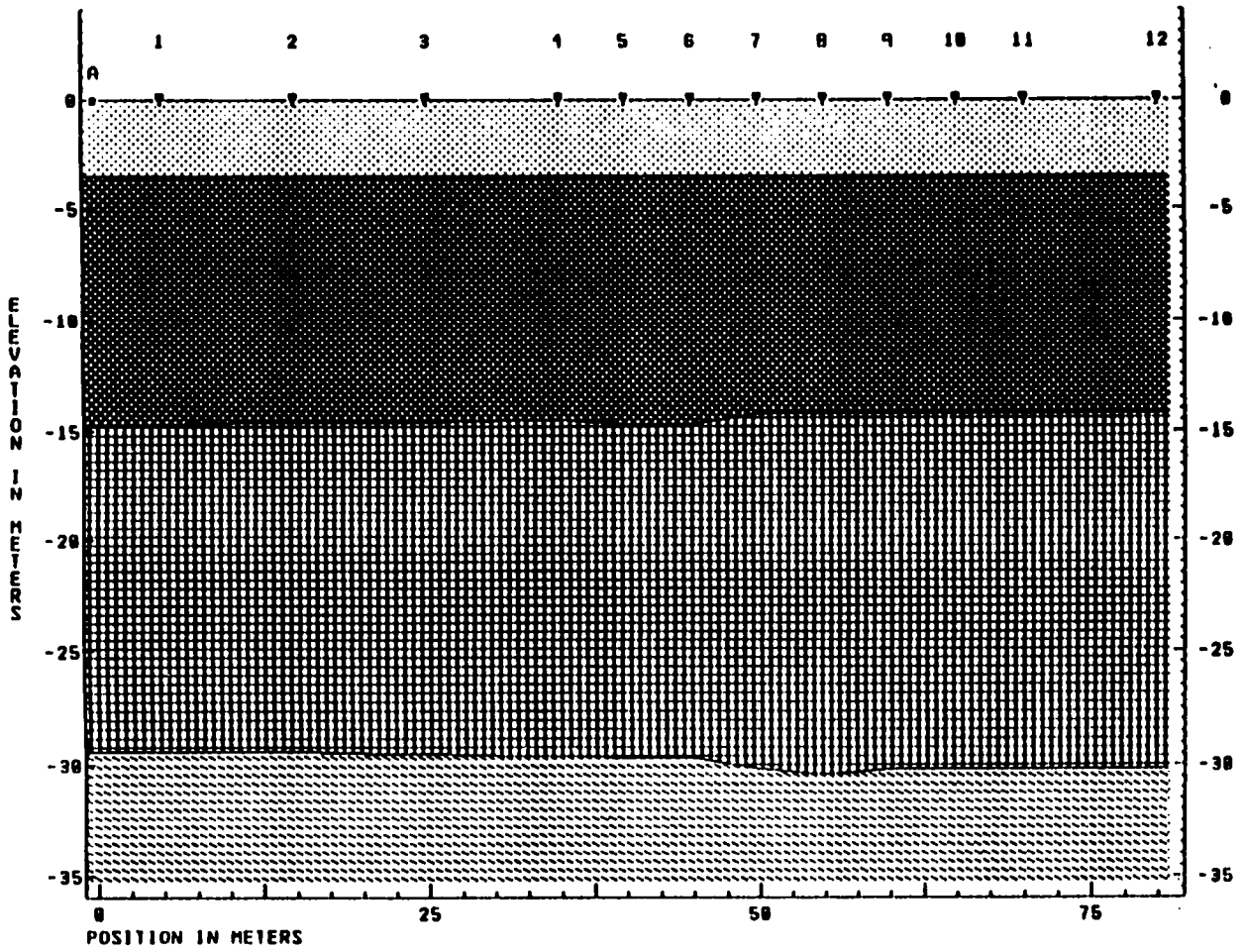

LEGEND

LAYER	VEL	SPREAD	
	155	A	
	1553	A	
	2183	A	
	3968	A	The Khobar Aquifer

FILE SP5000.SIP
MASTER THESIS - SEISMIC PROFILE NO. 5000 - THE KHOBAR AQUIFER
SPREAD A

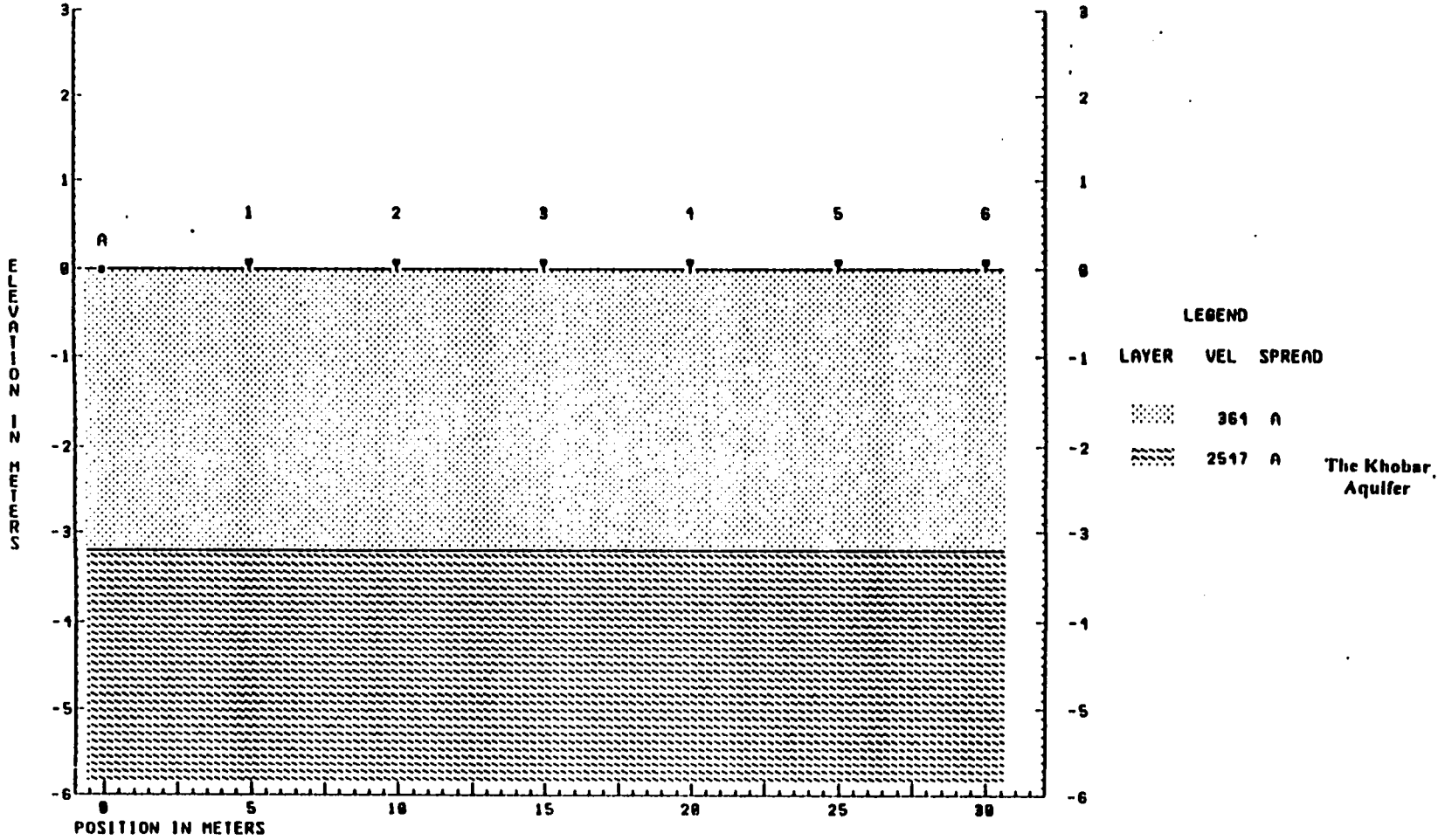

FILE SP6000.SIP
MASTER THESIS - SEISMIC PROFILE NO. 6000 - THE KHOBAR AQUIFER
SPREAD A